

Forsmark site investigation

Helicopter borne geophysics at Forsmark, Östhammar, Sweden

H Jan S Rønning, Ola Kihle, John Olav Mogaard
NGU

Peter Walker
Geophysical Algorithms, Canada

Hossein Shomali, Peter Hagthorpe, Sören Byström
Geological Survey of Sweden

Hans Lindberg, Hans Thunehed
GeoVista AB

May 2003

Svensk Kärnbränslehantering AB

Swedish Nuclear Fuel
and Waste Management Co
Box 5864

SE-102 40 Stockholm Sweden

Tel 08-459 84 00

+46 8 459 84 00

Fax 08-661 57 19

+46 8 661 57 19



Forsmark site investigation

Helicopter borne geophysics at Forsmark, Östhammar, Sweden

H Jan S Rønning, Ola Kihle, John Olav Mogaard
NGU

Peter Walker
Geophysical Algorithms, Canada

Hossein Shomali, Peter Hagthorpe, Sören Byström
Geological Survey of Sweden

Hans Lindberg, Hans Thunehed
GeoVista AB

May 2003

Keywords: Geophysics, helicopter, magnetometry, electromagnetic, radiometric, data processing

This report concerns a study which was conducted for SKB. The conclusions and viewpoints presented in the report are those of the authors and do not necessarily coincide with those of the client.

A pdf version of this document can be downloaded from www.skb.se

Preface

On behalf of Svensk Kärnbränslehantering AB (SKB), geophysical measurements from helicopter have been carried out in the Forsmark site investigation area. This report summarizes the three steps taken to secure a complete data set to be used for interpretation. Each step is described in a section of the report produced by the organisation responsible.

- *Section A* describes the instrument tests, data acquisition procedure, processing of data, map production and data delivery, performed by the Geological Survey of Norway (NGU).
- *Section B* describes the adjustment to the magnetic data to compensate for the disturbance of a DC cable in the survey area. The adjustments were carried out by the Geological Survey of Sweden (SGU).
- *Section C* describes a levelling made on the uranium channel in the radiometric data. The levelling, made by SGU, applies only to the area flown in north-south direction.

For details on data handling during each step in the process, please refer to each separate section. However, the following scheme of deliveries and input/output of data in different processes is important for the traceability of the final data delivery.

Raw final deliverable data (XYZ ASCII data) by NGU, as described in Section A, is a complete set of raw survey data apart from 2 aspects:

1. The effect from a major DC cable is present in the magnetic data delivered from NGU, Section A. Since the effect of the DC cable was not fully understood at the onset of the survey, SGU carried out a correction of the magnetics for the DC effect. Thus the corrected magnetic data is not included in the final delivery of XYZ ASCII data from NGU. The corrected magnetic raw data is found in a delivery from SGU, see Section B.
2. An error in level of the uranium channel of the north-south data at Forsmark was corrected by SGU after the delivery of the final data. The levelling is likely to be contributed to anomalous concentrations of radon in the air during the survey of a few of the flight lines. The corrected uranium data in XYZ ASCII format, including a full set of the other spectrometer data channels in the file, is described in section C.

In order to produce useful maps and grids for the final delivery, NGU used the corrected version of the magnetic data for grid and map production. Thus, the final grids delivered from NGU are based on DC corrected magnetic data.

The report structure is as follows:

Section A	p. 5
Section B	p. 113
Section C	p. 129

Forsmark site investigation

Helicopter borne geophysics at Forsmark, Östhammar, Sweden

H Jan S Rønning, Ola Kihle and John Olav Mogaard
NGU

Peter Walker
Geophysical Algorithms, Canada

April 2003

Keywords: Geophysics, helicopter, magnetometry, electromagnetic, radiometric, data processing

Summary

Svensk Kärnbränslehantering AB (SKB) has decided to carry out site investigations in the Forsmark area after decisions by the Swedish government and the municipality of Östhammar and approval from local landowners. As a part of this, geophysical measurements from helicopter were carried out in the area according to the general and site-specific programmes. The Geological Survey of Norway (NGU) was chosen to operate this survey. The NGU used NorCopter AS and Geophysical Algorithms as subcontractors. The main purpose of the geophysical measurements was to provide information about the bedrock geology in the Forsmark area.

Measurements were performed along north-south directed flight lines in a diamond shaped area of approximately 10 x 11 km in size. A sub area, 6 x 6 km in size, was flown east-west with the purpose to better resolve geological structures in a N-S direction south east of the nuclear power plant (i.e. in the central part of the Forsmark site investigation area). The line spacing was 50 metres and the nominal flying height 60 metres. Tie-lines were measured for each 500 metres. Altogether, 2819 kilometres were measured.

The quality control and first step of processing took place on site, while the final processing was made at Geophysical Algorithms in Canada. Maps in scale 1: 20 000 were produced at the NGU in Trondheim. This report describes instrument tests, data acquisition, processing of data, map production and data delivery.

Contents

1	Introduction	11
2	Objectives and scope	12
3	Methodology	13
3.1	Methods	13
3.2	Equipment	13
3.2.1	Magnetic	13
3.2.2	Electromagnetic	13
3.2.3	Radiometric	13
3.2.4	Very Low Frequency ElectroMagnetic (VLF-EM)	13
3.2.5	Navigation	14
3.2.6	Altimeter	14
3.2.7	Datalogger	14
3.2.8	Helicopter	14
3.3	Performance	14
3.4	Base of operation	15
3.5	Activity plan, quality assurance and control	15
4	Tests and calibration	17
4.1	Pre mobilization tests	17
4.2	Tests before, during and after the surveying	17
4.3	Daily tests	18
4.4	Quality of data	18
5	Processing of data	19
5.1	On-site processing	19
5.2	Post survey processing	19
6	Results and data delivery	21
6.1	Digital data	21
6.2	Geophysical maps	21
	References	23
Appendix A	Pre survey report	25
Appendix A1	Mail from Peter Walker (NGU) to Søren Bystrøm (SGU)	37
Appendix A2	Calibration report for Bendix/King KRA 405 B Radar altimeter	39
Appendix B	Forsmark Quality Control Tests	43
Appendix C	Helicopter geophysical data processing methods	65
Appendix D	Data delivery formats	75
Appendix E	Gridding and Map production	79
Appendix F	Produced and delivered maps	83

1 Introduction

Svensk Kärnbränslehantering AB (SKB) has decided to carry out site investigations in the Forsmark area after decisions by the Swedish government and the municipality of Östhammar and approval from local landowners. As part of this, geophysical measurements from helicopter were carried out according to general and site-specific programmes /1/, /2/. The Geological Survey of Norway (NGU) was chosen to operate this survey. The NGU used NorCopter and Geophysical Algorithms as subcontractors.

The survey in the Forsmark area, Figure 1-1, was conducted immediately prior to a similar survey at Simpevarp. Due to this, parts of the calibrations and instrument tests refer to the Simpevarp survey.

This report presents the methodology, calibrations and data gained in helicopter borne geophysics at Forsmark, which is one of the activities performed within the site investigation. The work was conducted according to activity plan AP PF 400-02-25 (SKB internal controlling document) under supervision of activity leader Rune Johansson, SGU, and assistant activity leader, Hans Lindberg, GeoVista AB.



Figure 1-1. Area covered by geophysical measurements from helicopter. Measurements were performed along north-south lines in the larger area while line direction was east west in the smaller area. Tie-lines were flown in the opposite directions.

2 Objectives and scope

The main purpose of the geophysical measurements was to provide information about the bedrock geology in the Forsmark area. Knowledge about any bedrock structures that might possibly be water bearing is very important for the safety analysis of a potential repository. The survey also provides information about soil cover. Helicopter surveys are very efficient in acquiring relatively detailed data with good spatial coverage. This will reduce the need for ground based methods and hence reduce the environmental impact of the site investigation.

3 Methodology

3.1 Methods

According to “Method description for helicopter borne geophysical surveying” (SKB MD 211.002), magnetic, electromagnetic, radiometric and Very Low Frequency ElectroMagnetic (VLF-EM) methods were used.

3.2 Equipment

The equipment used during the survey was as follows:

3.2.1 Magnetic

Mobile magnetometer: Scintrex CS-2 cesium magnetometer, resolution 0.001 nT, 10 samples per second, giving a data spacing of approximately 3 metres. The magnetometer was located in the electromagnetic sonde.

Base magnetometer: Scintrex MP-3 Proton magnetometer, resolution 0.1 nT, one sample every 3 seconds. As a backup, a Scintrex ENVI-mag base magnetometer was used.

3.2.2 Electromagnetic

Geotech Hummingbird, 5 frequency sonde, resolution 0.1 ppm, 10 samples per second. Coplanar 880, 6606 and 34133 Hz, Coaxial 980 and 7001 Hz. The four lower frequency coils are separated by 6 metres; the 34133 Hz coils are 4.2 metres apart. The sonde was towed on a cable approximately 30 metres in length.

3.2.3 Radiometric

Exploranium GR 820 with crystal volume 16 litres downward looking and 4 litres upward looking. The spectrometer has 256 channels, covering an energy window from 0.2 MeV to 3.0 MeV. Channel width is 12.5 keV. Channel 255 (cosmic) covers energies above 3 MeV. The crystal pack was thermally stabilized and mounted on a frame located between the skids of the helicopter. The system accumulates radiation in one second before data are stored (one sample each 30 metres).

3.2.4 Very Low Frequency ElectroMagnetic (VLF-EM)

Hertz Totem 2A, total field from two orthogonal stations, IN LINE and ORTHO (orthogonal). The system was sampled 5 times per second, which results in approximately 6 metre station distance. Usually the transmitter GBR (16,0 kHz) was used as the INLINE station and NAA (24 kHz) as the ORTHO station for the north–south profiling, and the opposite for east–west profiling. Occasionally NPM (23,4 kHz) replaced NAA when this was not operating. The sensor antenna was mounted on the tow cable approximately 10 metres below the aircraft. Due to instrument failure, VLF data was not available at the first five flights (western part of large area).

3.2.5 Navigation

An Ashtech G12 GPS receiver was used for navigation, with an Aztec RXMAR1 RDS receiver for differential corrections from the EPOS system and a Picodas PNAV2000 to provide real time navigation control data to the pilot. The antenna was mounted on the tail of the aircraft. The position is updated once every second. The resulting sampling increment was approximately 30 metres and not 20 metres as described in the method description for helicopterborne geophysical surveying (SKB MD 211.002). Differential GPS gave accuracy better than ± 5 m (see Appendix B).

3.2.6 Altimeter

Bendix/King KRA 405B, radar altimeter mounted on the helicopter. Accuracy is 5% of measured altitude.

3.2.7 Datalogger

Geotech datalogger, an integrated part of the EM-system.

3.2.8 Helicopter

AS 355 Twin engine, operated by NorCopter AS, Stavanger Norway.

3.3 Performance

The size and location of the two surveyed areas are as shown in Figure 1-1. Measurements were performed along north-south lines in the diamond shaped area. This area was originally limited by the following coordinates 1632471E / 6706371N, 1640249E / 6698596N, 1633178E / 6691522N and 1625400E / 6699300N with deviations for the power plant. Due to lack of time, profiles in the western and eastern corner were not measured.

The smaller area, selected with the purpose to better resolve possible geological structures in a N-S trend, was limited by the following coordinates 1630000E / 6702000N, 1636000E / 6702000N, 1636000E / 6696000N and 1630000E / 6696000N with deviations for the power plant.

The line spacing was 50 metres and nominal flying height 60 metres. Tie-lines were measured for each 500 metres.

Data were collected from August 22th to September 17th. Altogether, 2819 kilometres were surveyed.

The survey was performed using the following staff:

Equipment operators: John Olav Mogaard and Janusz Koziel, NGU

Quality control: Peter Walker, Geophysical Algorithms, Canada

Pilots: Frode Belsby and Johan Falkenberg, NorCopter AS

3.4 Base of operation

The base of operations was located at the Storskäret where flights began and ended and where re-fuelling took place. Fuel was available from a fuel truck. Location of the helicopter base was: 1634500E, 6697800N (RT90). On-site processing office was provided by a local farmer.

A test line was proposed between coordinates 1632000E / 6698000N and 1634000E / 6698000N. The test line was eventually placed between coordinates 1633700E / 6697900N and 1634900E / 6697900N (RT 90) with a length of 1.2 km. A two turn cable test loop, approximately 80 by 80 metres, was laid across the testline at the following coordinates: 1634437E / 6697862N, 1634442E / 6697901N, 1634435E / 6697943, 1634360E / 6697939N, 1634359E / 6697899N and 1634356E / 6697862N. The loop was closed during testing of EM lag, for calibration and system repeatability tests, and during the quality control line which was a part of every flight.

The base station magnetometer was located in a grove of trees just north of the barn used as base of operation. A second base station magnetometer, located at SFR (1632500E / 6701300N), was used as a backup. Due to influence from a DC power line north of the Forsmark power plant, none of these could be used to correct measured data. Instead, data from the FIBY laboratory were used in the final data processing (see Appendix C).

3.5 Activity plan, quality assurance and control

With a few nonconformities, the measurements at Forsmark followed the activity plan AP PF 400-02-25, version 1.0 (SKB internal controlling document) made specifically for the survey. Quality assurance and control followed the plan. Nonconformities were reported according to the standard SKB routine ("Rutin SD-006", SKB internal controlling document).

4 Tests and calibration

Tests and calibration were performed in three stages: (1) pre mobilization, (2) before, during, and after surveying and (3) daily tests.

4.1 Pre mobilization tests

Before the survey started, all instruments were tested and calibrated at the NGU in Trondheim. A pre survey report was delivered to SKB before the survey commenced, and is presented here in Appendix A.

4.2 Tests before, during and after the surveying

According to the activity plan, the following tests and calibrations should be performed before, during (after 10 days of operation) and after the surveying, Table 4-1.

Reports from these tests/calibrations are presented in Appendix B. Due to different events, there are some reported deviations from this plan (see Appendix C and nonconformity reports).

Table. 4-1. Tests before, during and after the surveying.

Method	Test/calibration	Before	During	After
Magnetic	Clover-leaf	X	X	X
	Lag test	X		X
	Base – bird side by side	X		X
ElectroMagnetic	Lag test	X		X
	Phase and calibration	X	X	X
	Temperature drift	X		
Radiometric	Cosmic correction	X		
	Upward-downward relation	X		X
	Altitude attenuation	X		X
GPS navigation	Accuracy test	X		X

4.3 Daily tests

Daily instrument test were mainly performed as described in the activity plan and the NGU quality assurance plan. Deviations were reported directly to SKB, according to the standard SKB protocol (Rutin SD-006).

4.4 Quality of data

All magnetic data were collected without any diurnal disturbances giving a very good data quality. However, the data were influenced by the DC power line located north of Forsmark power plant. The DC current was varying as a function of time, which gave effects that were necessary to correct for. The correction was performed by SGU, and the data given back to NGU for map production (see Appendix E). The data given to SGU missed parts of lines due to bad navigation (see Appendix E). These profiles were planned to be remeasured, but lack of time made this impossible. Originally measured data are included in final data delivery.

Additional noise sources in the area affecting the electromagnetic measurements were the DC rectifier with possible effects from the ground approach radar at Arlanda airport, a military installation located near Storskäret, and various broadcast antennae. It was subsequently noted in the Oskarshamn survey that the pulsed current used to energize electric fences seriously degraded the data, and such fences could have a similar effect, if present, on the data acquired in Forsmark. Due to this, it was difficult to do a proper nulling of the EM system. From time to time, instrument drift did not fulfil method specifications, but this gave minor problems compared with the external noise. In sum, these problems resulted in bad EM data quality, and in some areas it was not possible to calculate reliable resistivity data. This is also the reason why EM lines 350, 570, 640, 650, and 700 are missing in the final delivery. Due to lack of time and no possibility to overcome external noise sources, no re-measurements were made.

Radiometric data were collected within project specifications giving a good data quality.

At the beginning of the survey, the VLF receiver broke down. It took some time before this was replaced with new equipment from the company RMS in Canada. Meanwhile, data acquisition was performed without VLF (first five flights). Data quality was good for the rest of the survey except for lines 1818 to 2100 in the large area. When these lines were measured, there was no acceptable VLF station available.

Due to safety considerations, there were numerous deviations from flying height specifications (60 +/- 18 metres), described in the SKB deviation report. Actual flying height can be inspected in data delivery files (RALTM, see Appendix E).

From time to time, strong wind resulted in some deviations from line specifications. In agreement with the SKB representative, no lines were remeasured due to this. Flight paths can be inspected in Map 2002.095-01A (large area) and -01B (small area).

5 Processing of data

5.1 On-site processing

On-site processing was mainly performed as described in the activity plan. Raw and preliminary processed data were delivered to the SKB representative at the base of operation. Deviations are reported and accepted according to the standard SKB protocol. Processing steps for each method are described in Appendix C.

5.2 Post survey processing

Post survey processing was mainly performed as described in the activity plan. Deviations are reported and accepted in standard SKB manner. Processing steps for each method are described in Appendix C.

6 Results and data delivery

6.1 Digital data

Processed digital data from the survey are delivered on data CD (NGU CD 2002.095-1). In agreement with an SKB representative, data are not presented as described in the method description (SKB MD 211.002). Data are delivered in ten files; EW Radiometric data, NS Radiometric data, EW EM data, NS EM data and NS EW Magnetic and VLF data. Production and Test/calibration lines are separated. Data formats (Geosoft XYZ) are described in Appendix D.

The delivered data have been inserted in the database (SICADA) of SKB. The SICADA reference to the present activity is Field note Forsmark 42.

6.2 Geophysical maps

Based on the final processed data (see Appendix C), coloured contour maps were produced using filtering techniques described in Appendix E. In areas where data quality was so poor as to prevent the calculation of apparent resistivity, data were interpolated and are noted as such on the maps with hatched pattern. Maps from the large area are marked A, while maps from the small area are marked B. The following maps are produced and delivered to SKB (digital versions on NGU CD 2002.095-2, see also Appendix E).

Table 6-1. Produced and delivered maps to SKB.

Map number	Title	Scale
2002.095-01 A and B	Flight Path.	1: 20 000
2002.095-02 A and B	Magnetic Total Field.	1: 20 000
2002.095-03 A and B	Magnetic Vertical Derivative.	1: 20 000
2002.095-04 A and B	EM Resistivity 880 Hz Coplanar.	1: 20 000
2002.095-05 A and B	EM Stacked Profiles 980 Hz Coaxial	1: 20 000
2002.095-06 A and B	EM Resistivity 6606 Hz Coplanar	1: 20 000
2002.095-07 A and B	EM Resistivity 7001 Hz Coaxial	1: 20 000
2002.095-08 A and B	EM Resistivity 34133 Hz Coplanar	1: 20 000
2002.095-09 A and B	Radiometric Total Count	1: 20 000
2002.095-10 A and B	Radiometric Potassium	1: 20 000
2002.095-11 A and B	Radiometric Uranium	1: 20 000
2002.095-12 A and B	Radiometric Thorium	1: 20 000
2002.095-13 A and B	Radiometric RGB Composite Map	1: 20 000
2002.095-14 A and B	VLF-EM Total In-Line	1: 20 000
2002.095-15 A and B	VLF-EM Total Orthogonal	1: 20 000

Due to low signal, no resistivity map for EM 980 Hz Coaxial was produced.

References

- /1/ **SKB, 2001.** Platsundersökningar. Undersökningsmetoder och generellt genomförandeprogram. SKB R-01-10, Svensk Kärnbränslehantering AB.
- /2/ **SKB 2001.** Program för platsundersökning vid Forsmark. SKB R-01-42, Svensk Kärnbränslehantering AB.

Pre survey report

Geophysical measurements from helicopter

Forsmark and Simpevarp

Report, pre survey tests

Person responsible:	Jan S. Rønning, NGU
Responsible magnetometers:	Janusz Koziel, NGU
Responsible electromagnetic:	John Olav Mogaard, NGU
Responsible radiometric:	Mark A. Smethurst, NGU
Responsible altimeter:	NorCopter AS

A.1 Introduction

According to the activity plan for “Geophysical measurements from helicopter, Investigations in the Forsmark area” (AP PS 400-02-25, SKB internal controlling document), pre survey calibration test of the equipment should be performed and reported. This preliminary report describes tests made at NGU in Trondheim during the summer of 2002. Calibration of the radar altimeter was done by Scandinavian Avionics a/s as per an order from NorCopter. Test and calibration of all instruments were performed according to the manuals.

A.2 Test of Magnetometers

The manuals for the magnetometers describe no test and calibration routines. However, the Scintrex MP-3 proton magnetometers (two of them) have been tested using an external frequency source¹. Both magnetometers responded correctly at the external field.

The Scintrex Cs-2 sensor has no test procedure except for running a 4th difference filter. This was done on data from previous surveys, and we found that these data were far out of specifications for the project at Forsmark and Simpevarp. More detailed research documented that the magnetic system does not filter data, and we could document that there is probably an interference between the lowest frequencies at the EM and the magnetometer (see Figure A-1 and Appendix A1). Without disturbances from EM and the magnetic sensor at a fixed location, there is no problem to fulfill the requirement of a 4th difference less than 0,1 nT . To fulfill the requirement in practical work, we need to use a low pass filter before the 4th difference is calculated. This low pass filter would simulate the filtered output from other systems.

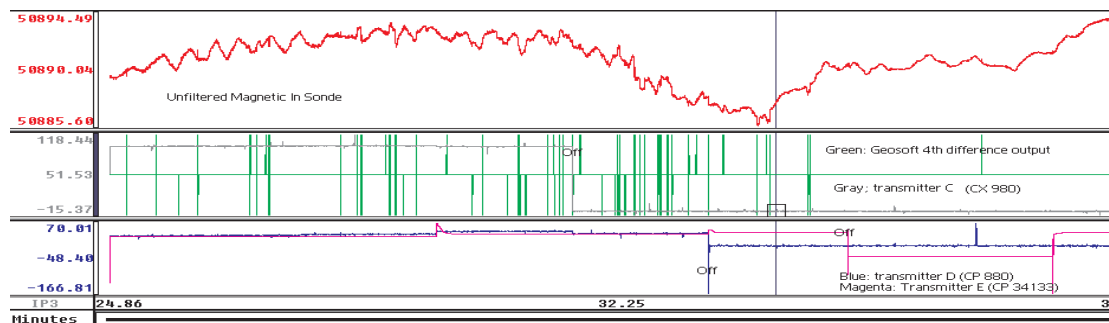


Figure A-1. Magnetic data recorded at NGU showing that a 4th difference less than 0,1 nT is achieved when EM transmitters are turned off.

¹ Ing. S. Paulsen, Trondheim Norway, Tester for proton magnetometer.

A.3 The Hummingbird HEM system

The Hummingbird HEM system was checked in Bymarka outside of Trondheim by J.O. Mogaard and J. Koziel on August 7, 2002. The checks included phasing and calibration checks in accordance with the manufacturers specifications. The five frequencies were initially phased. Once the phasing checks were done, the amplitudes were then set on each of the in-phase and quadrature channels.

In the phasing and the calibration mode, it is impossible to sample the data, but a printout is possible. Figure A-2 shows how the system is out of phase giving response of the quadrature until the phasing was done. After that time, In phase increases a little bit, while quadrature falls back to zero level. Figure A-3 shows phase test on all frequencies at a time. All In phase components response to the ferrite rod, while all quadratures give no response.

Figure A-4 shows how EM Coplanar 6606 Hz responds to external and internal Q-coil tests. With external, the response is equal for In phase and quadrature, and the signal showed up to be 65 ppm as expected. (Note that it is impossible to read out the values on the printout, but this is seen on the operators screen.) Using the internal Q-coils, the response of In phase and quadrature slightly differs, which is caused by a small irregularity in position of this Q-coil.

The system was then turned on and heated for about one hour and the drift was then monitored for about 4100 seconds. High frequency noise on all channels was low (within a few ppm, see Figure A-5 a–e), and consistent with the levels one might expect from spheric activity. Drift was good for all channels except on the highest frequency (coplanar 34133 Hz), where the highest rate was approximately 280 ppm/hour (quadrature). This is attributed to bird warm-up, and the drift rate tends to stabilize on this frequency once thermal equilibrium is reached. The drift on the coplanar 34133 Hz channels, although high, was linear and therefore would be correctable using normal correction methods. Observed rates of drift after the EM system has been warmed up during a night, tend to be substantially lower, and appear to follow a model that can be described as a thermal relaxation with time constants on the order of 0.02 (inverse) minutes.

A minor step in level at some of the measured parameters between 1300 seconds and 2400 seconds are probably caused by a car coming within the influence of the EM system.

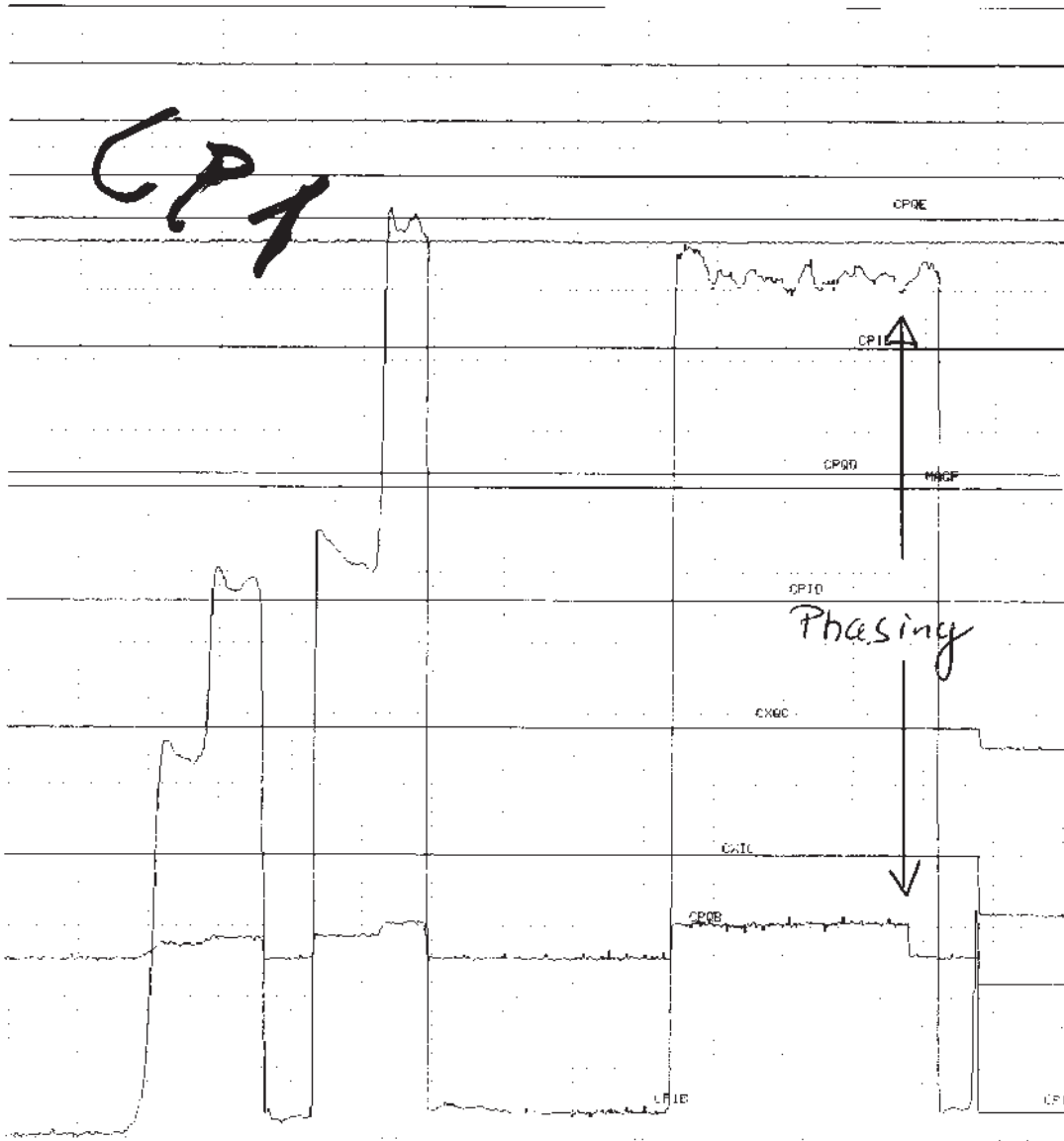


Figure A-2. Example of phase correction on EM Coplanar 6606 Hz.

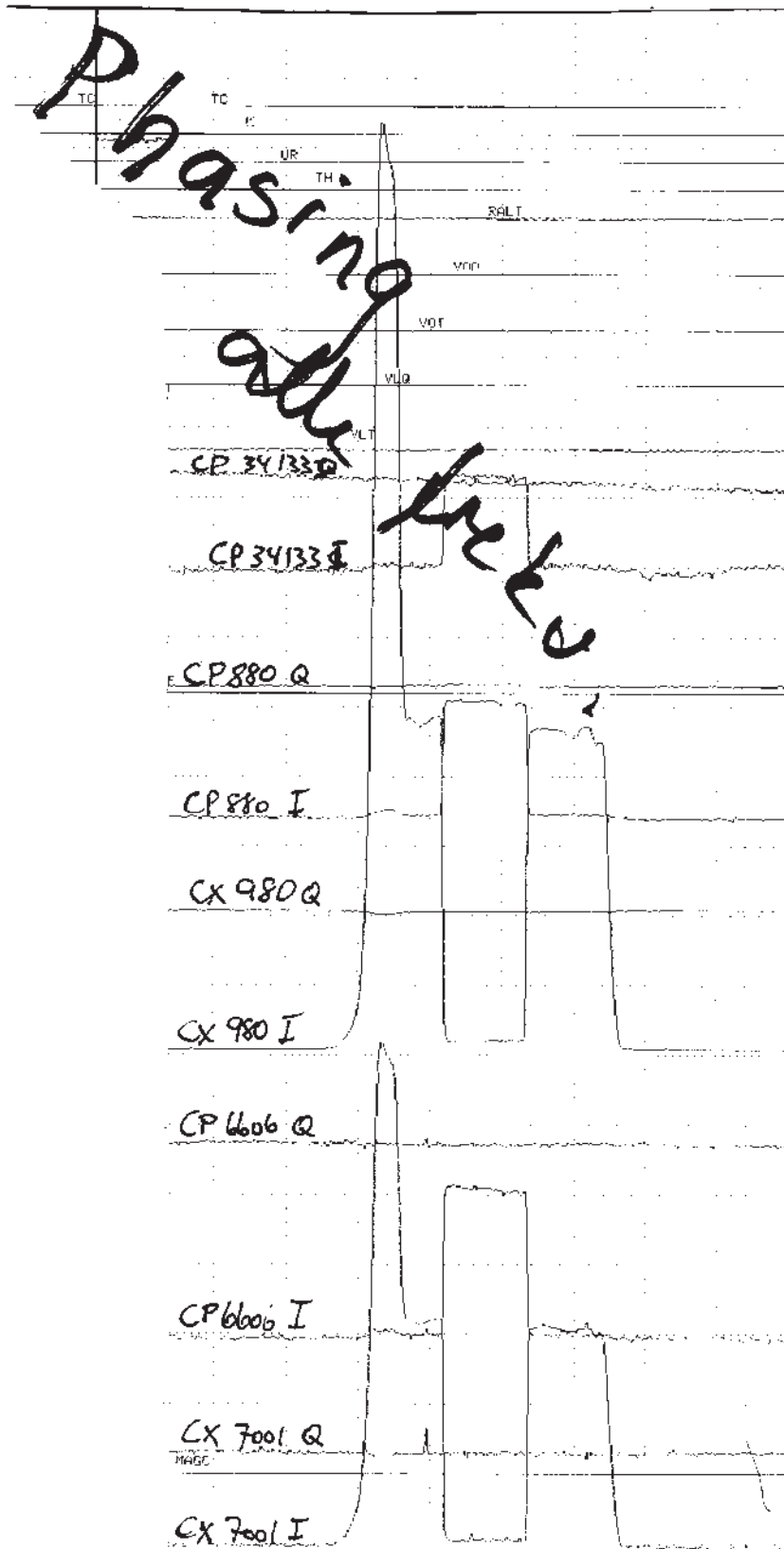


Figure A-3. Phase test of all frequencies. In phase components respond to a ferrite rod, while all quadratures give no response.

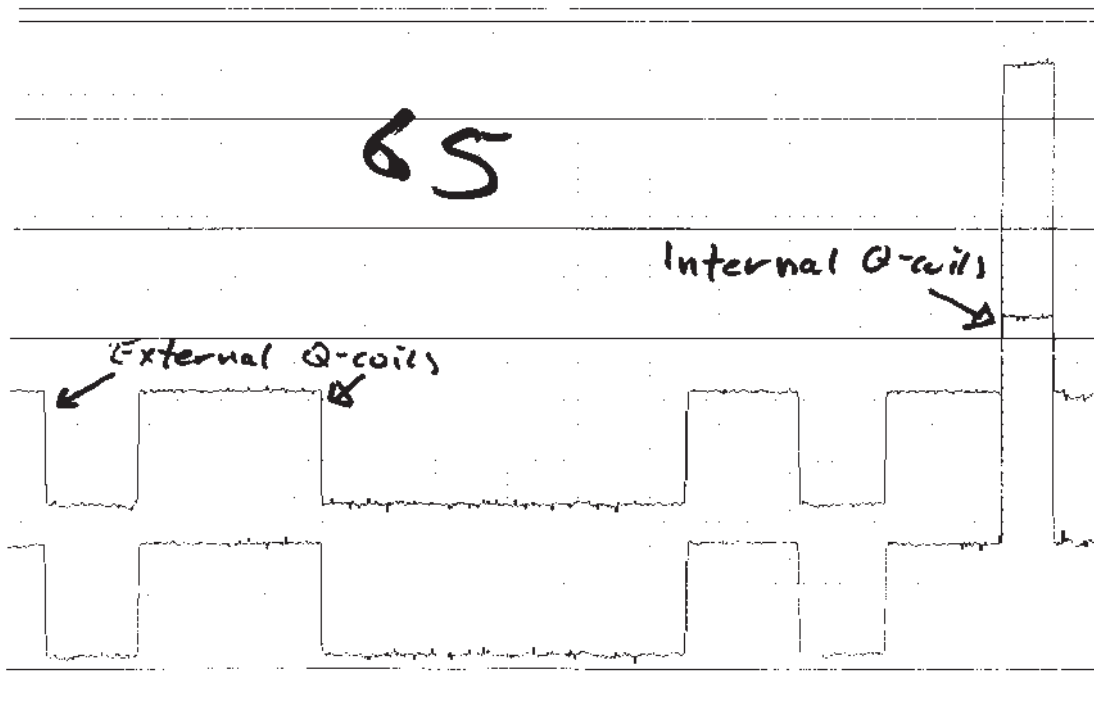


Figure A-4. External and internal Q-coil test for EM Coplanar 6606 Hz.

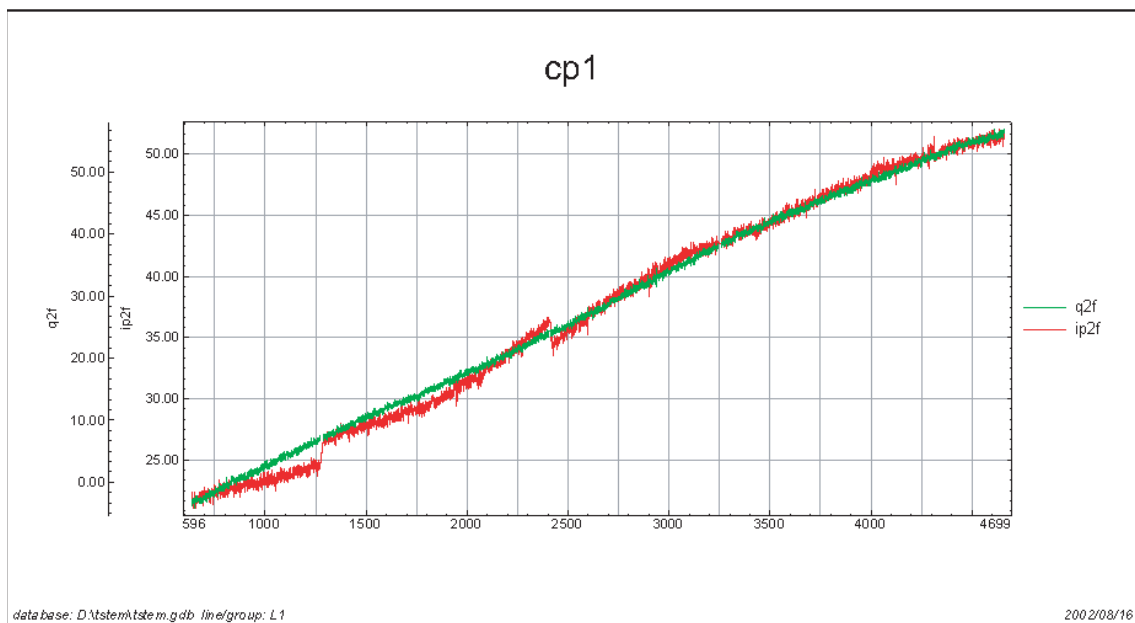


Figure A-5a. Drift registration for CP 6606 Hz (CP1) (time in seconds).

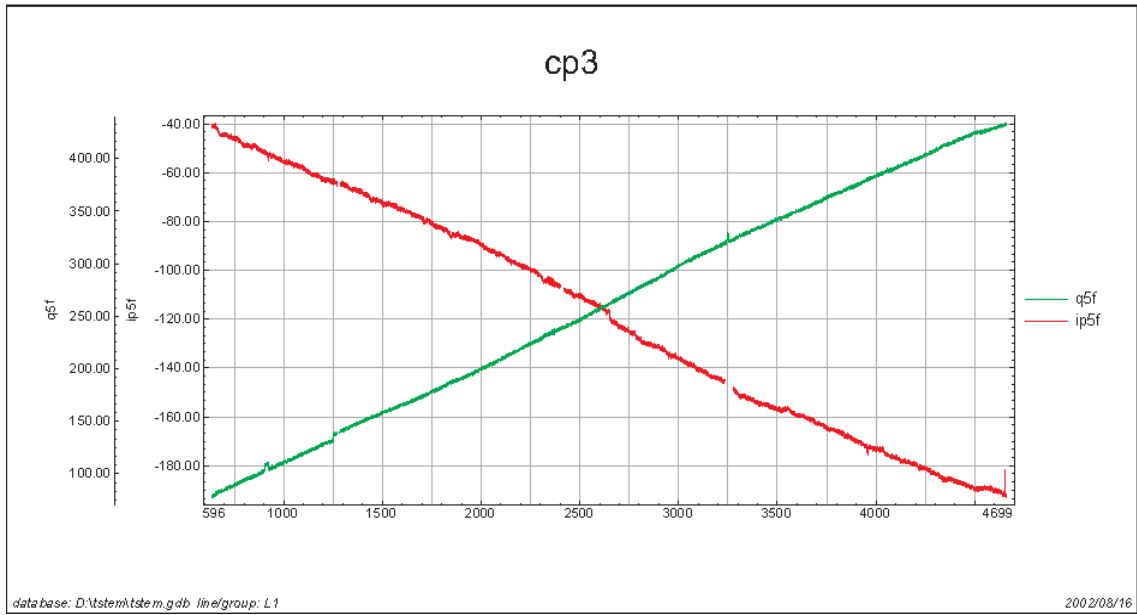
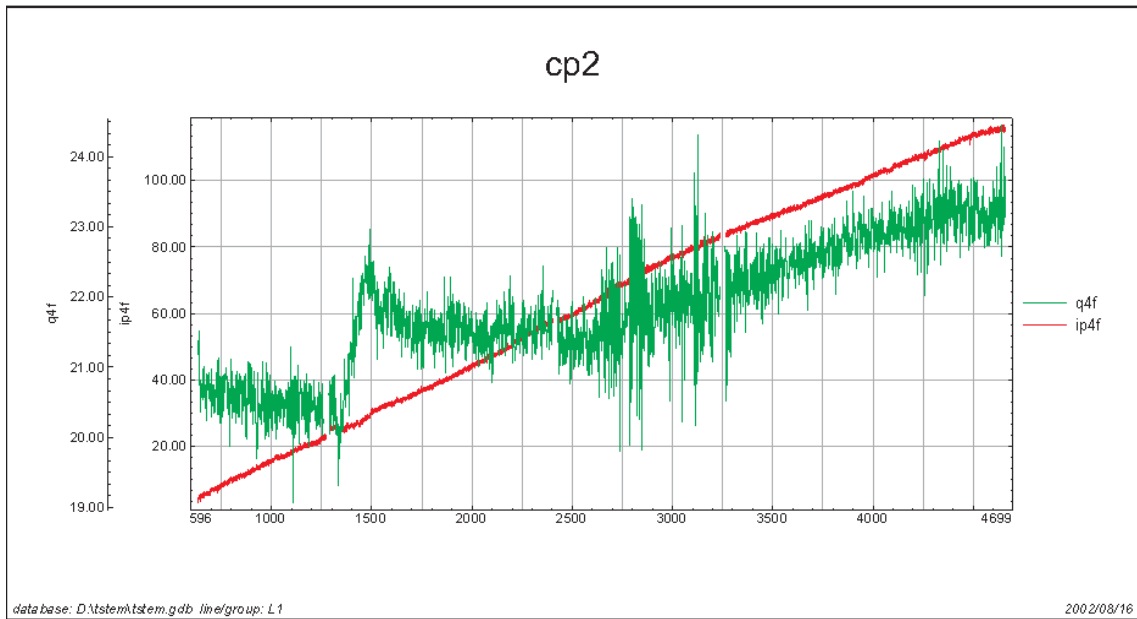


Figure A-5b and c. Drift registration for CP 880 Hz (CP2) and CP 34133 Hz (CP3) (time in seconds).

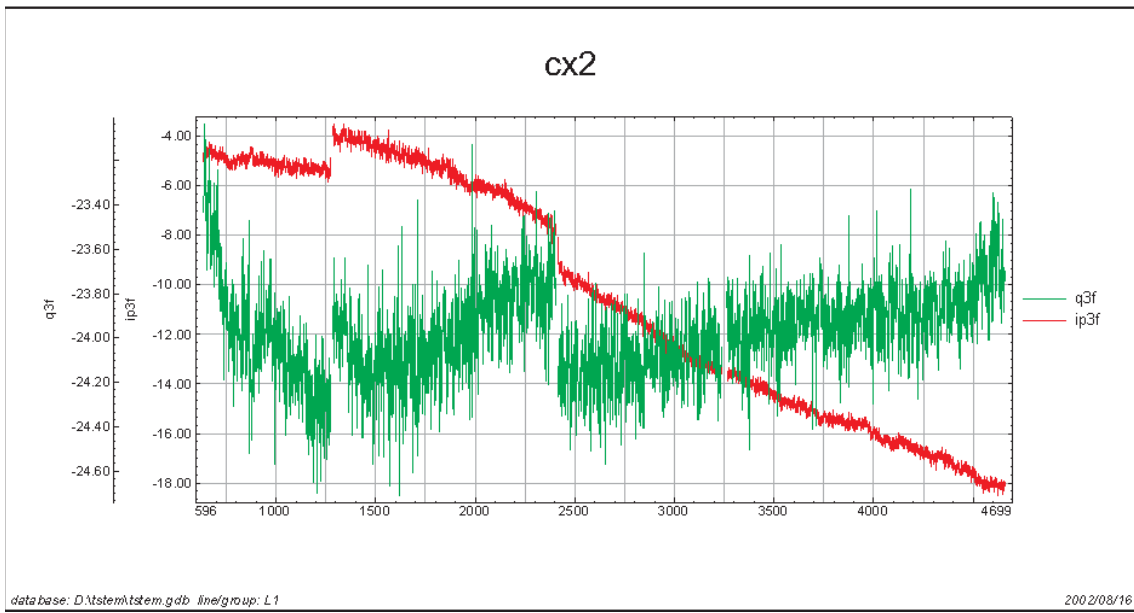
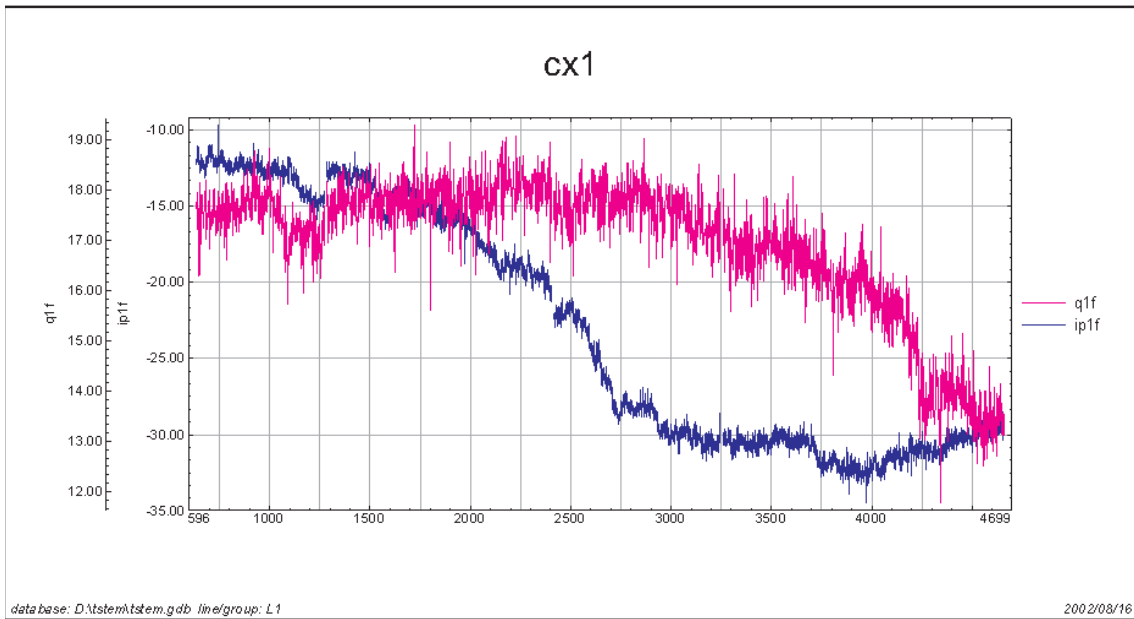


Figure A-5d and e. Drift registration for CX 7001 Hz (CX1) and CX 980 Hz (CX2) (time in seconds).

A.4 Calibration of the GR820 Gamma Ray Spectrometer (M.A. Smethurst)

Calibration of the gamma ray spectrometer at NGU was done using four portable concrete pads to determine the stripping coefficients and sensitivity conversion from counts to apparent element concentrations. The procedure for determining these coefficients is described below.

A.4.1 Description of calibration pads:

The NGU utilizes four concrete calibration pads measuring 1 m x 1 m x 30 cm each. The pads consist of a background pad, and pads containing known quantities of K-40, U-238 and Th-232. The pads produce approximately 85% of the count rate obtained from infinite sources and geometric corrections can be applied to the measurement data to simulate infinite sources. Detailed descriptions of the pads and their mode of use are offered by the manufacturer W. Grasty in the document "Transportable Calibration Pads for Portable Gamma-ray Spectrometers" (available upon request from the NGU).

Measurements are made on the pads in an area of ground that is flat and relatively homogeneous in its radioactivity. Our current practice is to use one of the parking lots at the NGU, emptied of cars. A mark is made on the ground where measurements are to take place. All pads are placed at least 30 metres away from this mark. First the background pad is placed on the mark and the gamma ray detector placed centrally and orthogonal on it. A measurement of the pad is made over approximately 10 minutes, sometimes more. The background pad is then removed and the K-40 pad placed on the mark. The detector is placed on the K-40 pad and a 10-minute measurement is made. The background pad is then re-introduced and measured, followed by the U-238 pad, the background pad again, and finally the Th-232 pad.

All measurements are stored digitally in full-spectrum and window count rate forms. Window count rates for the K, U and Th pads are background corrected using measurements on the background pad made immediately before. Geometric corrections to simulate infinite sources are then applied and stripping factors determined. Source sensitivities for K, U and Th are calculated given the known concentrations of radioisotopes in the calibration pads. Also FWHM (full width half maximum) values for the K (1.46 MeV), U (Bi-214 1.76 MeV) and Th (Tl-208 2.63 MeV) photo-peaks, are determined from background corrected full spectrum data.

This document summarises the measurement data and derived calibration values for the calibration experiment carried out 07.05.2002 using the NGU's GR820 gamma ray spectrometer and detector with steel mounting for attachment to the underside of a helicopter.

A.4.2 Spectrometer coefficients

Altitude attenuation coefficients for K, U and Th Channels, cosmic stripping and aircraft background coefficients will be computed from measurements made on site following procedures outlined by the IAEA. Airborne radon stripping coefficients a_u , a_k and a_t will be computed from data acquired during the surveys from those line segments over water, as variations in atmospheric radon concentration are necessary to properly derive these data, and such variations can only be expected to occur over a period of several days.

Calibration work carried out:

Date: 07.05.02
By: M.A. Smethurst & J.O. Mogaard
Instrument: GR820
Pad placement: NGU parking lot near delivery bay – pad position marked
Instrument placement: Central and orthogonal on top of pad, contacts facing south
Measurement chronology:

1) Background pad 11:25	1525 seconds
2) Background pad 11:40	773 seconds
3) U-238 pad	756 seconds
4) Background pad 12:20	715 seconds
5) K-40 pad	743 seconds
6) Background pad 12:55	527 seconds
7) Th-232 pad	637 seconds

Properties of the NGU calibration pads:

Pad	Concentration	Unit	Pad density g/cm ³	Geometric factor to infinite source
K-40	6.64	%	2.13	1.16
U-238	52.35	ppm	2.2	1.17
Th-232	107.72	ppm	2.3	1.19

Background corrected window values on the pads (counts per second)

Pad	K-40 window	U-238 window	Th-232 window	Cs-137 window
K-40	775.67	0.00	0.00	192.38
U-238	393.66	515.35	36.39	1059.28
Th-232	263.82	156.24	513.57	735.89

Stripping factors

Alpha	0.3042
Beta	0.5137
Gamma	0.7639
a	0.0706
b	0.0000
g	0.0000
K into Cs-137	0.2480
U into Cs-137	2.0555
Th into Cs-137	1.4329

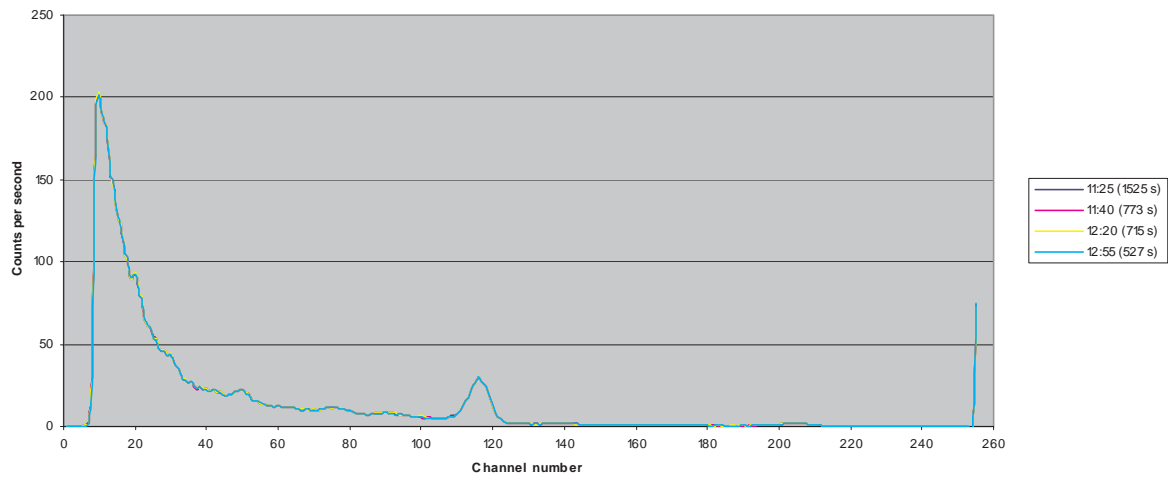
Conversions to concentrations

Sensitivities	Factor	Unit
K-40	0.00738	percent/cps
U-238	0.08682	Ppm/cps
Th-232	0.17626	Ppm/cps

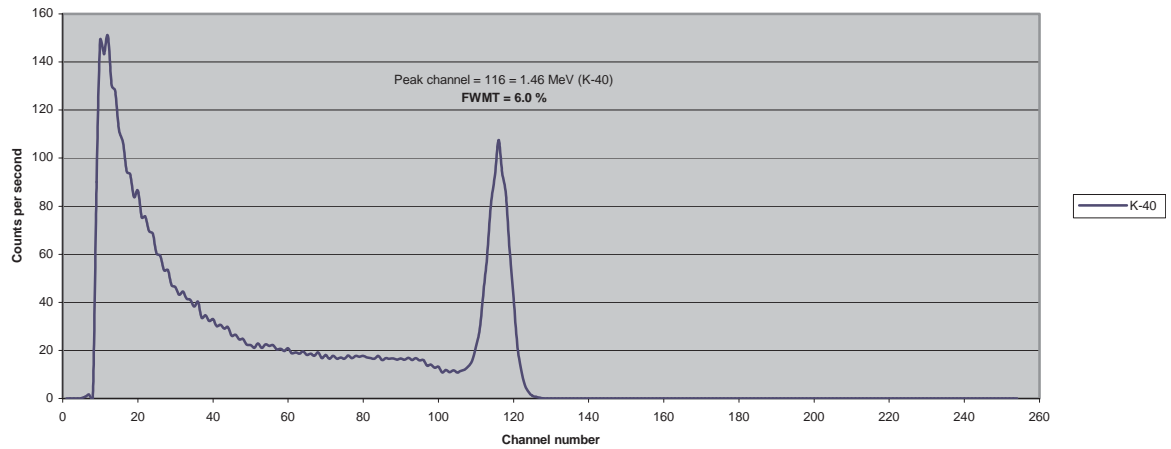
FWHM Full width at half maximum (%)

K-40 1.46 MeV	6.0
U-238 1.76 MeV	4.9
Th-232 2.63 MeV	4.6

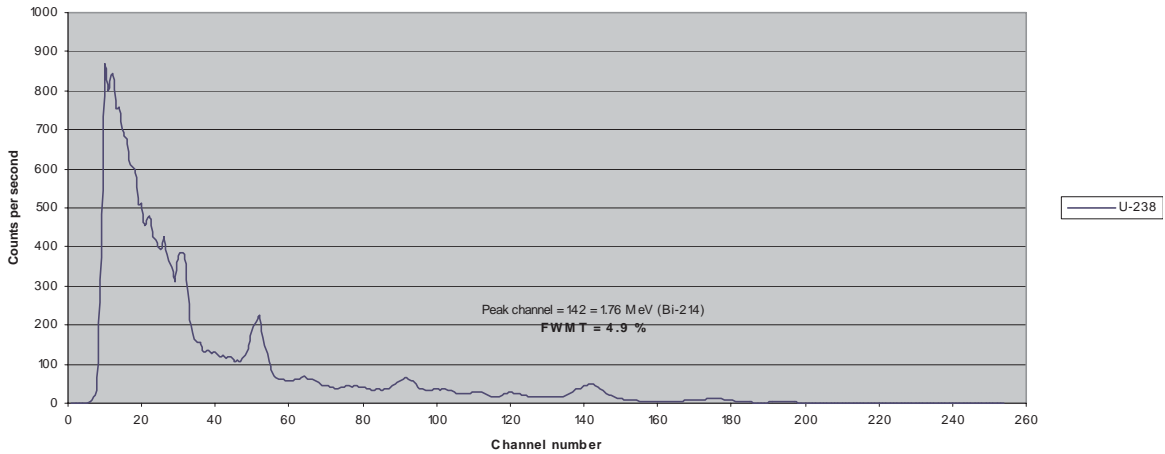
Background at 11:25, 11:40, 12:20 and 12:55 (07.05.2002)



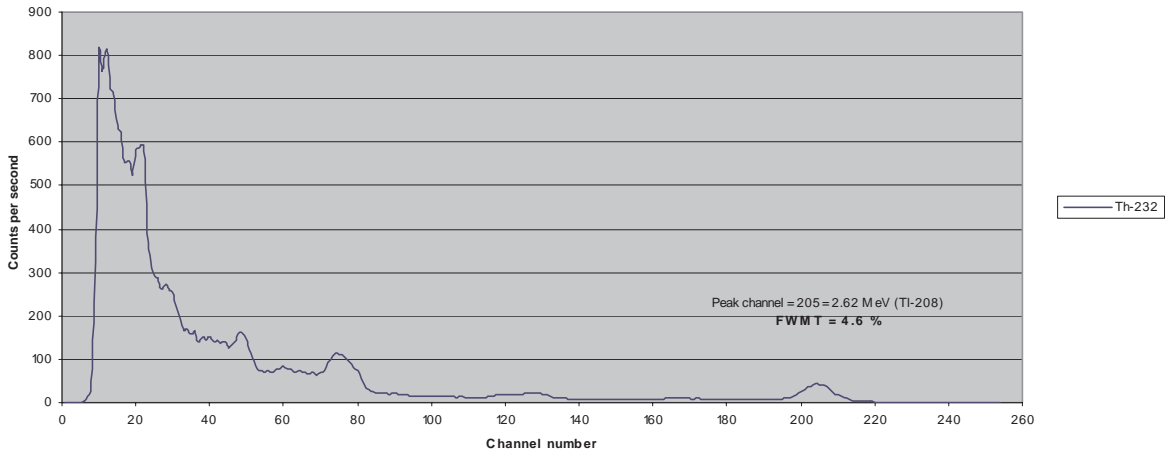
K-40 (743 s) measured after and corrected for background 12:20 (715 s)
07.05.2002



U-238 (756 s) measured after and corrected for background 09:36 (773 s)
07.05.2002



Th-232 (637 s) measured after and corrected for background 12:55 (527 s)
07.05.2002



A.5 Calibration of altimeter, Bendix / King KRA 405B

The altimeter (Bendix / King KRA 405B) was calibrated by Scandinavian Avionics as. Results from tests are shown in Appendix A2. The report confirms that output voltage on AUX_OUT_2 (the output signal which is used by NGUs logging system) is 0,4 V/100 feet as described in manual.

Mail from Peter Walker (NGU) to Søren Bystrøm (SGU)

Testing of the effect of the EM transmitters on the magnetometer

Dear Søren,

This afternoon we set out the EM sonde at NGU and let the EM system warm up for about an hour. Then we turned off the EM transmitters one by one until no transmitter was on. We then briefly turned on the high frequency EM transmitter.

We recorded the magnetic field from the sensor in the EM sonde and computed the 4th difference. We note a gradual increase in 4th difference noise, followed by a general decrease when the lower frequency EM channel are turned off.

The lower frequency transmitters would be expected to have the highest NIA, and therefore cause the largest magnetic field of all the transmitters on board.

The transmitters were turned off at 2 minute intervals.

The manual for the magnetic sensor states that an AC field in the presence of the magnetometer, and orthogonal to the static field, will cause an anomalous reading. I have so far been unable to find a specification for the NIA of the transmitters and so have not been able to calculate the AC field strengths involved.

The data are attached. My number at NGU is 47 73 90 4405.

Please feel free to contact me if you have any comments or suggestions.

Regards,

Peter Walker

Calibration report for Bendix/King KRA 405 B Radar altimeter

16.AUG.2002.1: 9:14'AX +45 NORCOPTER AS'AN-AVIONICS NO.505 P.1/4001/004
 +45 79508099



TELEFAX MESSAGE

SCANDINAVIAN AVIONICS A/S

Billund Airport
 P.O.Box 59, Lufthavnevej 45
 DK-7190 Billund
 Denmark

Phone: +45 7950 8000
 Fax: +45 7950 8099
 E-Mail: sa@scanav.com
 CVR-no.: 83 82 04 11

If this telefax transmission is incomplete, please notify by one of above contact methods

TO:	Norcopter	FROM:	Torben Hym
ATTN:	Karl Arvid Andersen/Tor Stenberg	OUR REF:	2012596
YOUR REF:	026	DATE:	2002.08.15
SUBJECT:	Calibration of Radar Altimeter	PAGES:	1 of 4

I hereby send a copy of the calibration report for the Radar Altimeter KRA405B S/N 2285

Torben Hym
 th@scanav.com

KOPI: JAN S. PUNNING

UVH
 G. Sten

AlliedSignal
 BENDIX/KING COMPONENT MAINTENANCE MANUAL
 KRA 405B RADAR ALTIMETER

CALIBRATION REPORT

RADAR ALTIMETER:

P/N: 066-01152-0101

S/N: 2285 WITH INDICATOR S/N 3610
 KM 416.

Altitude (ft)	Altitude Test Input(v)	Ana_Alt_1/Aux_Out_1	Aux_Out_2 (-0101)	Aux_Out_2 (-0202)	Pre_Equ_Out
0	0.000	0.400	0.000	0.400	0.000
10	0.100	0.600	-0.040	0.600	-0.100
20	0.200	0.800	-0.080	0.800	-0.200
30	0.300	1.000	-0.120	1.000	-0.300
40	0.400	1.200	-0.160	1.200	-0.400
50	0.500	1.400	-0.200	1.400	-0.500
60	0.600	1.600	-0.240	1.600	-0.600
70	0.700	1.800	-0.280	1.800	-0.700
80	0.800	2.000	-0.320	2.000	-0.800
90	0.900	2.200	-0.360	2.200	-0.900
100	1.000	2.400	-0.400	2.400	-1.000
110	1.100	2.600	-0.440	2.600	-1.100
120	1.200	2.800	-0.480	2.800	-1.200
130	1.300	3.000	-0.520	3.000	-1.300
140	1.400	3.200	-0.560	3.200	-1.400
150	1.500	3.400	-0.600	3.400	-1.500
160	1.600	3.600	-0.640	3.600	-1.600
170	1.700	3.800	-0.680	3.800	-1.700
180	1.800	4.000	-0.720	4.000	-1.800
190	1.900	4.200	-0.760	4.200	-1.900
200	2.000	4.400	-0.800	4.400	-2.000
210	2.100	4.600	-0.840	4.600	-2.100
220	2.200	4.800	-0.880	4.800	-2.200

+45 79508099

AlliedSignal
BENDIX/KING COMPONENT MAINTENANCE MANUAL
KRA 405B RADAR ALTIMETER

Altitude (ft)	Altitude Test Input (v)	Ana Alt 1/ Aux Out 1	Aux Out 2 (-0101)	Aux Out 2 (-0202)	Pre Equ Out
240	2.400	5.200	-0.960	5.200	-2.400
250	2.500	5.400	-1.000	5.400	-2.500
260	2.600	5.600	-1.040	5.600	-2.600
270	2.700	5.800	-1.080	5.800	-2.700
280	2.800	6.000	-1.120	6.000	-2.800
290	2.900	6.200	-1.160	6.200	-2.900
300	3.000	6.400	-1.200	6.400	-3.000
310	3.100	6.600	-1.240	6.600	-3.100
320	3.200	6.800	-1.280	6.800	-3.200
330	3.300	7.000	-1.320	7.000	-3.300
340	3.400	7.200	-1.360	7.200	-3.400
350	3.500	7.400	-1.400	7.400	-3.500
360	3.600	7.600	-1.440	7.600	-3.600
370	3.700	7.800	-1.480	7.800	-3.700
380	3.800	8.000	-1.520	8.000	-3.800
390	3.900	8.200	-1.560	8.200	-3.900
400	4.000	8.400	-1.600	8.400	-4.000
410	4.100	8.600	-1.640	8.600	-4.100
420	4.200	8.800	-1.680	8.800	-4.200
430	4.300	9.000	-1.720	9.000	-4.300
440	4.400	9.200	-1.760	9.200	-4.400
450	4.500	9.400	-1.800	9.400	-4.500
460	4.600	9.600	-1.840	9.600	-4.600
470	4.700	9.800	-1.880	9.800	-4.700
480	4.800	10.000	-1.920	10.000	-4.800
490	4.900	10.200	-1.960	10.198	-4.900
500	5.000	10.400	-2.000	10.392	-5.000
600	6.000	10.700	-2.400	12.151	-6.000
700	7.000	11.000	-2.800	13.646	-7.000
800	8.000	11.300	-3.200	14.947	-8.000
900	9.000	11.600	-3.600	16.000	-9.000

+45 79600099

AlliedSignal
BENDIX/KING COMPONENT MAINTENANCE MANUAL
KRA 405B RADAR ALTIMETER

Altitude (ft)	Altitude Test Input(v)	Ana Alt 1/ Aux_Out_1	Aux Out 2 (-0101)	Aux Out 2 (-0202)	Pre_Equ_Out
1000	10.000	11.900	-4.000	17.129	-10.000
1100	11.000	12.200	-4.400	18.065	-11.000
1200	12.000	12.500	-4.800	18.920	-12.000
1300	13.000	12.800	-5.200	19.770	-13.000
1400	14.000	13.100	-5.600	20.630	-14.000
1500	15.000	13.400	-6.000	21.410	-15.000
1600	16.000	13.700	-6.400	21.790	-16.000
1700	17.000	14.000	-6.800	22.355	-17.000
1800	18.000	14.300	-7.200	22.920	-18.000
1900	19.000	14.600	-7.600	23.450	-19.000
2000	20.000	14.900	-8.000	23.962	-20.000
2100	21.000	15.200	-8.400	24.446	-21.000
2200	22.000	15.500	-8.800	24.907	-22.000
2300	23.000	15.800	-9.200	25.347	-23.000
2400	24.000	16.100	-9.600	25.769	-24.000
2500	25.000	16.400	-10.000	26.174	-25.000

Altitude vs. Precision Output Voltages
 Table 101, Sheet 3

Forsmark Quality Control Tests

B.1 Introduction

This document reports the various methodologies used to calibrate and measure the various instrument parameters required to accurately process integrated helicopter survey data.

Results of the various tests at Forsmark are reported herein, together with results from Simpevarp, where applicable.

The quoted Simpevarp tests were conducted subsequent to demobilization from Forsmark, and are equally applicable to the Forsmark data since the system used was identical.¹ For the radiometric data, the time constraints imposed during the Forsmark survey meant that all the calibration parameters were not determined during the Forsmark tests, and the calibration data acquired at Simpevarp were therefore used. Other test data acquired at the beginning of the Forsmark survey may have limited applicability because at that time, the pilots were fairly new to helicopter geophysical surveys, and so had difficulty maintaining standard elevation, line tolerances and speeds. Such inexperience would affect the applicability of the lag tests, where precise location and speed are of paramount importance in acquiring accurate lag information.

We would like to acknowledge the help of Sören Byström, Peter Hagthorpe, and Hossein Shomali of SGU, Hans Thunehed and Hans Lindberg of GeoVista, Rune Johansson and the staff at SKB for their untiring support of our work in acquiring accurate calibration parameters.

B.2 Magnetometer

B.2.1 *Mag Cloverleaf*

The magnetic cloverleaf test is carried out to determine the heading correction that should be applied to the magnetic field data acquired by an aircraft. The procedure is to acquire magnetic data along intersecting, orthogonal profiles, each of which are repeated in opposite directions. Two magnetic cloverleaf tests were done at Simpevarp (both over the magnetic low at 1545000 E and 6367000 N (RT90)) and one at Forsmark over a magnetic low near Storskäret. These anomalies were chosen because they were large enough to be laterally uniform within the positioning tolerances of the aircraft, thus minimizing the possibility of a heading error being derived as a result of a positioning error.

¹ The only conceivable difference being due to some problem that could have occurred when the EM and VLF sondes were detached from the helicopter, in Forsmark, transported by ground to Simpevarp where they were re-attached. In the interim, the helicopter had a 100 hour service done in Karlskoga.

Ideally, magnetic heading errors should be determined over sedimentary basins, where the magnetic gradients are low. Unfortunately, both Forsmark and Simpevarp are located in magnetically active areas, and cloverleaf tests are affected by the presence of these gradients.

Heading errors were measured in Forsmark by flying at 300 metres over a magnetically quiet area near Storskäret in the four cardinal directions. The results over this test are using the base levelled data from Test Flight, acquired on Aug 25. A base magnetometer fluctuation occurred on the 5002 crossing causes the discrepancy that is seen on that line. A point taken further down the line (5002a in the Table B-1) is felt to be satisfactory since the gradients in the N-S direction over the crossing point were low. A heading error of 0.5 gamma is noted in the EW/WE directions and .75 gamma in the NS/SN directions. Errors of this size can easily be caused by the slight variations in position/altitude due to the presence of small magnetic gradients. As the manufacturer quotes a heading error of 0.1 nT for the CS-3 magnetometer being used on the survey, no compelling evidence was found to apply a heading correction to the data.

The first Simpevarp cloverleaf test was done at the beginning of the survey during flight 1 at 2000 feet altitude. The 2000-foot altitude was chosen in an attempt to minimize errors in the cloverleaf test due to positioning and altitude variations along the 4 profiles.

Unfortunately, these flight 1 results are compromised because of noise on the base magnetometer, subsequently determined to be due to the area lighting at Oskarshamns airport. Additionally, the radar altimeter response was clipped at 5 volts, or 1250 feet, making it impossible to confirm that the altitudes during each of the segments of the cloverleaf were sufficiently precise.

Accordingly, the cloverleaf was re-flown at the end of the survey during flight 20 using a 1200 feet altitude so as to have radar altimeter data available. The results are presented below (Table B-3), using a filter on the base mag of 18 seconds/unfiltered base mag.

Little difference occurs as a result of filtering the base magnetometer. Results comparing the two Simpevarp cloverleaf test data sets indicate a difference of 100 gammas vertically over 800 feet, or +1/8 gamma per foot or +0.4 gamma/metre. Thus 1.6 gammas should be added to the results for line 5005 in comparison to 5006, and to line 5008 in comparison to line 5007. Accordingly, the data corrected for altitude are as shown in Table B-4.

While there is apparently a 5 gamma heading difference in the magnetic heading from west to east compared with east to west, the heading difference between north to south and south to north is 1.5 gamma. This difference could easily be accounted for by radar altimeter differences, as it amounts to an elevation difference of 3 metres. Given the results of the Forsmark tests, heading corrections were not deemed to be worthwhile.

Table B-1. Forsmark magnetic heading result

Line	UTM X – WGS84	UTM Y – WGS84	Magnetic Reading (nT)
5000 N->S	348012	6695898	52187.06
5001 E->W	349029	6695894	52187.65
5002 S->N	348043	6695893	52179.17
5003 W->E	348051	6696882	52188.61
5002a (S->N)	348041	6695949	52188.50

Table B-2. Simpevarp flight 1 Cloverleaf

Line	Magnetic data (nT)	E RT90	N RT90	Radar altitude (m)
5001 S-N	50481.90	1545016	6366980	380.76 clipped
5002 N-S	50482.54	1545017	6366966	380.94 clipped
5003 W-E	50486.27	1544950	6367004	380.76 clipped
5004 E-W	50478.92	1544900	6367005	380.76 clipped

Table B-3. Simpevarp 20 Cloverleaf.

Line	Magnetic Data (nT)	E RT90	N RT90	Radar altitude (m)
5005 S-N	50377.35 / 50377.68	1545005	6366953	370.76
5006 N-S	50380.53 / 50380.47	1545000	6366954	374.97
5007 E-W	50381.52 / 50381.89	1544973	6367001	364.94
5008 W-E	50375.08 / 50374.39	1544960	6367006	360.56

Table B-4. Simpevarp 20 Cloverleaf corrected for altitude

Line	Magnetic Data (nT)	E RT90	N RT90	Radar altitude (m)
5005 S-N	50379.0	1545005	6366953	370.76 Corrected
5006 N-S	50380.5	1545000	6366954	374.97
5007 E-W	50381.5	1544973	6367001	364.94
5008 W-E	50376.5	1544960	6367006	360.56 Corrected

B.2.2 Magnetic Lag

The magnetic lag test is done to determine the time delay of the magnetic data logged on the data system in comparison to the corresponding navigational data. These differences can be due to the time differences required to acquire the data, or can be caused by the difference in locations of the various sensors. In a helicopter system using the configuration adopted by the NGU, with the GPS sensor on the tail of the helicopter, and the magnetic sensor in the EM sonde, the lag will be a function of flying speed, where higher speeds cause increased lag since air drag causes the sonde to “ride” farther behind the helicopter.

The lag was measured prior to the survey at Forsmark by following the straight section of the road to Storskäret just off the main road between Forsmark and Osthrammar. This path was chosen because it was orthogonal to the strike of a fairly narrow magnetic feature that crossed the road, and because at the outset of the survey, the pilot was unfamiliar with the navigation system and a road was considered to be an easier path to follow. From the analysis of the data (see Figure B-1), the lag was determined to be 2 fiducials (0.2 sec or about 6 metres).

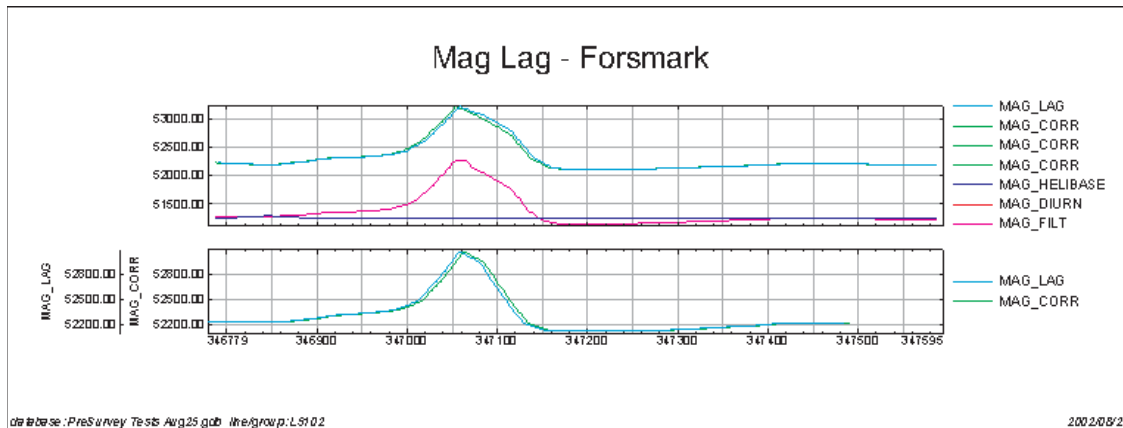


Figure B-1. Forsmark magnetic lag results.

These results were considered to be suspect for several reasons; one being that the helicopter was flown slowly so as to follow the road exactly, with the slow velocity causing the bird to drop below the helicopter, thus reducing the apparent lag². Accordingly, it was resolved to re-fly the magnetic lag data, but the opportunity to do this never presented itself until the system was taken to Simpevarp.

The initial magnetic lag test line at Simpevarp was selected from a gridded magnetic data set supplied by the SGU. Magnetic lag was tested over a large magnetic gradient by taking the second derivative (Geosoft 1st derivative is offset, and not useful for lag). Data were recorded on lines 5100 and 5101. From this, the lag was determined to be 0.2 seconds. However, this lag test was not very satisfactory, as it was difficult to precisely align the anomalies to accurately measure the time difference over the same feature.

One of the difficulties with a lag test is that a sharp anomaly is required, and gridded data sets are not always suitable for this. It was noted in the course of processing the data that a stone pile (the result of Äspö tunnel excavation) north of Simpevarp nuclear plant provided such an anomaly. The lag was measured on Flight 19 and was determined to be 0.45 seconds. The results are presented below (Figure B-2), and can be viewed in lines 5100 and 5101 in the Simpevarp Flight 19 data.

B.2.3 Base station/bird magnetometer comparison

The base station (proton) and bird magnetometer (cesium) were compared in Forsmark during the spectrometer calibration lines. The base station exhibited some spikes and some excursions of 4–6 seconds in duration. This may be related to the EM noise seen on this flight.

It should be noted that the various proton magnetometers used in the project exhibit a similar behaviour. As such, this behaviour is attributed to the noisy electrical environment in which the magnetometers were located; the base magnetometers, being proton precession magnetometers, were more sensitive to noise than the cesium magnetometer that was located in the EM sonde.

² Sören Byström also pointed out that the lag measurements were affected by the “17 second jump effect” that resulted from the CPU timing problem in the data acquisition system (see Appendix C, this report), since the data in the figure predate the correction software developed to account for this effect.

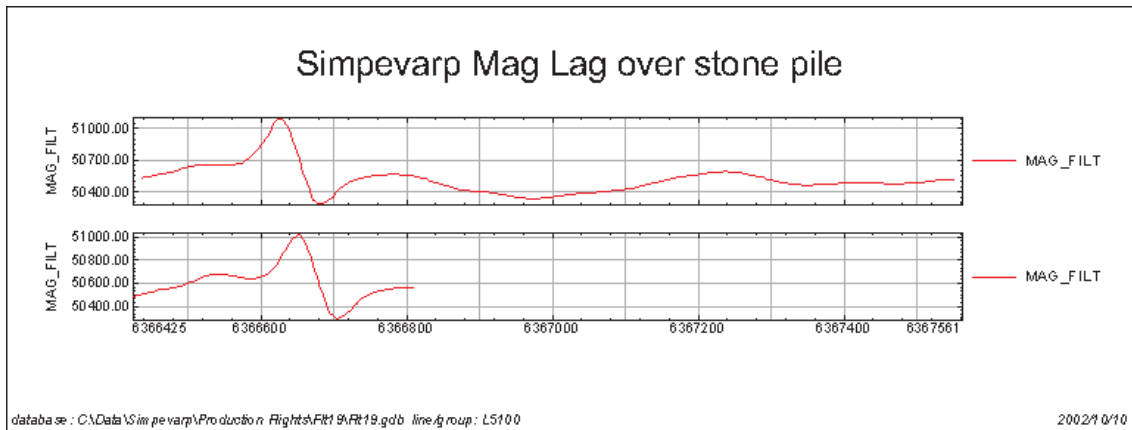


Figure B-2. Control of magnetic lag over a stone pile.

To make the comparison, the base magnetometer data were loaded into the database and subtracted from the bird magnetometer to yield a MAG_BASE_DIFF channel. The base magnetometer was located some 50 metres from the bird, resulting in a difference of approximately 50 gamma in level. Sections of lines 3000, 3001, 3002 and 3003 were selected and Geosoft statistics computed for them (see Table B-5). The selected areas of the line were without the excursions.

4th Difference after 5-point filtering and spike removal:

Processing using the Geosoft QC software of test flight 3 was shown to Peter Hagthorpe and was deemed to be acceptable at Forsmark.

B.2.4 Base Station High Pass RMS Error

At the outset of the Forsmark survey, Peter Hagthorpe outlined the following procedure for processing and accepting base magnetometer data. According to this procedure, the base magnetometer was high pass filtered with a cutoff of 3 seconds (30 fids), with the result deemed to be acceptable if under 0.3 nT. Sample results, for sections of the data unaffected by 4–6 second excursions and spikes, are summarized in Table B-6. These deviations were deemed to be acceptable.

Table B-5. Base magnetometer – bird magnetometer comparison (nT).

Line	Min Difference	Max Difference	Av. Difference	Deviation
3001	-53.7	-52.0	-52.6	.30
3001	-53.4	-51.4	-52.5	.53
3000	-55.1	-51.7	-52.7	.54
3000	-53.7	-51.7	-52.6	.44
3003	-53.2	-51.8	-52.6	.35
3002	-53.6	-52.1	-52.7	.35

Table B-6. Base magnetometer high pass filter results (gammas).

Line	Minimum	Maximum	Average	Deviation
3001	-2.2	1.2	0.0	0.24
3001	-0.2	0.2	0.0	0.06
3000	-0.1	0.3	0.0	0.07
3000	-0.1	0.1	0.0	0.04
3003	-0.1	0.1	0.0	0.03
3002	-0.2	0.1	0.0	0.04

B.3 EM System

B.3.1 EM Lag

EM Lag occurs for the same reason as the magnetic lag. At Forsmark the EM lag data were acquired on Test Flight 3, and were loaded into lines 4100 and 4101. The lag was determined to be 0.7 seconds (1.4 seconds between peaks plotted on lines traversing in opposite directions). Since this was the first flight the pilot flew with the bird, the results are probably not representative, and these data were not used in determining the EM lag³.

As a result of production pressures, no further lag tests were undertaken at Forsmark and the lag data from Simpevarp were therefore used.

The Simpevarp EM lag test was completed on test line data from Oct 3, Flight 16, lines 4201, 4202, 4203. The results indicated a lag of 0.5 second.

B.3.2 EM Calibration

The following tests were carried out on Aug 23 at the Forsmark base. Various calibration checks were undertaken during the course of the survey, but only the initial ones are presented here.

Drift: Drift was measured over a period of approximately 3 hours and recorded in line 4009 in database “EM Ground Test Aug 23”. Drift was monotonic and fairly well behaved, with numerical data furnished in Table B-7 and the actual drift plotted in Figure B-5.

Instantaneous Noise: Drift profiles were inspected for instantaneous noise. Noise was approximately 1 ppm in all channels.

Calibration: Calibration of the coils is recorded prior to the Forsmark survey on August 23 in lines 4002 (A), 4003 (B), 4004 (C), 4005 (D) and 4006 (E). Calibration is automatically controlled by the system and was done in accordance with the manufacturers specifications.

EM calibration was also checked at the beginning of the Simpevarp survey and was found to be consistent with the Forsmark calibration. EM calibration is really controlled by the manufacturer, and must be set using the on-board software functions supplied with the system.

³ The Forsmark EM lag data are uncorrected for the navigation problem that resulted from the slow CPU time clock (see discussion of the magnetic lag data at Forsmark, and Appendix C).

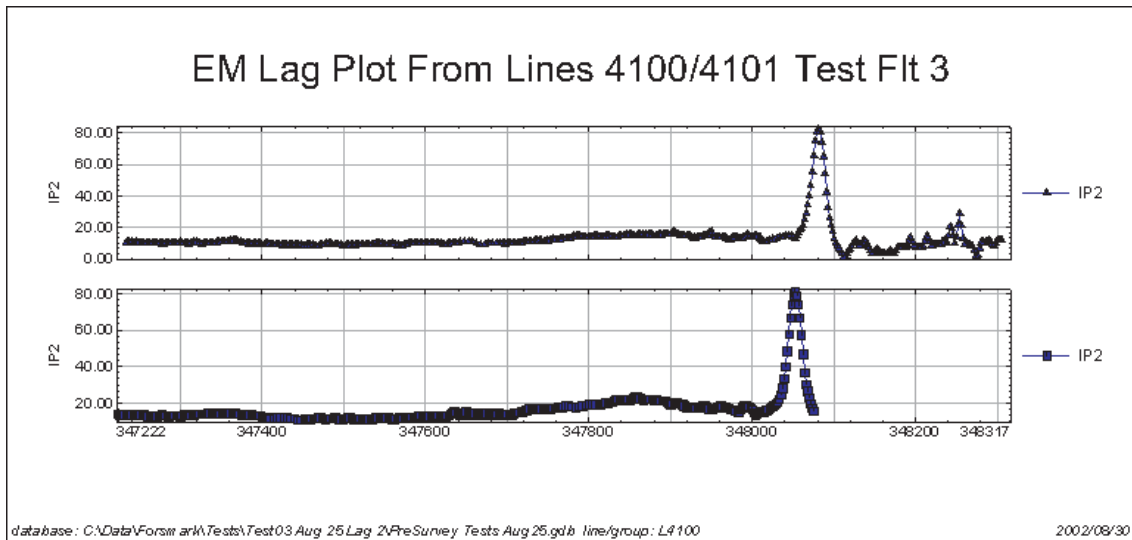


Figure B-3. EM lag test at Forsmark.

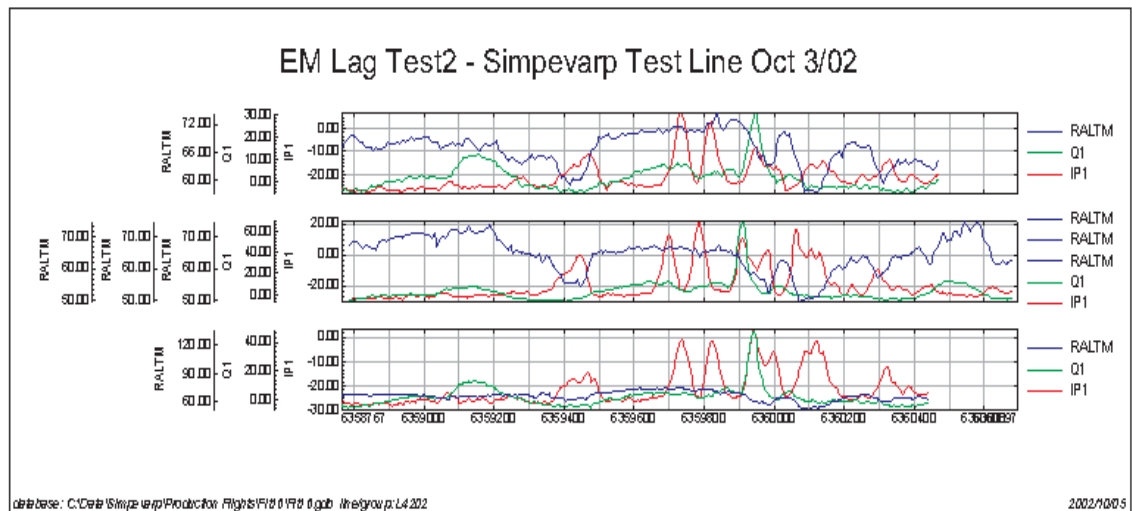


Figure B-4. EM lag test at Simpevarp, 7001 Hz Coaxial.

Table B-7. EM Drift Summary, Aug 23, 2002.

Channel	Start (0.0 hrs)	End (2.9 hrs)	Change	Rate/Hour
IP1	-5	-156	-151	-52
Qd1	4	13	9	3
IP2	-45	122	167	57
Qd2	-14	-75	-61	-20
IP3	-7	-68	-61	-20
Qd3	-14	-5	9	3
IP4	10	54	44	15
Qd4	-33	-74	-41	-14
IP5	5	96	91	31
Qd5	21	226	205	71

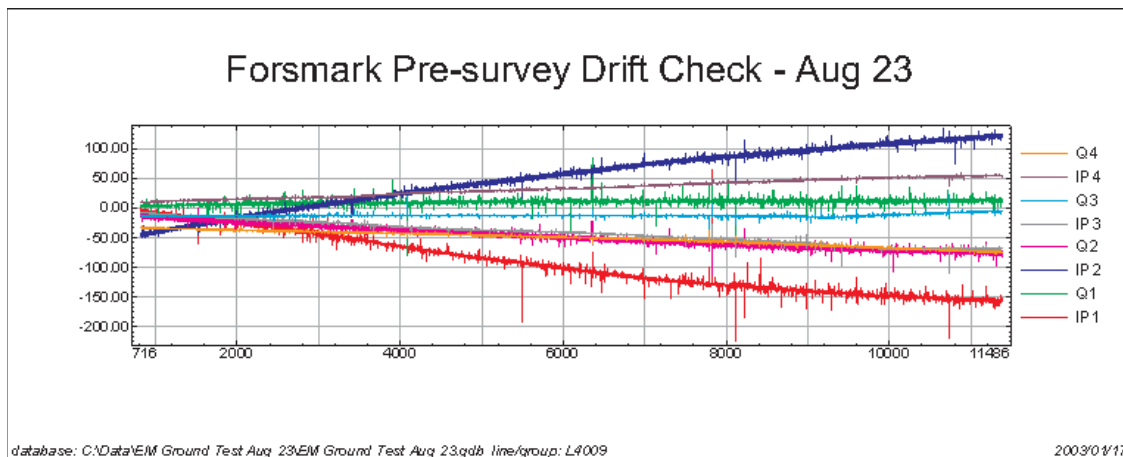


Figure B-5. Forsmark EM drift test.

Phasing: The pre-survey phasing check is recorded in line Forsmark 4001 and is shown below (Figure B-6). The quadrature channels show no response and phasing is ok.

B.3.3 EM Test line

The test line, located on an east-west line crossing the Storskaret helibase, was set out with a loop approximately 80 metres square laid across it. This test line was flown at the beginning of the Forsmark survey several times on August 25, with the results shown below (Figure B-7).

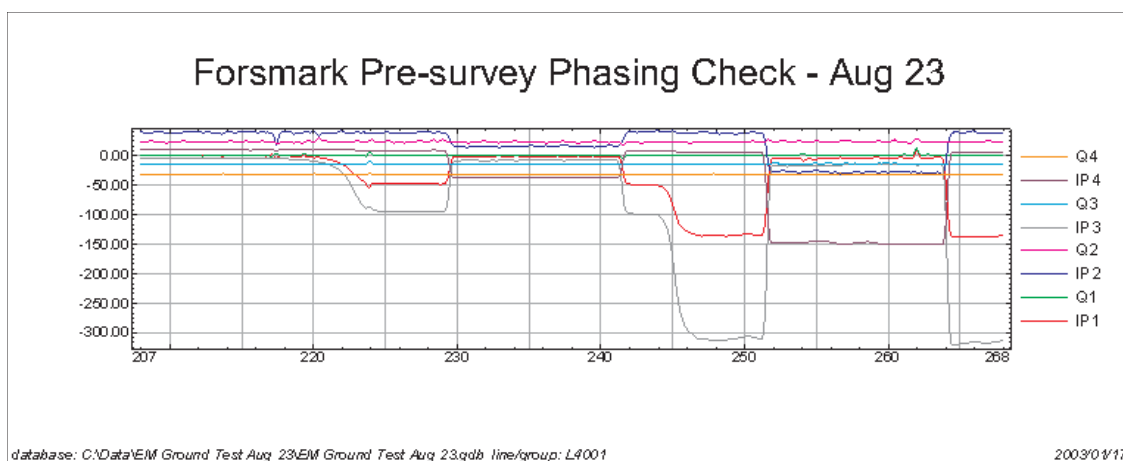
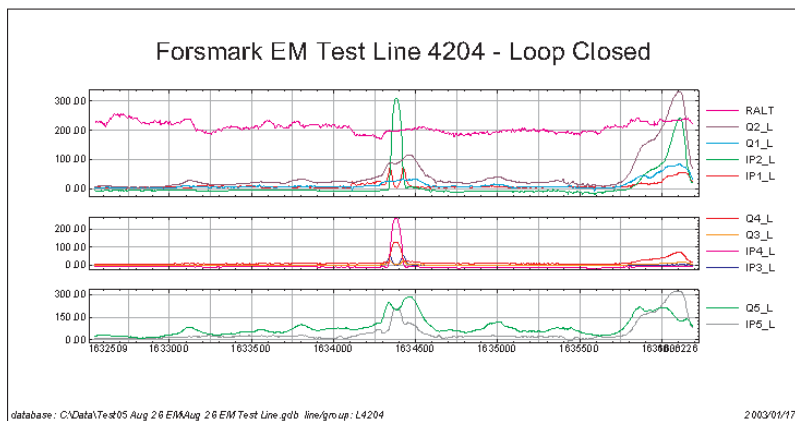
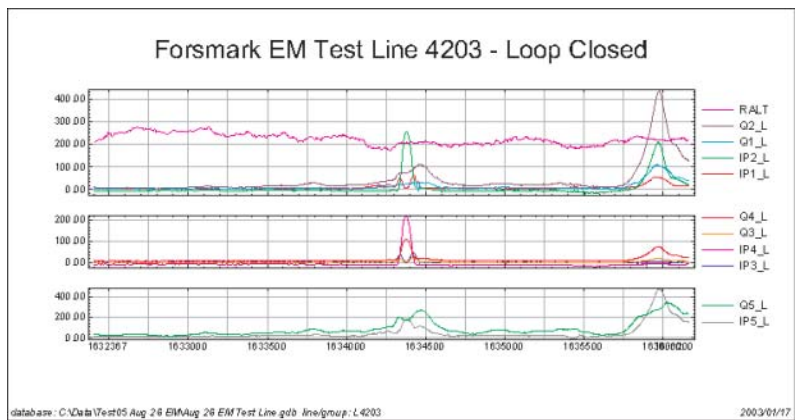
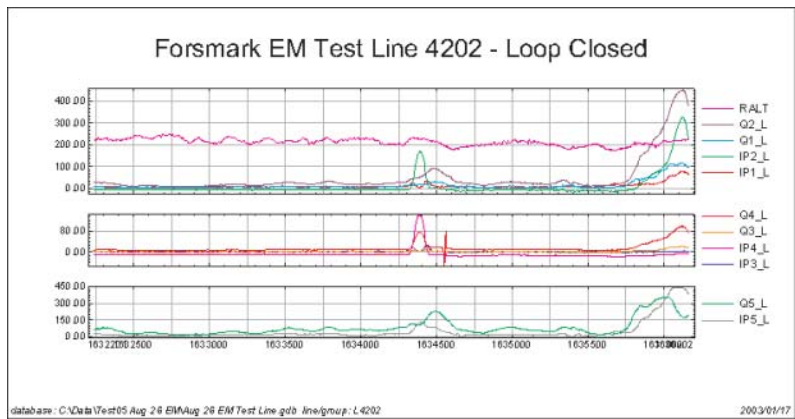
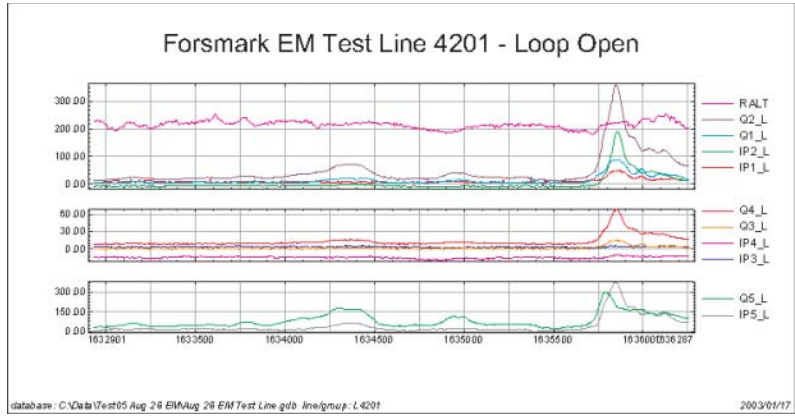


Figure B-6. Forsmark pre-survey phasing test.



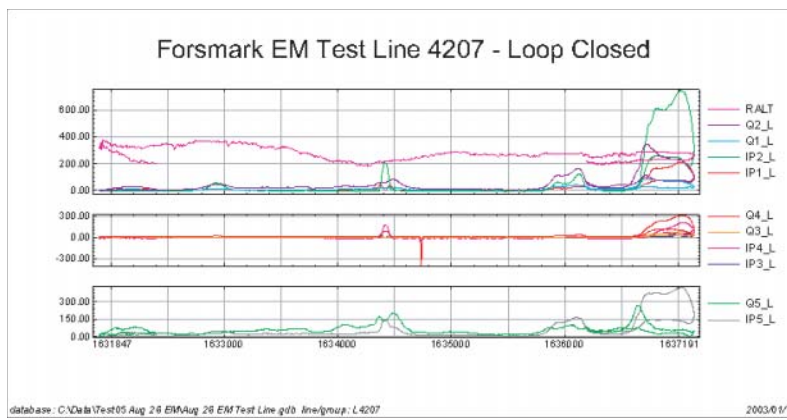
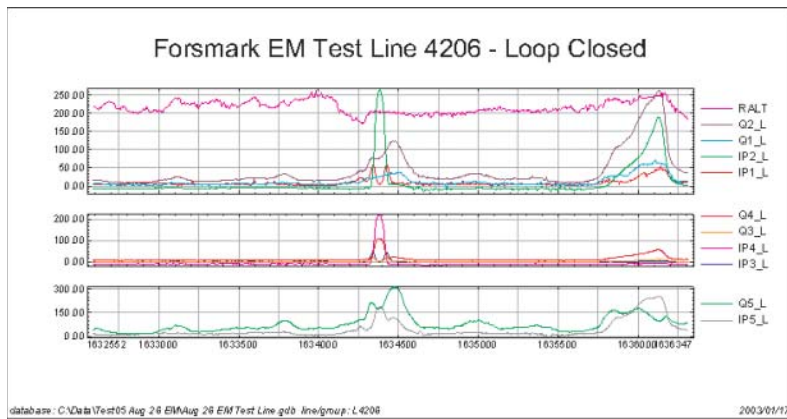
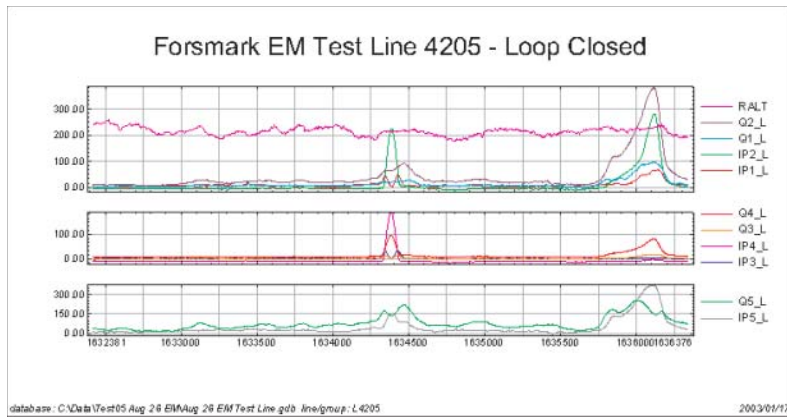


Figure B-7. Repeated EM measurements at the Forsmark test line.

Drift on the test line flight is as follows:

Table B-8. Drift Results (PPM) on the Test Line.

UTC	Line	Rec	IP1	Qd1	IP2	Qd2	IP3	Qd3	IP4	Qd4	IP5	Qd5
8:11	8000	1663	-10	12	-24	22	3	1	-25	-24	-13	-31
8:33	8001	2905	-9	13	-39	38	12	0	-33	-16	-65	49
8:47	8002	3662	-7	14	-42	44	15	0	-29	-16	-91	119
9:01	8003	4557	-5	12	-43	46	17	1	-19	-16	-120	174
9:18	8004	5440	-5	11	-42	55	19	1	-13	-15	-151	263

B.4 GPS accuracy test.

The navigation system was tested during approximately 3 hours at the helicopter base while the EM drift was being recorded (Aug 23, 2002 EM Ground Test Line 4009). The WGS 84 XY and RT90 results are summarized in Tables B-9–B-12 below and have been approved by Hans Thunehed of Geovista.

B.5 Radar altimeter

The radar altimeter was calibrated prior to the Forsmark survey by NorCopter, the helicopter service company used in the Forsmark survey (see Appendix A). The radar altimeter was checked prior to the Forsmark survey by hovering for 1 minute with the tow cable on the bird fully extended so that the bird was just touching the ground. The average altimeter reading was found to be 107.2 feet, with a minimum, maximum and deviation of 100.7, 117.2 and 3.1 feet respectively.

Table B-9. WGS84 xy test results (metres).

Channel	Minimum	Maximum	Mean	Standard Deviation
X	347971.3	347976.4	347947.6	1.09
Y	6696401.1	6696406.5	6696403.8	1.32

Table B-10. WGS84 LAT/LONG test results (degrees).

Channel	Minimum	Maximum	Mean	Standard Deviation
LatWGS84	18.242 540	18.242 632	18.242 601	0.000 020
LongWGS84	60.375 403	60.375 453	60.375 428	0.000 019

Table B-11. RT90 LAT/LONG test results (degrees).

Channel	Minimum	Maximum	Mean	Standard Deviation
LatRT90	18.246 075	18.246 154	18.246 124	0.000 019
LongRT90	60.376 019	60.376 069	60.376 045	0.000 012

Table B-12. RT90 LAT/LONG test results (X Y).

Channel	Minimum	Maximum	Mean	Standard Deviation
X_RT90	1634444.9	1634449.3	1634447.8	1.01
Y_RT90	6697752.5	6697758.1	6697755.3	1.34

B.6 Gamma ray spectrometer tests

The calibration of the gamma ray spectrometer was a complicated task, and involved tests undertaken at NGU, at the beginning of the Forsmark survey, during the Forsmark and Simpevarp surveys, and at the end of the Simpevarp survey. Calibration of the spectrometer could not have been completed without the help of Sören Byström and Hossein Shomali of SGU, who provided calibrated ground spectrometer data that could be used to cross check the pad calibration data acquired at NGU. The extended effort to acquire calibration data was caused in part by bad luck (rain and position errors), the need to complete the Forsmark data acquisition so as to begin the Simpevarp survey, and the need to acquire enough data with a large enough variation in the uranium-thorium ratio to accurately determine the stripping coefficients A1 and A2.

Windows:

The spectrometer was configured to generate the following windowed channels:

U	132–148	1660 keV–1860 keV
Th	189–220	2410 keV–2810 keV
K	109–125	1370 keV–1570 keV
TC	34–220	410 keV–2810 keV

To verify these windows, spectral data from line 3004, test flight 2, on Aug 22 were loaded into an excel spreadsheet for processing. The counts at the thorium channel were summed and the resulting peak at channel 205 had half maxima (determined from inspection) at approximately channels 199.5 and 209.5, a span of 10 channels, or a FWHM of approximately 4.9%. This is close to the 4.6% figure quoted by Smethurst and Mogaard (see below).

Stripping factors:

The stripping factors were determined by Mark Smethurst and John Mogaard at the NGU and are as follows (see Appendix A):

Alpha	0.3042	(Th-> U)	Beta	0.5137	(Th-> K)
Gamma	0.7639	(U-> K)	a	0.0706	(U->Th)
b	0.0000	(K->Th)	g	0.0000	(K-> U)

Sensitivity factors:

The pad sensitivity factors were determined by Mark Smethurst and John Mogaard at the NGU and are as follows (see Appendix A):

K-40	0.00738%/cps
U-238	0.08682 ppm/cps
Th-232	0.17626 ppm/cps

The pad sensitivity factors must be corrected to the nominal survey altitude of 60 metres.

Full width at half maximum (FWHM):

The FWHM coefficients were determined by Mark Smethurst and John Mogaard at the NGU and are as follows (see Appendix A):

K-40	6.0%	Accepted value	6%
U-238	4.9%	Accepted value	6%
Th-232	4.6%	Accepted value	6%

The spectral data from line 3004, test flight 2, on Aug 22 were loaded into an excel spreadsheet (Thorium-line3004- test flight.xls). The counts in the thorium window were summed and the resulting peak at channel 205 had half maximum (determined from inspection) at approximately channels 199.5 and 209.5, a span of 10 channels, or a FWHM of approximately 4.9%. This is close to the 4.6% figure quoted by Smethurst and Mogaard and under the 6% tolerance.

B.6.1 Cosmic correction

The cosmic stripping coefficients were computed from a cosmic background flight over the Baltic Sea about 3–10 kilometres east of the Forsmark nuclear plant. The cosmic flight data are recorded as Test1 in the flight reports, and consisted of a series of 10 minutes lines flown at 4500, 5500, 7000, 8500, 9500 and 10500 feet⁴. The data at each elevation were corrected for deadtime with the Geosoft RPS package (except the Uranium window from the upward looking detector, where the correction was done manually) and averaged using Geosoft's averaging software. Results are as follows, with the results in brackets being given as typical by the IAEA, Table B-13.

Table B-13. Aircraft background and cosmic stripping coefficients

U down	aircraft background	= 2.9	cosmic stripping coefficient = 0.029	(.041)
U up	aircraft background	= 0.53	cosmic stripping coefficient = 0.0077	(.0084)
Th	aircraft background	= 0.91	cosmic stripping coefficient = 0.034	(.055)
K	aircraft background	= 6.3	cosmic stripping coefficient = 0.039	(.050)
TC	aircraft background	= 62	cosmic stripping coefficient = 0.68	(.81)

⁴ The upper altitude was limited by safety due to the lack of oxygen.

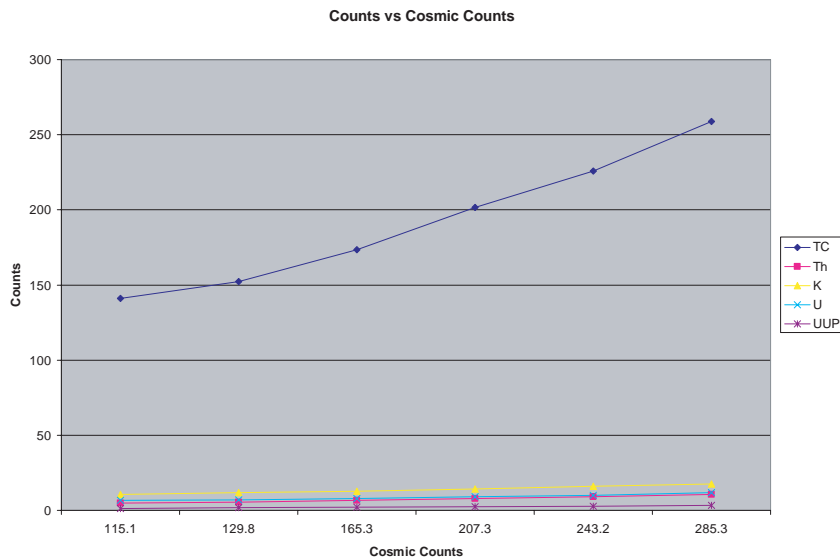


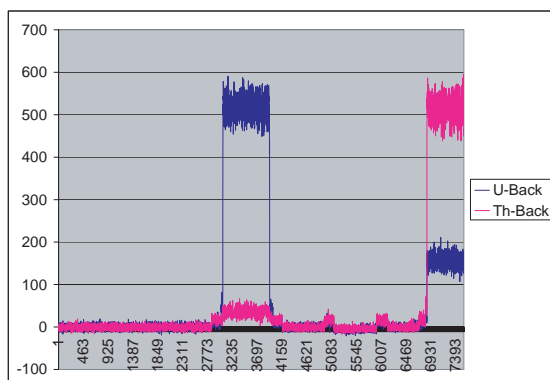
Figure B-8. Total counts vs. cosmic counts at height 4500, 5500, 7000, 8500, 9500 and 10500 feet.

B.6.2 Radiometric Constants A1 and A2

The radiometric constants A1 and A2 were determined from the NGU pad calibration data (shown left below), and are as follows, together with the standard errors and the R2 coefficient of fit.

Pads are not optimal for determining A1 and A2 because pad data are subject to localization and do not include atmospheric scattering. (IAEA values are A1= 0.0339 and A2 = 0.0162).

To measure A1 and A2, a number of sites near the Simpevarp reactor were selected to maximize variation of ground uranium and thorium. Each site was selected for adjacency to water, so as to provide background measurement, and for accessibility. Data were acquired at the following points, and are recorded in lines 500000 in flight 19. An initial attempt prior to commencing the Forsmark survey proved to be unsuccessful because the measured ranges of uranium and thorium concentrations were not large enough to generate significant results, and because the areas selected were too far removed from water for the over-water backgrounds to be sufficiently accurate.



	A2	A1
Value	0.00544564	0.04164194
Error	0.00031151	0.00030653
R2	0.99989972	0.14949547

Figure B-9. Pad data for computing A1 and A2.

The Simpevarp A1/A2 data (background corrected with individual backgrounds) are as follows:

Line/Background	Udown	Th	Uup	E (RT90)	N (RT90)
503011/12	53.6	89.7	3.9	1553500	6366647
503013/14	28.4	34.7	2.8	1552867	6368109
503015/16	26.4	28.8	3.6	1552971	6366449
503017/18	27.8	41.3	3.3	1551423	6366519
503019/20	23.8	26.2	2.3	1550249	6365027
503021/22	23.6	25.1	1.4	1551314	6366860
503023/24	29.8	38.1	1.7	1553939	6367850

The results are hypersensitive to the background levels determined for the upward looking uranium crystal, and regression using these data yields a negative coefficient for A2. Accumulating the background into a common “line” that is used to correct all data results in:

Line	Udown	Th	Uup
503011	53.6	89.7	3.9
503013	28.4	34.7	2.8
503015	26.4	28.8	3.6
503017	27.8	41.3	3.3
503019	23.8	26.2	2.3
503021	23.6	25.1	1.4
503023	29.8	38.1	1.7
Common Background	3.5	0	1.25

Using these data, the following analysis resulted in the sky shine coefficients that were used in the processing, Table B-14.

Table B-14. Coefficients for correction of atmospheric radon content.

Compute a least squares fit using Equations 4.17, 4.18 IAEA manual page 29					
Line	a Ud/ \bar{A}^2	b Th/ \bar{A}^2	C Ud*Th/ \bar{A}^2	d Uu*Ud/ \bar{A}^2	e Uu*Th/ \bar{A}^2
3011	258.76390	829.49380	463.29590	13.687110	24.505670100
3013	79.48846	154.37050	110.77310	4.948077	6.895512821
3015	51.41275	81.31765	64.65882	5.275980	6.635294118
3017	59.64545	172.29190	101.37270	5.031818	8.552020202
3019	52.16329	86.89114	67.32405	2.698101	3.482278481
3021	50.50125	78.75125	63.06375	0.376875	0.470625000
3023	100.24490	210.37830	145.22170	1.715217	2.484782609
Sum	652.22000	1613.49500	1015.71000	33.733180	53.026183330

Determinant=	20686.59	Determinant = ac-bb
a1	0.02751	(ce-bf)/det
a2	0.015547	(af-be)/det

B.6.3 Radiometric upward and downward window relationships

A Geosoft GX was written (cal_over_water) to select all points with cosmic corrected thorium and total counts as an indicator of the presence of water. Thorium was selected as a water “detector” channel because it is least affected by the variations in atmospheric radon; high concentrations of atmospheric radon could cause a water auto-detect algorithm based on other channels to indicate land, biasing the results to include only those data sampled during lower radon concentrations.

Data were accumulated from each corrected channel for each line on the survey, with the criteria that thorium counts < 10/sec, total counts < 250/sec, such that at least 10 such occurrences were encountered on a particular line. Processed data included both the over-water background and survey lines, and written to an ASCII file whence they were read into excel and processed to yield the required linear relationships. The best fit was achieved using only the over water lines, indicating that the “water test” parameters in the “GX” were not perfect, but could be used to reject suspect points in the over water lines, which in Simpevarp traversed many shallow shoals. These data are presented below (Table B-15).

B.6.4 Radiometric altitude attenuation:

An initial radiometric altitude attenuation test was made over a large field near the helicopter base at Forsmark. This was an ideal location, devoid of trees, flat, near water for a good background and with a relatively high background radioactivity. The only problem was that during the course of the measurements, a light rain⁵ drastically changed the apparent ground uranium concentration and the test results were thus of dubious quality.

⁵ As luck would have it, pretty much the only significant rain that occurred during the survey at Forsmark happened half-way through this experiment.

Table B-15. Data from Simpevarp over-water background lines and resulting regression.

Uup	K	Th	TC	Ud	Uup vs Udown		
1.53	2.96	0.397	43.6	3.07	a_u, b_u	0.291535	0.448503
1.74	3.62	0.381	41.4	3.51	Std.err a,b	0.02982	0.095653
0.813	1.62	-0.121	15.9	1.2	R2,SEY	0.819861	0.299258
1.11	3.76	0.7	42.1	2.32	F,df	95.5769	21
1.37	2.2	0.58	28.3	1.28	SSReg,SSres	8.559426	1.880663
1.5	1.83	0.959	34.3	2.46	K vs Udown		
1.72	6.86	0.742	89.7	5.68	a_k, b_k	0.998442	1.308666
3.17	9.89	2.1	141	8.39	Std.err a,b	0.13552	0.434699
0.819	2.52	0.149	21.9	1.19	R2,SEY	0.721042	1.359985
1.16	4.47	1.34	57.2	2.15	F,df	54.28006	21
0.4	0.298	0.11	0.779	0.11	SSReg,SSres	100.3942	38.84073
0.901	3.17	0.737	28.9	0.87	Th vs Udown		
0.953	2.96	0.501	34.7	1.72	a_t, b_t	0.11563	0.409933
0.941	6.07	0.625	50.9	2.27	Std.err a,b	0.069988	0.224496
0.112	-0.31	0.644	-0.918	-0.803	R2,SEY	0.115028	0.702352
1.05	1.71	0.652	11.9	0.0398	F,df	2.729569	21
0.161	4.92	1.19	37.8	0.926	SSReg,SSres	1.34649	10.35925
2.23	8.84	1.03	96.4	5.79	TC vs Udown		
0.385	1.35	-0.185	17.9	0.943	a_tc, b_tc	14.63316	8.692883
0.993	5.82	2.78	65.8	2.55	Std.err a,b	1.002029	3.214148
0.729	2.57	-0.312	29.9	1.85	R2,SEY	0.910357	10.05568
1.79	4.17	-0.285	72.8	5.12	F,df	213.263	21
1.04	4.63	1.18	55.9	3.28	SSReg,SSres	21564.47	2123.453

- Notes: 1. a_x and b_x are the regression of channel x against uranium down: $x = a_x u_d + b_x$
2. Std Err, a,b are the standard errors in a_x and b_x
3. R2 and SET are the R2 and standard error in Y (channel x) statistic
4. F, df are the F statistic and the degrees of freedom
5. SSReg and SSRes are the regression sum of squares and residual sum of squares

Table B-16. Forsmark altitude attenuation results.

ln(th) vs ht		ln(k) vs ht		ln(u) vs ht		ln(tc) vs ht	
-0.00894	4.026017	-0.01144	5.801488	-0.004707	3.6248605	-0.00804	7.859611
0.000589	0.040184	0.000145	0.009925	0.000891	0.0608128	0.000211	0.014386
0.991395	0.029760	0.999677	0.007350	0.933105	0.0450380	0.998628	0.010654

The altitude attenuation data computed from the hover test during flight 34 at Forsmark are shown in Table B-16, with data extracted from an excel spreadsheet having been computed with the LINEST function. The data for each element are presented as pairs as follows:

- The second row gives the attenuation constant and the log(e) of the projected counts on the ground.
- The third row gives the standard errors of both the attenuation constant and the projected counts.
- The first element of each pair in the last row gives the r2 coefficient of fit.

The r2 fits are very good, apart from uranium, which was affected because of a light rain that began during the tests, altering the bismuth concentration in the air and on the ground.

The projected count rates and conversion to element concentrations are shown in Table B-17, with the element concentrations having been measured under the direction of SGU (Sören Byström, Hossein Shomali). Note that according to Sören Byström, the slight rain caused the uranium ground concentration to increase from 1.8 to 4 ppm during the course of the measurement, and is probably the source of discrepancy in the uranium measurement.

Table B-17. Forsmark radiometric sensitivity results.

Channel	Ln (Projected Ground Counts)	Projected Ground Counts	Ground Concentration (average of SGU data)	Sensitivity	Sensitivity (NGU Pads)
Th	4.026	56	10 ppm	5.6 c/ppm	5.7 c/ppm
U	3.62	37	2.6 ppm	14.2 c/ppm	11.5 c/ppm
K	5.80	330	2.52%	131c/%	135.5 c/%
TC	7.85	2565			

The experiment was retried on flight 20, Simpevarp, using ground spectrometer data for calibration supplied by Hossein Shomali. Altitude attenuation was measured over a field south east of the intersection with the Sybilla at Farbo, near Simpevarp. This site was selected because it is near to water for background measurement, relatively flat, clear of trees and compositionally homogenous. Hossein Shomali from the SGU measured the test area with a calibrated hand spectrometer on October 9th in the afternoon. A test flight was flown on October 10th, Flight 20, lines 34XX. Data are reduced using data averaged at 200, 250, 300 and 400 feet. Tables illustrating the computations are presented below:

The following table shows the original data, deadtime corrected, with radar altimeter corrected to STP conditions using temperature 7°C and pressure 1025 mb. Samples are averaged over 1 minute:

Line No	Nom.Ht (feet)	TC (cnts)	Th (cnts)	K (cnts)	U (cnts)	Uup	COSMIC	Corr HT to STP(m)
3420	200	1649	35.1	257	29.2	4	69	53.3
3425	250	1467	30.8	214	27.8	4.7	71	68.5
3430	300	1371	28.4	201	24.9	3.6	67	77
3440	400	1114	23.7	151	22.2	3	68	106
420000	200	199	4.6	16	8.4	2.4	64	57

The next step is to remove backgrounds. This removes radon and cosmic scattering. The results are:

Nom.Ht (ft)	TC	Th	K	U	Uup	Corr HT (m)
200	1450	30.5	241	20.8	1.6	53.3
250	1268	26.2	198	19.4	2.3	68.5
300	1172	23.8	185	16.5	1.2	77.0
400	915	19.1	135	13.8	0.6	106.0

The background corrected data are now stripped. The stripped counts with the background removed are as follows:

Nom.Ht (ft)	TC	Th	K	U	Corr HT (m)
200	1450	30.77093	223.5074	11.3679400	53.3
250	1268	26.33873	181.2385	11.1914700	68.5
300	1172	24.02067	170.7932	8.8739350	77.0
400	915	19.26413	122.4228	7.4372290	106.0

To compute the attenuation coefficients, fit linear line through the \log_e of the count rate as a function of height:

Nom.Ht (ft)	TC	Th	K	U	Corr HT (m)
200	7.279319	3.426571	5.409444	2.430797	53.3
250	7.145196	3.271041	5.199814	2.415152	68.5
300	7.066467	3.178915	5.140453	2.183118	77.0
400	6.818924	2.958245	4.807481	2.006498	106.0

The resulting linear fits produce the decay coefficients below in the second column (Table B-18). Note the discrepancies with the IAEA thorium results which appear to be unreliable compared with the results presented for Forsmark and Simpevarp. The columns to the right illustrate the count rate projected to occur at ground level using the Simpevarp decay coefficients.

Table B-18. Comparison of various attenuation factors.

	Decay coefficients vs height			Convert to counts at ground level		
	Simpevarp	Forsmark	IAEA p36	IAEA Graph	Ln(Counts)	Counts
U	-0.00864	-0.004707	-0.0084	-0.00828	2.917281	18.49093
Th	-0.0088	-0.00894	-0.0066	-0.00783	3.879237	48.38729
K	-0.01123	-0.01144	-0.0082	0.00945	5.995269	401.5246
TC	-0.00873	-0.00804	-0.0067	-0.00782	7.74288	2305.101

(Note the error in the Forsmark uranium attenuation caused by rain). The Simpevarp attenuation factors generate the following factors used to convert counts from ground level to counts at a nominal survey altitude of 60 metres (Table B-19).

Table B-19. Attenuation factors used in processing.

U	0.420967
Th	0.441402
K	0.359731
TC	0.445392

B.6.5 Conversion to a calibrated count rate

Rain not only affected the altitude attenuation coefficients for the Forsmark test, but also cast the conversion to ground concentration parameters into doubt because of the apparent ground uranium concentration changed during the course of the survey.

Altitude attenuation was therefore re-measured over a field south east of the intersection at Fårbo, in the Simpevarp survey, as noted above. This site was independently measured with a calibrated ground spectrometer operated by Hossein Shomali on a grid of points over the field where the test was made. Conversion units determined from the SGU data are compared with the pad calibration factors from calibration done at NGU. Results compare well in view of the precision of the data, as measured by the standard deviation of the SGU ground data, see Table B-20.

The thorium and potassium attenuation coefficients are almost identical to those computed for Forsmark; results for uranium and total count are different, with the uranium coefficient being more compatible with that expected in comparison, for example, with thorium. This is likely explained by the fact that at Forsmark, the rain, which changed the apparent uranium ground concentrations during the course of measurement, and thus destroyed the uranium attenuation coefficient experiment. Summarizing the sensitivity data (Table B-21), the results are reiterated below, with the NGU pad sensitivity data: any geometric effects due to restricted pad size must be minor indeed!

Table B-20. Ground spectrometer data, Farbo field near Simpevarp.

Element	Counts at ground level	Error in counts at ground level	Ground spectrom. elemental concent.	Units for ground spectrom data	Units/cps from SGU ground data	Standard deviation: SGU ground spectrom.	Error/cps from SGU ground data	Units/cps from NGU pad calibration
U	18.49093	err ~1.3%	1.1	ppm	0.059489	0.4 ppm	0.021632	0.08682
Th	48.38729	err ~2.5%	9.2	ppm	0.190133	1.3 ppm	0.026867	0.17626
K	401.5246	err ~2.5%	3.10	%	0.007721	0.2%	0.000498	0.00738

Table B-21. Summary of computed sensitivities.

Channel	Sensitivity (Simpevarp)	Sensitivity (Forsmark)	Sensitivity (NGU Pads)
Th	5.2 c/ppm	5.6 c/ppm	5.7 c/ppm
U	16.8 c/ppm	14.2 c/ppm	11.5 c/ppm
K	130 c/ppm	131 c/%	135.5 c/%

Accordingly, the following data were used in the processing (Table B-22).

Table B-22. Apparent sensitivity used for converting cps to ground concentration of Th, U and K.

Channel	Pad Sensitivity	Attenuation coefficient	Factor to convert pad sensitivity to 60 metres	Apparent sensitivity at 60 metres
Th	5.67 c/ppm	-0.00894	1.71	3.32 c/ppm
U	11.5 c/ppm	-0.00864	1.68	6.86 c/ppm
K	135.5 c/%	-0.01144	1.98	68.4 c/%
TC		-0.00873		

Helicopter geophysical data processing methods

Used in the SKB Forsmark and Simpevarp surveys:

Discussion of the Forsmark survey

A report prepared on behalf of the Geological Survey of Norway
for Svensk Kärnbränslehantering AB by

Peter Walker
Geophysical Algorithms

Ola Kihle, John Mogaard and Jan Steinar Rønning
Geological Survey of Norway

December 2002

Geological Survey of Norway
Leiv Erikssons vei 39N-7491
Trondheim
Norway

Geophysical Algorithms
99 Queen Street South
Mississauga, Ontario
L5M 1K7 Canada

C.1 Introduction

This document describes the data processing sequence used to reduce helicopter geophysical data on behalf of Svensk Kärnbränslehantering (SKB) in the Forsmark and Simpevarp surveys that were undertaken in August, September and October, 2002, with particular emphasis on the Forsmark survey.

The survey apparatus consisted of an integrated data acquisition package consisting of a 5 frequency “Hummingbird” EM system, a Scintrex cesium vapour magnetometer, a Herz Totem VLF, real time differential GPS, radar altimeter, and a 256 channel spectrometer.

Testing and calibration of this equipment for the Forsmark and Simpevarp surveys is described in Appendix A and Appendix B.

C.2 Line numbering conventions

Lines represent a time sequence of data used for a particular purpose. The term line originates from the interpretation that this sequence of data represents a usual traverse or survey line. However, as additional calibration checks have been added, lines are used to define sequences of data used to measure various background, verification, and calibration checks.

Line numbering conventions for production lines at Forsmark are as follows:

Type	Description	Number Range
Traverse	Forsmark survey, NS lines, large area	0–3020 by increments of 10
Traverse	Forsmark survey, repeated lines, large area	1–3029 not ending with 0
Traverse	Forsmark survey, NS lines north of reactor	50000–59999
Tie Line	Forsmark survey, EW Tie Line	60000–69999
Traverse	Forsmark survey, EW lines, small area	70000–79999

Note that some of the test and calibration measurements are common for the Forsmark and the Simpevarp survey. Navigation at test and calibration lines were not always processed, (position does not matter) and hence coordinates are sometimes equal to 0.

Line numbering conventions for test and calibration lines are as follows:

Type	Description	Number Range
Rejected	Turns, Aborted Lines, Ferry To Area	9XXX, 99XXX
Bk, Cs,U, Th	Background and Radiometric Samples	3001–3004
Bk, Cs,U, Th	Samples FF = Flight No.	3FFXXX
Hover	Spectrometer Altitude Hover Testing	301X
Altitude	Spectrometer Attenuation Testing	3400–3499
OverWater	Spectrometer Water Line Forsmark	3200–3399
Cosmic	Cosmic Calibration $xy = \text{height (ft)}/100$	34XY
EM	Ground Calibration	4000–4099
Test Line	Forsmark and Simpevarp	4200–4299
EM Lag		41XX
Mag Heading	Cloverleaf check	50XX
Mag Lag		51XX
Radar	Hover at full tow cable extension	6XXX
EM	Background test line	8XXX
EM	Nulling Background FF = Flight no	1FFXXX
Test line	Forsmark and Simpevarp	2FFXXX
Over Water	Spectrometer OverWater – Simpevarp	4FFXXX

C.3 Loading and initial inspection procedures

Processing the data begins by loading data generated by the Hummingbird Data Acquisition System. This system generates a “.HUM” file for every flight which is converted to a Geosoft compatible “.XYZ” file using the extractor program HUM2XYZ.

When the “.XYZ” file has been created, it is copied into a *_LINES.XYZ file, which is edited in conjunction with the flight reports to break the continuous stream of data from the flight into separate lines. Once the lines have been defined in the XYZ file, the data are loaded into a Geosoft database for processing and initial inspection.

The procedure is as follows.

Loading Hummingbird Data:

1. Data from hummingbird is extracted to xyz file using HUM2XYZ
2. *.xyz file is copied to *_lines.xyz.
3. Operators report is used to edit *_lines.xyz to insert line breaks
4. Database is loaded from the *_lines.xyz
5. Lines 9000–9999 and 90000–99999 are deselected in database

Loading Magnetic Base Station Data:

6. Base magnetometer file is copied to flight directory
7. Base magnetometer data are converted to .bas format with a 0 field offset
8. Base magnetometer data are loaded into the mag_heli_base channel using the geosoft leveling package. To do this the base mag is used to level fid 0 to generate MAG_HELI_BASE. Time reference is UTC from GPS. In the case of the Forsmark survey where the Fiby base station magnetometer was used, the Fiby base station data were loaded into MAG_FIBY, and then MAG_FIBY_300 was generated from MAG_FIBY to bring the Fiby base station magnetic values close to the MAG_HELIBASE values.
9. MAG_HELI_BASE is then multiplied by -1 to yield the base mag reading.
10. The channel RAWMAG is filtered with a 5 point lowpass to generate MAG_FILT
11. MAG_HELI_BASE is protected

Note: Following the Forsmark survey, magnetic data from Fiby observatory were used to level the magnetics, so as to largely eliminate the effect of the DC power cable. Prior processing had manually removed spikes in magnetic base station data. However, during the processing of the Fiby data, it was discovered these “spikes” were the result of 0:00:00.00 times occurring in the GPS time base channel. By defaulting these zero-time data, the base station corrections could be applied without such time-base error spike occurring.

Preparing Ancillary Data:

12. Radar altimeter RALT (feet) is converted to RALTM metres (= ft x 0.3049)
13. Temperature TEMP (degrees C) channel loaded using data from operators log
14. Barometric pressure BARO channel (mbars) loaded using data from operators log

Preparing GPS Data:

15. X_RT90, Y_RT90 are generated from X,Y (Zone 34N Forsmark, 33N Simpevarp)
16. Run GX to create repositioned RT90 data to correct timing error in GPS. This generates the channels X_RT90Fix, Y_RT90Fix

Initial Delivery:

17. Files in flight directory copied to CD and delivered to SKB

C.4 QC stage

In the QC stage, the quality control checks required by SKB were performed in the field. The QC stages are as follows:

Magnetic Diurnals:

18. High pass filter (cutoff = 30 fids) MAG_HELI_BASE to generate MAG_BASE_HP
19. MAG_HELIBASE is copied into MAG_DIURNAL. MAG_DIURNAL is edited to remove obvious spikes. In the case of Forsmark, where the Fiby magnetic base station was used, MAG_DIURNAL was copied from MAG_FIBY_300.

20. Stat report on MAG_BASE_HP is made to determine base mag noise. Limit is 0.3 nT. MAG_BASE_HP is plotted to determine the base station noise, with the average noise being under 0.3 nT. Spikes in manual MAG_DIURNAL are removed by manual editing.
21. MAG_HELI_BASE is inspected so that the diurnals do not exceed the following:
22. 100 nT; in 60 min or 35 nT in 10 min or 15 nT in 2 min
23. QC (4th difference) is run on MAG_FILT and a map plotted.

Flight Line Parameters:

24. QC is run on altimeter with geosoft parameters 60, 48, 18 50 and a map plotted. The map was inspected to locate bad sections of data.
25. QC is run on line separation using the geosoft parameters 50, 100, 75, 500 and a map plotted. The map was inspected to locate bad sections of data.

EM:

26. IP*,Q* -> IP_L,Q_L using Geosoft HEM leveling package. Drift inspected for the following limits between background null points:
 - A: IP1 < 20 ppm, B: Q1 < 20 ppm, C: IP2 < 20 ppm, D: Q1 < 20 ppm,
 - E: IP3 < 10 ppm, F: Q3 < 10 ppm, G: IP4 < 10 ppm, H: Q4 < 10 ppm,
 - I: IP5 < 30 ppm, J: Q5 < 30 ppm
27. Because noise was large and unpredictable in both areas, and sporadic and attributed to cultural effects outside the system, high frequency EM system noise was checked by observing the EM profiles over the radon water background lines. Targeted noise values were (99% of samples)
 - A: IP1 < 5 ppm; B: Q1 < 5 ppm; C: IP2 < 2 ppm; D: Q2 < 2 ppm;
 - E: IP3 < 5 ppm; F: Q3 < 5 ppm; G: IP4 < 2 ppm; H: Q4 < 2 ppm;
 - I: IP5 < 5 ppm; J: Q5 < 5 ppm

Spectrometer:

28. 256-channel spectra are copied into EXCEL. FWHM @ 2.62 Mev (Th) < 6% for the Thorium sample (Line 3004)
29. Th Peak at 205 (U at 140, K at 116, Cs at 55)
30. Criterion that no heavy rain had occurred verified.

Data Abundance:

31. A statistical report on the channels was run to verify that the following channels contained the required abundance of data:
 - X for more than 95% data, TC for more than 99% of data; RAWMAG for more than 99% of data;

Administration:

32. Lines are accepted for navigation
33. Lines are accepted for mag

34. Lines are accepted for em
35. Lines are accepted for spectrometer

PreProcessing:

36. Radiometric Data are processed using the Geosoft RPS package with the available coefficients. These coefficients change as calibration data became available during the surveys.
37. EM Data are levelled using the Geosoft HEM levelling package
38. VLF data are not pre-processed during the QC stage in any manner.
39. Magnetic-VLF, EM and Radiometric data are written out for each flight into separate XYZ data files for each data set and are then imported into a database for each data set. East-West Lines and North-South line data from Forsmark are initially loaded into separate databases, but the final Fiby processed mag data are written into a single database with both north-south and east-west lines. Simpevarp North-South lines and the special area to the east of Simpevarp are loaded into separate databases.
40. Preliminary grids of uranium, thorium, potassium and total count generated from the radiometric database; Preliminary grids of magnetic field are generated from the magnetic database, and first and second derivative grids are generated from the magnetic field grid.

C.5 Post Processing: Differential GPS data.

Positions are defined in RT90 coordinates, and were generated using the Geosoft conversion function from the X, Y coordinate channels logged in WGS84 using UTM zone 34. These data were then relocated to account for a software bug in the Hummingbird data acquisition system using the GX “xyfix” that was written for the purpose. The data required relocation because the CPU clock in the data system ran slower than the GPS clock by a factor of 17/18, meaning that every 18 seconds (on average), 2 GPS samples were received during a “1 second” CPU cycle, only one sample of which was logged. This resulted in an apparent jump in position between one-second samples of approximately 56 metres, or equivalently, an apparent doubling of the helicopter speed during this one-second interval. The relocated data have been checked, and when profiles are plotted against the relocated positions, the sampling distance between points is uniform (not so when the apparent speed doubled), indicating the correction made is accurate.

The relocated data were then interpolated to generate the channels X_RT90FIXINT and Y_RT90FIXINT (See Appendix D) that were used for gridding. Based on these coordinates RT90_LAT and RT90_LONG are produced.

C.6 Post Processing: Forsmark Magnetic Data

This section describes the processing undertaken following the Forsmark survey to generate the final magnetic data sets. The magnetic data processed were loaded into the NewMagVLFWithFiby databases from the XYZ files generated from each flight. This database was created using the method in which the zero-times in the GPS time channel were defaulted prior to applying the necessary level corrections.

The original magnetic data, in nanoTesla, is archived in the RAWMAG channel. These data were low pass filtered using a 5-point (1/2 second) filter to generate the MagFixFilt Channel. Base station data are archived in the MAG_FIBY (nanoTesla) channel, and was then linearly interpolated to generate the MAG_FIBY_INT channel.

No tie line levelling was performed, since magnetic gradients in the area were large, and would introduce more levelling errors than the tie-line method could resolve. No heading errors were applied, owing to insufficient evidence that a significant heading dependence, in comparison to the gradients present in the survey area, could be measured.

The MAG_CORR channel contains the base station corrected magnetic data, and was generated with $MAG_CORR = MagFixFilt - MagFibyInt + 50900$. The MAG_CORR channel was then lagged by 0.4 seconds to generate the MAG_LAG channel. The MAG_LAG channel was then gridded to form a total magnetic field grid. The data were gridded using a cell size of 15 metres. Subsequent to this, the magnetic data were relevelled to account for the variations in the current in the DC power line by SGU. The relevelled data were then returned to NGU for gridding.

Standard first derivative filters were run over the magnetic data to generate first and second vertical derivative maps.

C.7 Post Processing: Forsmark EM Data

This section describes the processing undertaken following the Forsmark survey to generate the final EM and resistivity data sets. The EM data processed were loaded into the ForsmarkEM database from the XYZ files generated from each flight with NS lines. East-west lines were loaded into the EW ForsmarkEM database. These EM data included both the raw and the levelled data from each flight. The characteristics of the EM system are summarized in the table below.

Label	Frequency Label	Frequency (Hz)	Coil Orientation	Coil Separation (m)
A	F1	7001	Coaxial	6.0
B	F2	6606	H. Coplanar	6.0
C	F3	980	Coaxial	6.0
D	F4	880	H. Coplanar	6.0
E	F5	34133	H. Coplanar	4.2

An initial inspection of the EM data indicated that the in-phase channels for frequencies F1, F2, F3 and F4 were heavily influenced by magnetic susceptibility in the area since much of the area was highly resistive. Accordingly, the apparent resistivity maps were generated using the quadrature and apparent bird height channels to minimize the effect of susceptibility. To test this hypothesis, the effect of the apparent susceptibility on the in-phase response was calculated, and correlated well with the measured magnetic field strength.

The apparent bird height was calculated from the radar altimeter by subtracting 30 metres, the length of the tow cable. The resulting channel exhibited strong variations due, for example, to the effect of tree height, and so was filtered with a 40 point (4 second) non-linear filter to remove spurious variations. It is felt that 4 seconds corresponds to the amount of time the pilot would use to adjust the elevation of the helicopter when approaching a stand of trees.

Electromagnetic measurements are sensitive to the height of the measurement, with signal penetration falling off rapidly as a function of altitude. Accordingly, when the apparent bird height exceeded 60 metres, the calculated resistivity was defaulted out, the result being that large patches, often over power lines, are defaulted out and are not gridded.

The EM data in the Forsmark survey were heavily contaminated with pulsing noise, often to such an extent that on certain channels, it was difficult to determine what was the “pulse on” noise and what was pulse free data. The pulses affected both on-line data and background measurements, with the result being that much of the data required heuristic levelling. It proved to be difficult to develop a filter to identify the noise, and much of the noise was removed manually. This manual noise removal was accomplished by copying the levelled data (*_L) into a channel (*_LEDIT), and defaulting out sections of data contaminated with pulses. Often, due to the confusing quality of the pulses, this procedure was carried out on an iterative basis by comparing adjacent lines and related channels, working from where the noise initially appeared into where it became intense, until the suspect pulses were eliminated.

The resistivity data were generated from the level-edited channels (*_LEDIT), which were then filtered to generate (*_LFILT) and subsequently re-levelled data channels (*_LADJ). The filter applied was a 7 point (0.7 second) non-linear filter, which was necessary to remove noise from power lines in the survey area. Re-levelling was required to remove minor level variations that resulted from non-linearity in the drift between background null measurements, and because of the presence of the pulsating noise. Levels were adjusted where striping in the resistivity map was associated with a specific flight line or group of lines subject to common nulling measurements. Level adjustments were made over laterally uniform resistive patches of ground to quadrature channel until this striping was minimized. A certain amount of such striping will always occur in resistivity maps if there is a variation of resistivity with depth and a variation in bird height from line to line. The reason for this is that the average field penetration depth is a function of altitude, so different altitudes will yield different apparent resistivities over vertically inhomogeneous ground.

Resistivity channels generated were INV_RES_Q*H, where * represents the frequency number. A lag of 0.5 seconds was applied, and defaults (dummy values) applied where the apparent bird height exceeded 60 metres to generate the resistivity channel RES_?_LAG.

The processing of the XY channels to generate the positions for the grids is described in the section C.5.

C.8 Post Processing: Forsmark Radiometric Data

This section describes the processing undertaken following the Forsmark survey to generate the final radiometric data sets. The radiometric data on north-south lines were loaded into the ForsmarkRadiometrics database from the XYZ files generated from each flight. East-west line data were loaded into EW ForsmarkRadiometrics. These data included the raw and partially processed data from each flight. The partially processed data were discarded and the radiometric data were processed en masse using the Geosoft RPS software. Extensive documentation has been prepared on the calibration of the radiometric instrumentation in the Forsmark and Simpevarp QC reports (Appendix B).

The basic processing steps are as follows. The raw uranium (U), thorium (TH), potassium (K), total count (TC) and upward uranium (UPU) channels (all in counts per second) were deadtime corrected using the instrument livetime channel (LIVETIME, milliseconds). Cosmic corrections were then applied to the deadtime corrected channels using the COSMIC channel (counts per second). No filtering was applied to the data, except for the cosmic channel, which had a 5 second low pass filter applied to improve the counting statistics. Since the survey area was relatively flat, the cosmic count rate should be approximately uniform over it, and filtering should not degrade the resolution of the data. The resulting processed channels are labeled *_FILT.

Background was then removed using the upward looking crystal methods with a 4 second filter. This resulted in a number of RADREF channels being generated. The RADREF channels represent the predicted radon background levels for each radio-element channel. Long filters on the RADREF channel generated unsatisfactory edge effects on the end of the line, while the 4 second filter generated unsatisfactory short period oscillations, unlikely to be representative of the actual radon levels. The RADREF channels were therefore filtered with a 60-point non-linear filter over each line⁶, with the original RADREF channel being added to the output leveled channels (*_LVL), and the filtered RADREF then subtracted from the leveled data. Inspection of the profiles indicated this processing step was an effective method of representing the effect of the radon clouds. The resulting levelled channels are labelled *_LVL and represent the count rate per second due to radiometric sources on the ground.

The levelled data were then stripped and converted to apparent radioelement concentrations on the ground, with the potassium channel KCORR being in %, the THCORR and UCORR channels being in ppm, and the TCCORR being in counts. The channel TCEXP represents the exposure rate in micro-R/hr, and this value was computed using the default value provided by the Geosoft RPS processing package.

The radar altimeter channel (RALTM) was filtered using a 40 point (4 second) non-linear filter to remove variations, for example, due to reflections from trees and recorded in RALTM_FILT. Grids were prepared by processing the XY navigation data according to the method outlined in the section C.5.

Grids were prepared using a cell size of 15 metres for each of the corrected channels. Herringbone offsets of 56 metres were consistently noticed over the east-west trending shorelines, correlated with the flight path. This distance corresponds to approximately 2 seconds of flight time, and was removed by lagging the radiometric data by 1 second. The resulting data are stored in the *_LAG channels.

C.9 Post Processing: Forsmark VLF Data

Usually the transmitter GBR (16,0 kHz) was used as the INLINE station and NAA (24 kHz) as the ORTHO station for the north-south profiling, and the opposite for east-west profiling. Occasionally NPM (23.4 kHz) replaced NAA when this was not operating.

The only processing of these VLF data was a linear trend removal. Processing was performed at NGU in Trondheim. Map production is described in Appendix E.

⁶ In Simpevarp, a polynomial was used, and generated results equivalent to the non-linear filter. However, in Forsmark, the variable length of the lines made polynomial-fit filtering unreliable, with the filtering depending on the length of the line. Accordingly, a non-linear filter was employed.

C.10 Coordinate Transform Methodology in Geosoft

This section documents the transformation used to convert WGS84 XY to WGS84 lat-long and RT90 lat-long.

Define the coordinate system:

XY->WGS84-LAT-LONG

menu->COORDINATE->SET PROJECTION

[PROJECTION][MODIFY]

PROJECTED(X,Y) ->next-> WGS84/ UTMZONE 33 N -> next -> WGS84/
WGS84(WORLD) -> next -> METRE [ok]

Generate WGS84 lat-long:

menu->COORDINATE->NEW PROJECTED COORDINATE

x/Y/BLANK/IGNORE -> next -> OK -> LATWGS84/LONGWGS84 -> [MODIFY]
(define coordinate) GEOGRAPHIC LAT/LONG -> next

WGS84 -> next -> WGS84 -> OK

Generate RT90 lat-long:

menu->COORDINATE->NEW PROJECTED COORDINATE

x/Y/BLANK/IGNORE -> next -> OK -> LATRT90/LONGRT90 -> modify -> GEO-
GRAPHIC LAT/LONG -> NEXT (datum) RT90

-> (local datum xform) RT90 SWEDEN -> OK

Generate RT90 XY:

menu->COORDINATE->NEW PROJECTED COORDINATE

x/Y/BLANK/IGNORE -> next -> OK -> X_RT90/Y_RT90 -> modify -> Projected(x,y) ->
NEXT (datum) RT90 (projection method) Swedish National Projection

-> (local datum xform) RT90 SWEDEN -> OK

Data delivery formats

Forsmark Geosoft XYZ file formats, Final Delivery

Data are separated in files for Radiometric data, EM-data and Magnetic/VLF data. “Production lines” and “Test and Calibration lines” are also separated and named as indicated underneath (—**Test.xyz** indicating test and calibration data).

EW Forsmark Radiometric.xyz, EW Forsmark Radiometric Test.xyz, NS Forsmark Radiometric.xyz and NS Forsmark Radiometric Test.xyz

Flight		Flight number
Date		Date YMMDD; Y = year, MM = month, DD = Day of month
UTCtime		Universal time Hours:Minutes:Seconds.Decimal_seconds
recnum		Internal record number, ordinal, per flight; incremented at 0.1 per tenth of a second
X_RT90FIXINT	metres	X, RT90 corrected
Y_RT90FIXINT	metres	Y, RT90 corrected
RT90_LAT	deg:min:sec	Latitude, RT90, based on X_RT90FIXINT
RT90_LONG	deg:min:sec	Longitude, RT90, based on Y_RT90FIXINT
RALTM	metres	Radar altimeter, unfiltered
TCEXP_LAG	micoR/hr	Exposure
TCCORR_LAG		Apparent total count concentration, /Geosoft 2001/
UCORR_LAG	ppm	Apparent U concentration
THCORR_LAG	ppm	Apparent Th concentration
KCORR_LAG	%	Apparent K concentration
TEMP	Degrees C	Temperature
BARO	mBar	Barometric altimeter

EW Forsmark EM.xyz and EW Forsmark EM.Test.xyz

FLIGHT		Flight number
Date		Date YMMDD; Y = year, MM = month, DD = Day of month
UTCtime		Universal time Hours:Minutes:Seconds.Decimal_seconds
recnum		Internal record number, ordinal, per flight; incremented at 0.1 per tenth of a second
X_RT90FIXINT	metres	X, RT90 corrected
Y_RT90FIXINT	metres	Y, RT90 corrected
RT90_LAT	deg:min:sec	Latitude, RT90, based on X_RT90FIXINT
RT90_LONG	deg:min:sec	Longitude, RT90, based on Y_RT90FIXINT
RALTM	metres	Radar altimeter, unfiltered
BIRD_HT	metres	Computed bird height
IP1_LFILT	ppm	F1 Inphase (7001 Hz Coaxial)
IP2_LFILT	ppm	F2 Inphase (6606 Hz Coplanar)
IP3_LFILT	ppm	F3 Inphase (980 Hz Coaxial)
IP4_LFILT	ppm	F4 Inphase (880 Hz Coplanar)
IP5_LFILT	ppm	F5 Inphase (34133 Hz Coplanar)
Q1_LADJ	ppm	F1 Quadrature (7001 Hz Coaxial)
Q2_LADJ	ppm	F2 Quadrature (6606 Hz Coplanar)
Q3_LFILT	ppm	F3 Quadrature (980 Hz Coaxial)
Q4_LADJ	ppm	F4 Quadrature (880 Hz Coplanar)
Q5_LADJ	ppm	F5 Quadrature (34133 Hz Coplanar)
RES_1_LAG	ohm-m	F1 Resistivity (7001 Hz Coaxial)
RES_2_LAG	ohm-m	F2 Resistivity (6606 Hz Coplanar)
RES_4_LAG	ohm-m	F4 Resistivity (880 Hz Coplanar)
RES_5_LAG	ohm-m	F5 Resistivity (34133 Hz Coplanar)

NS Forsmark EM.xyz and NS Forsmark EM Test.xyz

FLIGHT		Flight number
Date		Date YMMDD; Y = year, MM = month, DD = Day of month
UTCtime		Universal time Hours:Minutes:Seconds.Decimal_seconds
recnum		Internal record number, ordinal, per flight; incremented at 0.1 per tenth of a second
X_RT90FIXINT	metres	X, RT90 corrected
Y_RT90FIXINT	metres	Y, RT90 corrected
RT90_LAT	deg:min:sec	Latitude, RT90, based on X_RT90FIXINT
RT90_LONG	deg:min:sec	Longitude, RT90, based on Y_RT90FIXINT
RALTM	metres	Radar altimeter, unfiltered
BIRD_HT	metres	Computed bird height
IP1_LFILT	ppm	F1 Inphase (7001 Hz Coaxial)
IP2_LFILT	ppm	F2 Inphase (6606 Hz Coplanar)
IP3_LFILT	ppm	F3 Inphase (980 Hz Coaxial)
IP4_LFILT	ppm	F4 Inphase (880 Hz Coplanar)
IP5_LADJ	ppm	F5 Inphase (34133 Hz Coplanar)
Q1_LADJ	ppm	F1 Quadrature (7001 Hz Coaxial)
Q2_LADJ	ppm	F2 Quadrature (6606 Hz Coplanar)
Q3_LFILT	ppm	F3 Quadrature (980 Hz Coaxial)
Q4_LADJ	ppm	F4 Quadrature (880 Hz Coplanar)
Q5_LADJ	ppm	F5 Quadrature (34133 Hz Coplanar)
RES_1_LAG	ohm-m	F1 Resistivity (7001 Hz Coaxial)
RES_2_LAG	ohm-m	F2 Resistivity (6606 Hz Coplanar)
RES_4_LAG	ohm-m	F4 Resistivity (880 Hz Coplanar)
RES_5IQ_INT_LAG	ohm-m	F5 Resistivity (34133 Hz Coplanar)

Note: Lines 350, 570, 640, 650, and 700 are missing.

NS EW Forsmark MAG VLF.xyz and NS EW Forsmark MAG VLF Test.xyz

Note: Data described here are delivered prior to corrections being applied for the current in the DC cable running from Forsmark power station to Finland. Parts of lines planned to be remeasured but were not are included in dataset as xxx1 lines. Line 350 is missing due to bad data quality.

FLIGHT		Flight number
Date		Date YMMDD; Y = year, MM = month, DD = Day of month
UTCtime		Universal time Hours:Minutes:Seconds.Decimal_seconds
recnum		Internal record number, ordinal, per flight; incremented at 0.1 per tenth of a second
X_RT90FIXINT	metres	X, RT90 corrected
Y_RT90FIXINT	metres	Y, RT90 corrected
RT90_LAT	deg:min:sec	Latitude, RT90, based on X_RT90FIXINT
RT90_LONG	deg:min:sec	Longitude, RT90, based on Y_RT90FIXINT
RALTM	metres	Radar altimeter, unfiltered
MAG_FIBY	nT	Base magnetic data from Fiby
MAGFixLag	nT	Levelled and lagged magnetic data
VLQ	%	Inline VLF Quadrature
VLT	%	Inline VLF Total
VOQ	%	Orthogonal VLF Quadrature
VOT	%	Orthogonal VLF Total
MAG_FIBY_NEW	nT	Base mag from Fiby, UTC time errors defaulted
MagFix	nT	Raw Magnetic data, preliminary filter applied to remove high frequency noise

Reference

Geosoft, 2001. Radiometric Processing System for OASIS Montaj. User guide and tutorial. Manual release 13.08.2001.

Gridding and Map production

Maps produced in scale 1: 20 000 were based on the final processed data (see Appendix C). Data treatment before map production is described in Table E-1. Note that navigation at lines west of line 310 is far out of specifications and due to this the data is only included in radiometric maps. Due to the same problem, parts of the lines 1530, 1540, 1550, 1930, 2030, 2080 and 60220 are not used in map production, but included in the final data delivery.

Table E-1. Maps from large area, measured in N-S direction.

Map number	Title, names and treatment of data.	Scale
2002.095-01 A	Flight Path. <i>Name - .map and - .tiff: FPATH_NS</i> <i>Grid names: forsmark1m.grd + forsmark2m.grd</i> No treatment of data Topographic background digitised from "Grøna Kartan"	1: 20 000
2002.095-02 A	Magnetic Total Field. <i>Name - .map and - .tiff: MAG_NS</i> <i>Grid name: mag_fin_m_ns.grd</i> Based on data corrected for DC line (SGU2002). Grid cell size 15 metres No treatment of data	1: 20 000
2002.095-03 A	Magnetic Vertical Derivative. <i>Name - .map and - .tiff: MAG_1VD_NS</i> <i>Grid name: Mag_vd1_ns.grd</i> Grid cell size 15 metres Calculation first order derivative /Geosoft, 1996/ No other treatment of data	1: 20 000
2002.095-04 A	EM Resistivity 880 Hz Coplanar. <i>Name - .map and - .tiff: RES4_NS</i> <i>Grid name: NSRES4_W.grd</i> Grid cell size 15 metres Decorrugation, Differential Median Filters /Mauring and Kihle, 2000/ 1D 500 metres, 2D 500 metres No other treatment of data	1: 20 000
2002.095-05 A	EM Stacked Profiles 980 Hz Coaxial. <i>Name - .map and - .tiff: EM_NS_980Hz</i> No treatment of data	1: 20 000
2002.095-06 A	EM Resistivity 6606 Hz Coplanar. <i>Name - .map and - .tiff: RES2_NS</i> <i>Grid name: NSRES2_W.grd</i> Grid cell size 15 metres Decorrugation, Differential Median Filters /Mauring and Kihle, 2000/ 1D 500 metres, 2D 500 metres No other treatment of data	1: 20 000

Map number	Title, names and treatment of data.	Scale
2002.095-07 A	EM Resistivity 7001 Hz Coaxial. <i>Name - .map and - .tiff: RES1_NS</i> <i>Grid name: NSRES1_W.grd</i> Grid cell size 15 metres Decorrugation, Differential Median Filters /Mauring and Kihle, 2000/ 1D 500 metres, 2D 500 metres No other treatment of data	1: 20 000
2002.095-08 A	EM Resistivity 34133 Hz Coplanar. <i>Name - .map and - .tiff: RES5_NS</i> <i>Grid name: NSRES5_W.grd</i> Grid cell size 15 metres Decorrugation, Differential Median Filters /Mauring and Kihle, 2000/ 1D 500 metres, 2D 500 metres No other treatment of data	1: 20 000
2002.095-09 A	Radiometric Corrected Total Count. <i>Name - .map and - .tiff: TC_NS</i> <i>Grid name: NS_TCCORR1_M-NEWW.grd</i> Grid cell size 15 metres No other treatment of data	1: 20 000
2002.095-10 A	Radiometric Potassium concentration. <i>Name - .map and - .tiff: K_NS</i> <i>Grid name: NS_KCORR1_MW.grd</i> Grid cell size 15 metres No other treatment of data	1: 20 000
2002.095-11 A	Radiometric equivalent Uranium concentration. <i>Name - .map and - .tiff: U_NS</i> <i>Grid name: NS_UCORR1_MW.grd</i> Grid cell size 15 metres No other treatment of data	1: 20 000
2002.095-12 A	Radiometric equivalent Thorium concentration. <i>Name - .map and - .tiff: Th_NS</i> <i>Grid name: NS_THCORR1_MW.grd</i> Grid cell size 15 metres No other treatment of data	1: 20 000
2002.095-13 A	Radiometric RGB Composite Map. <i>Name - .map and - .tiff: RAD_COMP_NS</i> <i>Grid nameS:</i> <i>NS_KCORR1_MW.grd, NS_UCORR1_MW.grd and NS_THCORR1_MW.grd</i> Grid cell size 15 metres RGB composite map produced using Geosoft routine /Geosoft, 1996/ No other treatment of data	1: 20 000
2002.095-14 A	VLF-EM Total In-Line. <i>Name - .map and - .tiff: VLF_LINE_NS</i> <i>Grid name: VLT_NS_m.grd</i> Grid cell size 15 metres No other treatment of data	1: 20 000
2002.095-15 A	VLF-EM Total Orthogonal. <i>Name - .map and - .tiff: VLF_ORTO_NS</i> <i>Grid name: VOT_NS_MED_M.grd</i> Grid cell size 15 metres Decorrugation, Differential Median Filters /Mauring and Kihle, 2000/ 1D 500 metres, 2D 500 metres No other treatment of data	1: 20 000

Table E2. Maps from small area, measured in E-W direction.

Map number	Title, names and treatment of data.	Scale
2002.095-01 B	Flight Path. <i>Name - .map and - .tiff: fpath_ew</i> <i>Grid name: forsmark1m.grd + forsmark2m.grd</i> No treatment of data Topographic background digitised from "Grøna Kartan"	1: 20 000
2002.095-02 B	Magnetic Total Field. <i>Name - .map and - .tiff: mag_ew</i> <i>Grid name: mag_fin_m_ew.grd</i> Based on data corrected for DC line (SGU2002). Grid cell size 15 metres No treatment of data	1: 20 000
2002.095-03 B	Magnetic Vertical Derivative. <i>Name - .map and - .tiff: mag_1vd_ew</i> <i>Grid name: mag_vd1_ew.grd</i> Grid cell size 15 metres Calculation first order derivative /Geosoft, 1996/ No other treatment of data	1: 20 000
2002.095-04 B	EM Resistivity 880 Hz Coplanar. <i>Name - .map and - .tiff: res4_ew</i> <i>Grid name: ewres4_w.grd</i> Grid cell size 15 metres Decorrugation, Differential Median Filters /Mauring and Kihle, 2000/ 1D 500 metres, 2D 500 metres No other treatment of data	1: 20 000
2002.095-05 B	EM Stacked Profiles 980 Hz Coaxial. <i>Name - .map and - .tiff: em_ew_980Hz</i> No treatment of data	1: 20 000
2002.095-06 B	EM Resistivity 6606 Hz Coplanar. <i>Name - .map and - .tiff: res2_ew</i> <i>Grid name: ewres2_w.grd</i> Grid cell size 15 metres Decorrugation, Differential Median Filters /Mauring and Kihle, 2000/ 1D 500 metres, 2D 500 metres No other treatment of data	1: 20 000
2002.095-07 B	EM Resistivity 7001 Hz Coaxial. <i>Name - .map and - .tiff: res1_ew</i> <i>Grid name: ewres1_w.grd</i> Grid cell size 15 metres Decorrugation, Differential Median Filters /Mauring and Kihle, 2000/ 1D 500 metres, 2D 500 metres No other treatment of data	1: 20 000
2002.095-08 B	EM Resistivity 34133 Hz Coplanar. <i>Name - .map and - .tiff: res5_ew</i> <i>Grid name: ewres5_w.grd</i> Grid cell size 15 metres Decorrugation, Differential Median Filters /Mauring and Kihle, 2000/ 1D 500 metres, 2D 500 metres No other treatment of data	1: 20 000
2002.095-09 B	Radiometric Corrected Total Count. <i>Name - .map and - .tiff: tc_ew</i> <i>Grid name: ew_tccorr_m_newww.grd</i> Grid cell size 15 metres No other treatment of data	1: 20 000
2002.095-10 B	Radiometric Potassium concentration. <i>Name - .map and - .tiff: K_ew</i> <i>Grid name: ew_kcorr_mw.grd</i> Grid cell size 15 metres No other treatment of data	1: 20 000

Map number	Title, names and treatment of data.	Scale
2002.095-11B	Radiometric equivalent Uranium concentration. <i>Name - .map and - .tiff: U_ew</i> <i>Grid name: ew_ucorr_mw.grd</i> Grid cell size 15 metres No other treatment of data	1: 20 000
2002.095-12 B	Radiometric equivalent Thorium concentration. <i>Name - .map and - .tiff: Th_ew</i> <i>Grid name: ew_thcorr_mw.grd</i> Grid cell size 15 metres No other treatment of data	1: 20 000
2002.095-13 B	Radiometric RGB Composite Map. <i>Name - .map and - .tiff: rad_comp_ew</i> <i>Grid name:</i> <i>ew_kcorr_mw.grd , ew_ucorr_mw.grd and ew_thcorr_mw.grd</i> Grid cell size 15 metres RGB composite map produced using Geosoft routine /Geosoft, 1996/ No other treatment of data	1: 20 000
2002.095-14 B	VLF-EM Total In-Line. <i>Name - .map and - .tiff: vlf_line_ew</i> <i>Grid name: vlt_ew_med2_m.grd</i> Grid cell size 15 metres Decorrugation, Differential Median Filters /Mauring and Kihle, 2000/ 1D 500 metres, 2D 500 metres No other treatment of data	1: 20 000
2002.095-15 B	VLF-EM Total Orthogonal. <i>Name - .map and - .tiff: vlf_orto_ew</i> <i>Grid name: vot_ew_m.grd</i> Grid cell size 15 metres No other treatment of data	1: 20 000

References

Geosoft, 1996. OASIS Montaj Version 4.0 User Guide, Geosoft Inc. Toronto.

Mauring E, Kihle O, 2000. Micro-levelling of aeromagnetic data using a moving differential median filter. NGU Report 2000.053.

Shomali H, Hagthorpe P, Byström S. Removal of DC power line influence on magnetic data in the Forsmark area – Section B of this report.

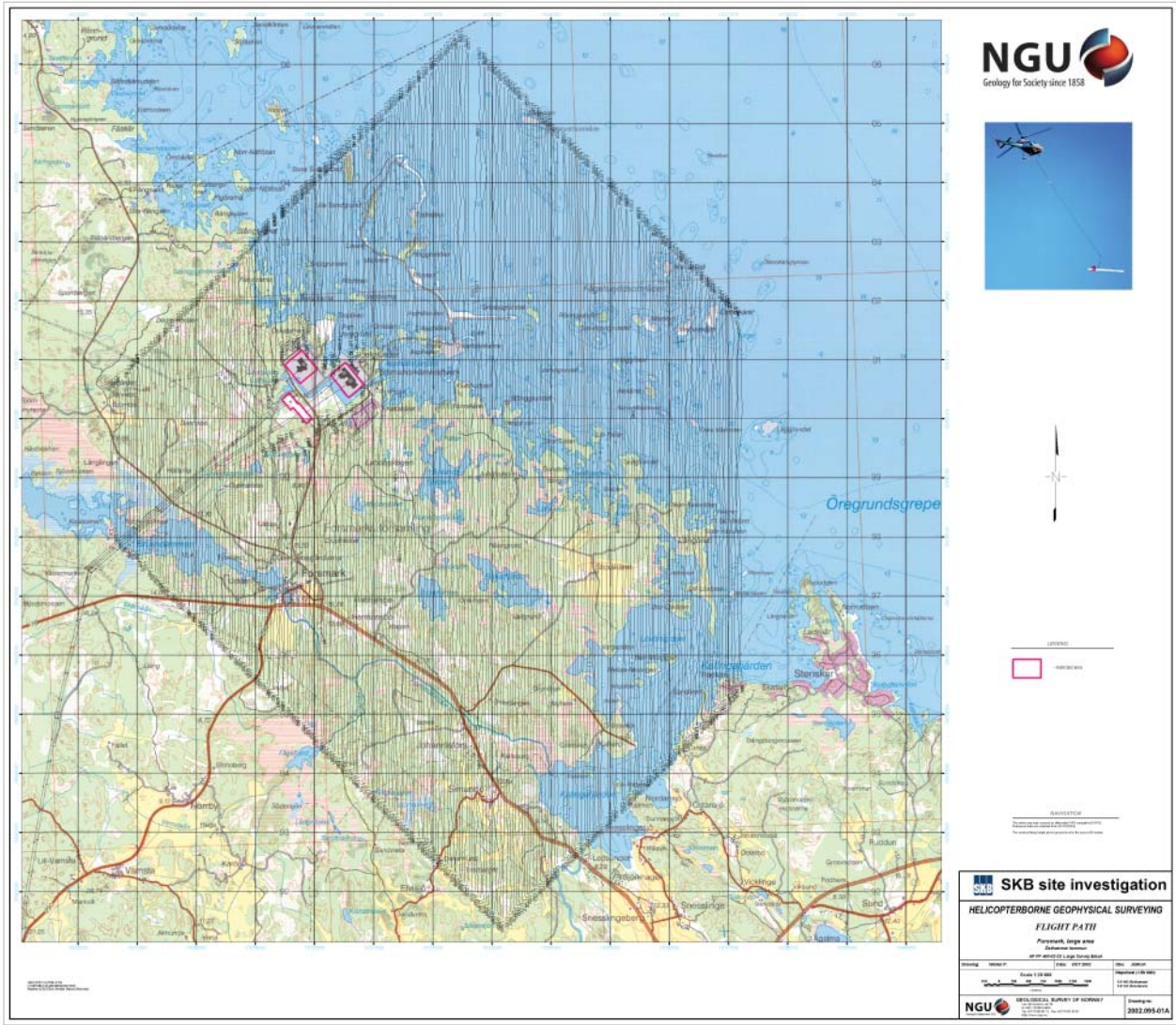


Figure F-1. Flight Path, North-South area. Map number 2002.095-01 A.

Produced and delivered maps

Appendix F

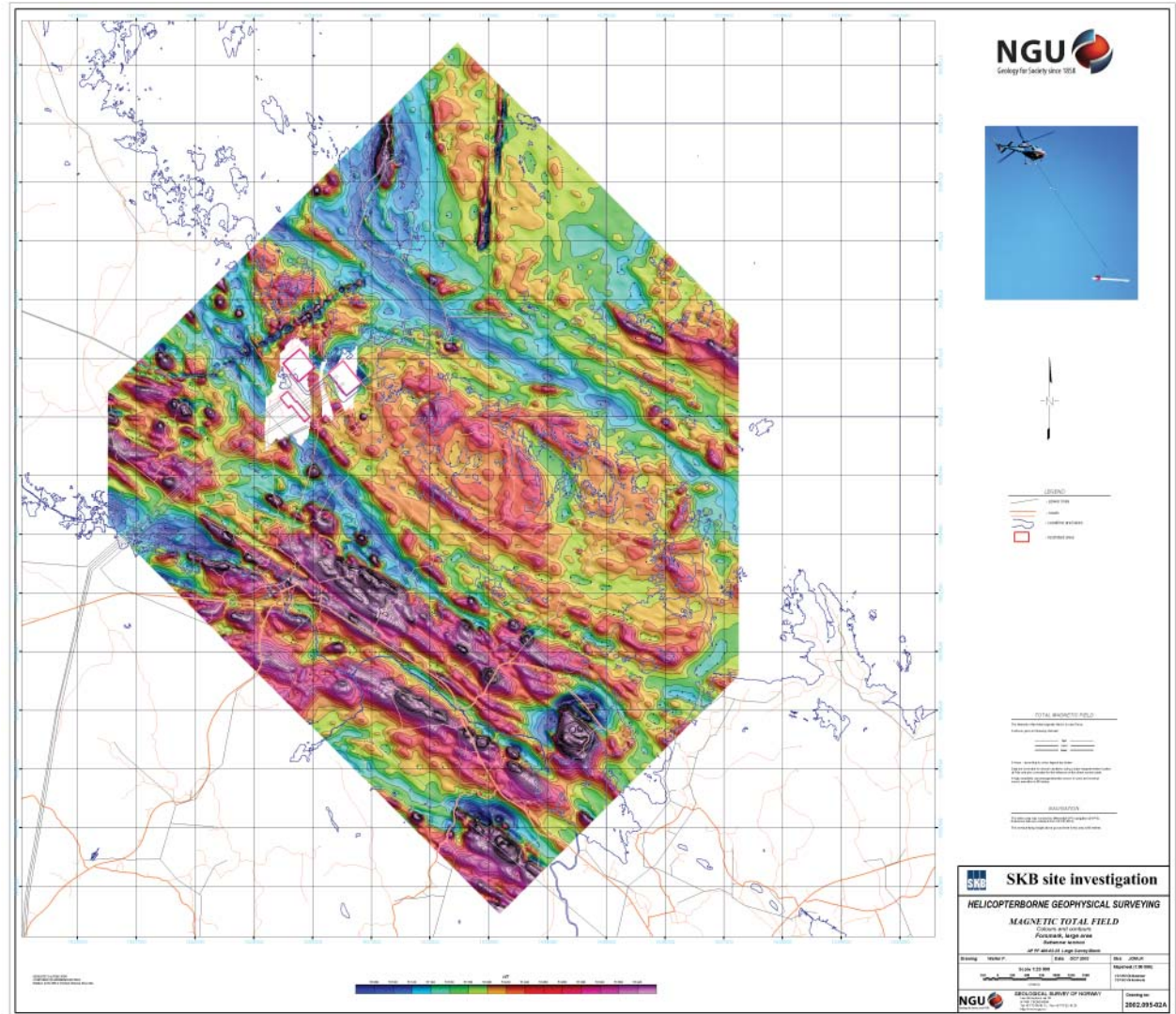


Figure F-2. Magnetic Total Field, North-South area. Map number 2002.095-02 A.

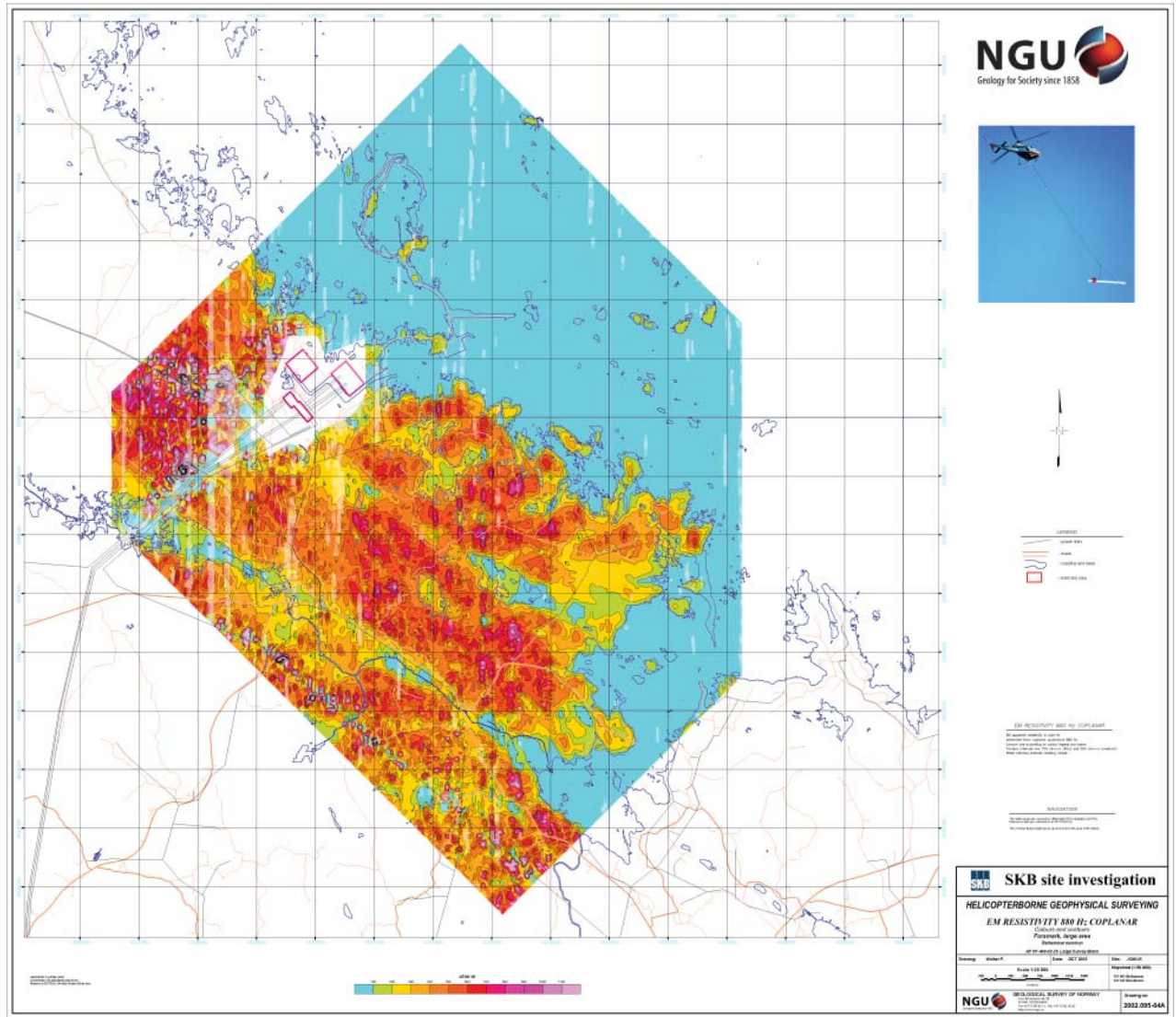


Figure F-4. EM Resistivity 880 Hz Coplanar, North-South area. Map number 2002.095-04 A.

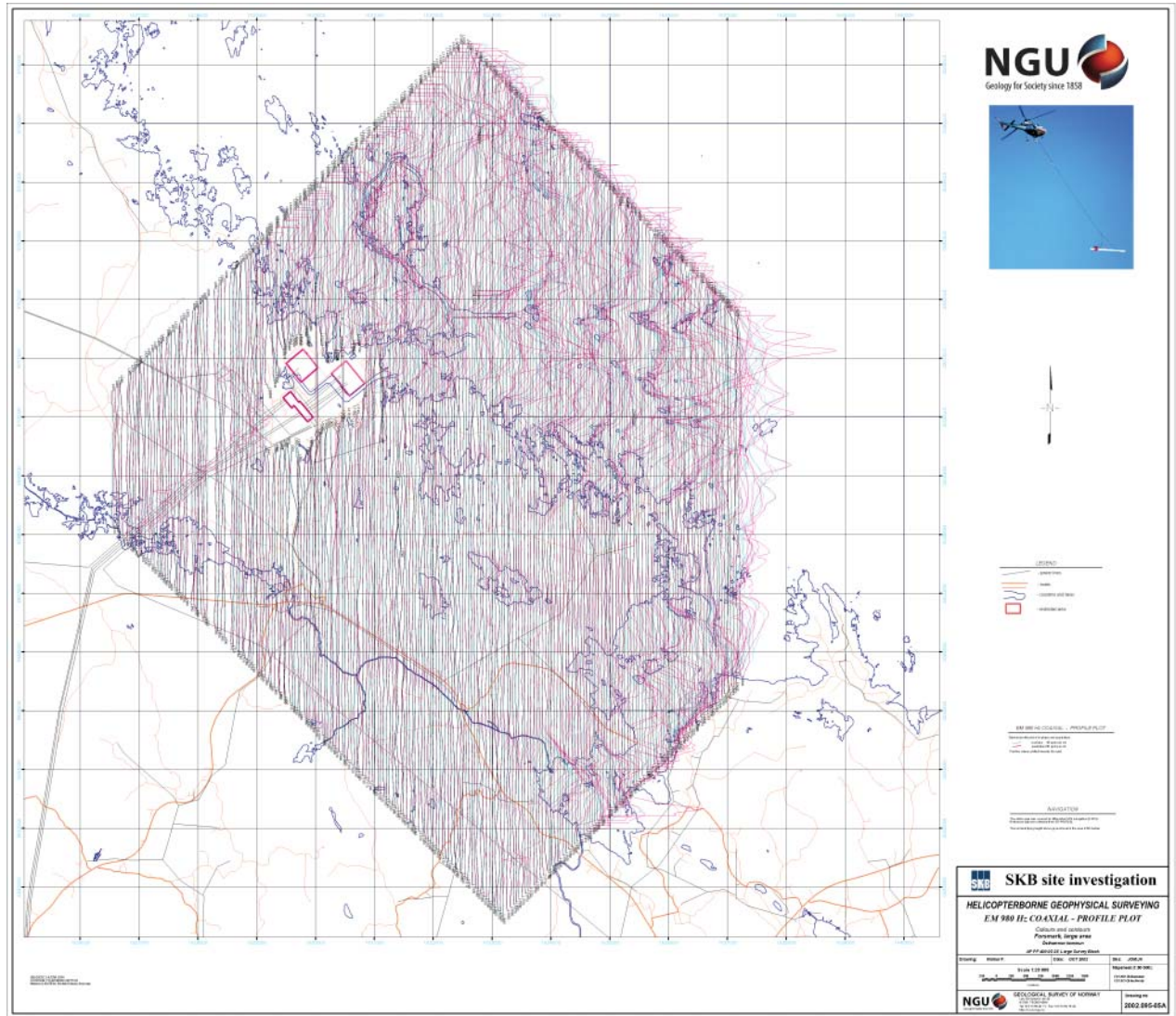


Figure F-5. EM Stacked Profiles 980 Hz Coaxial, North-South area. Map number 2002.095-05 A.

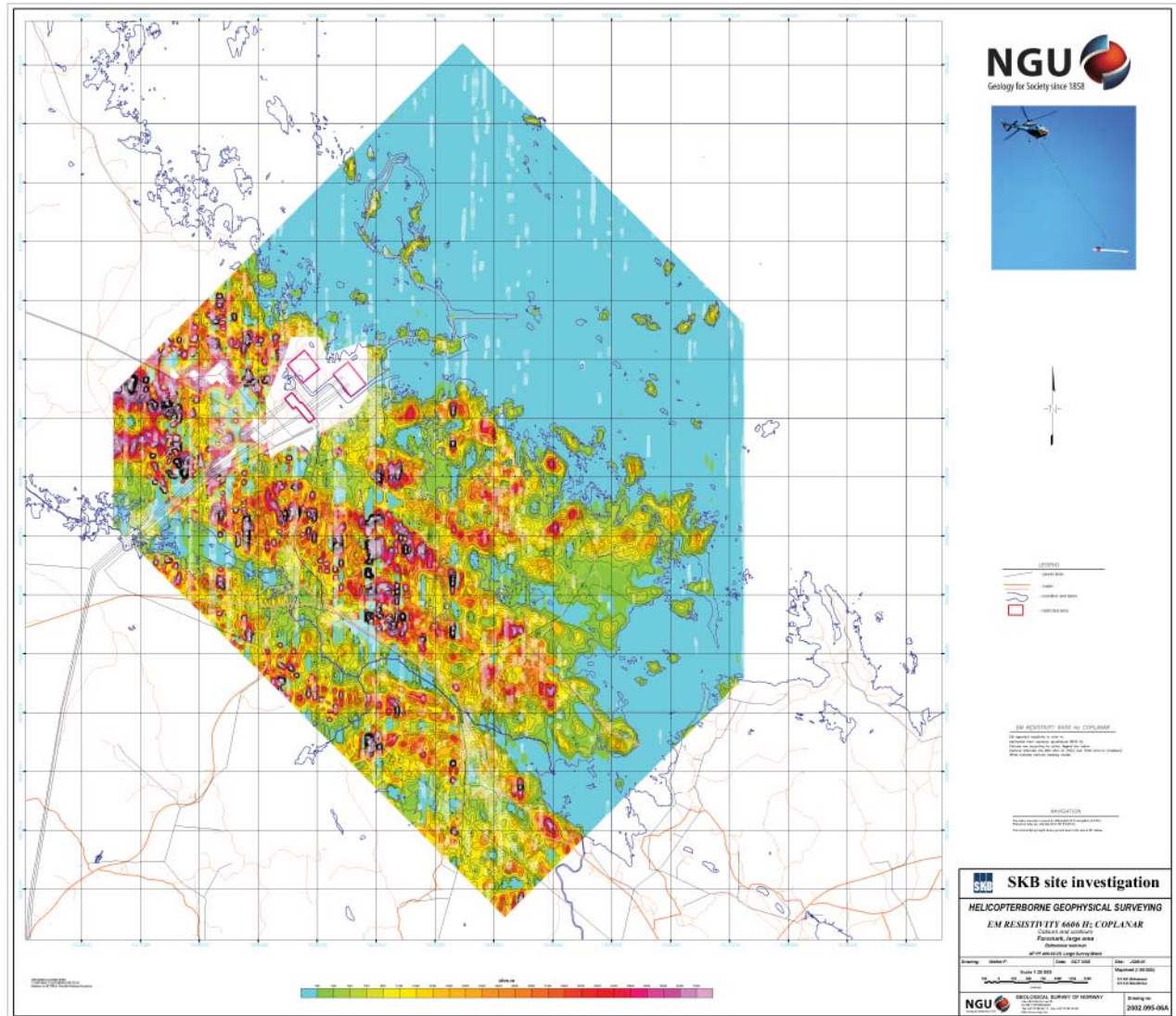


Figure F-6. EM Resistivity 6606 Hz Coplanar, North-South area. Map number 2002.095-06 A.

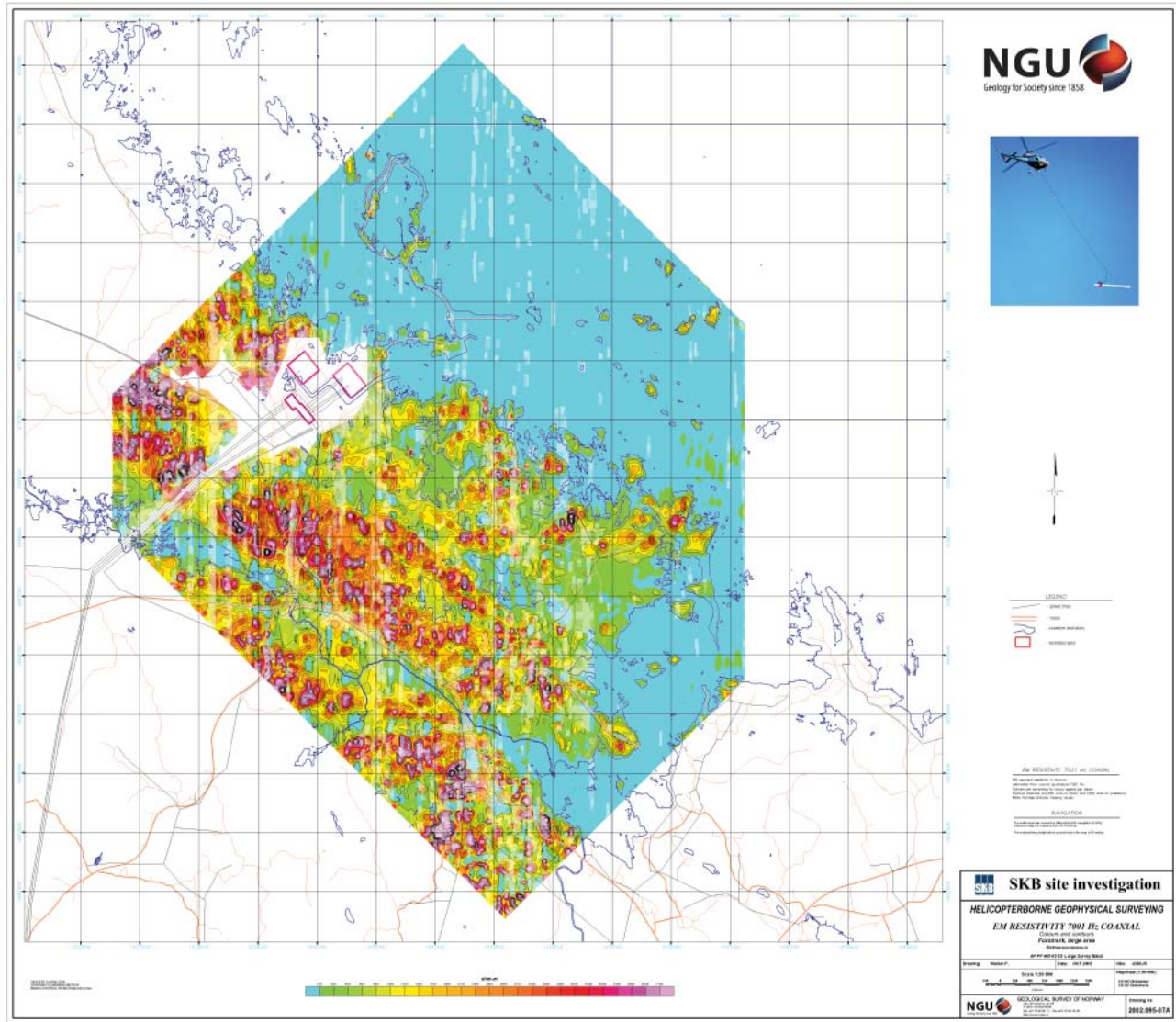


Figure F-7. EM Resistivity 7001 Hz Coaxial, North-South area. Map number 2002.095-07 A.

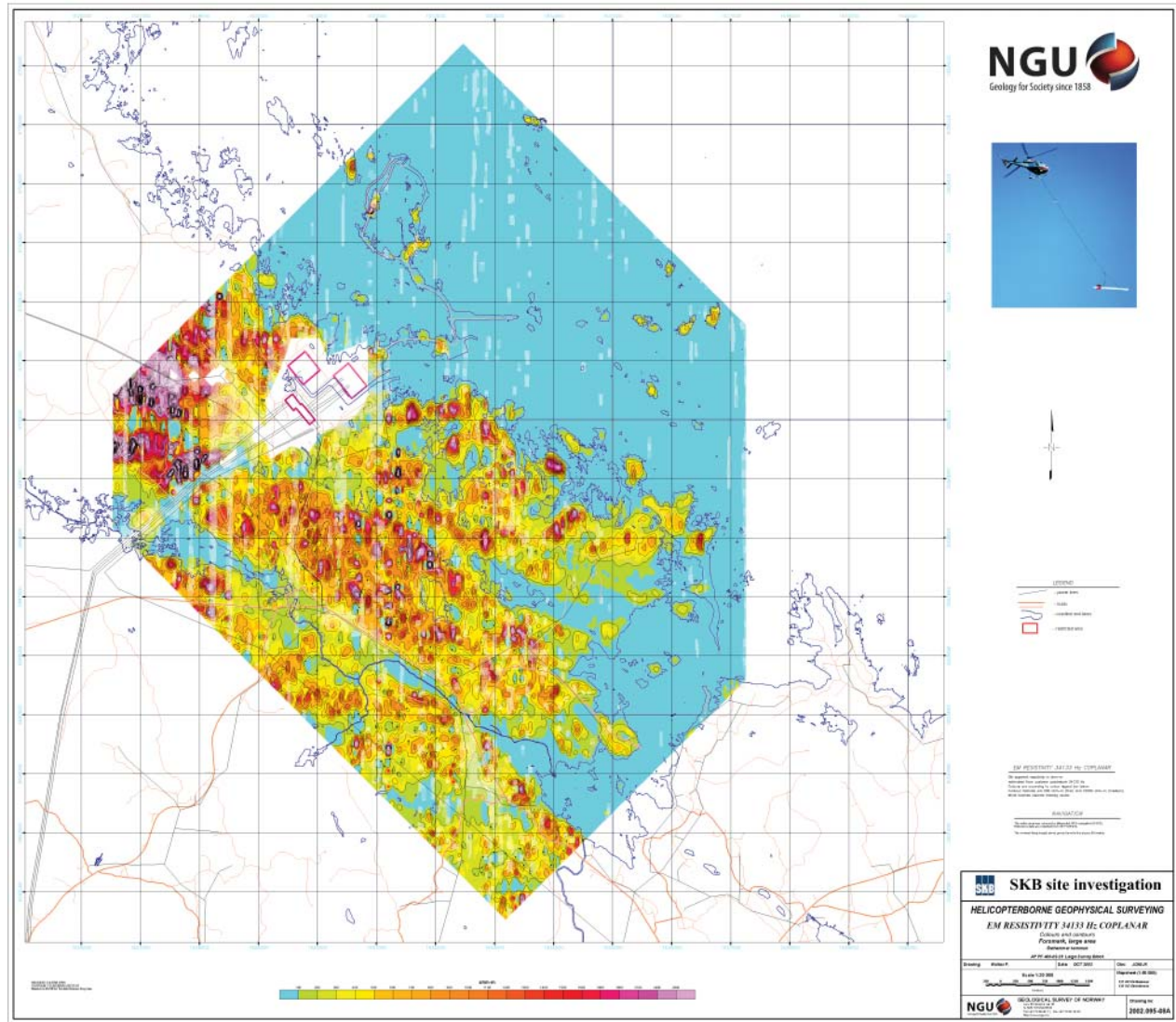


Figure F-8. EM Resistivity 34133 Hz Coplanar, North-South area. Map number 2002.095-08 A.

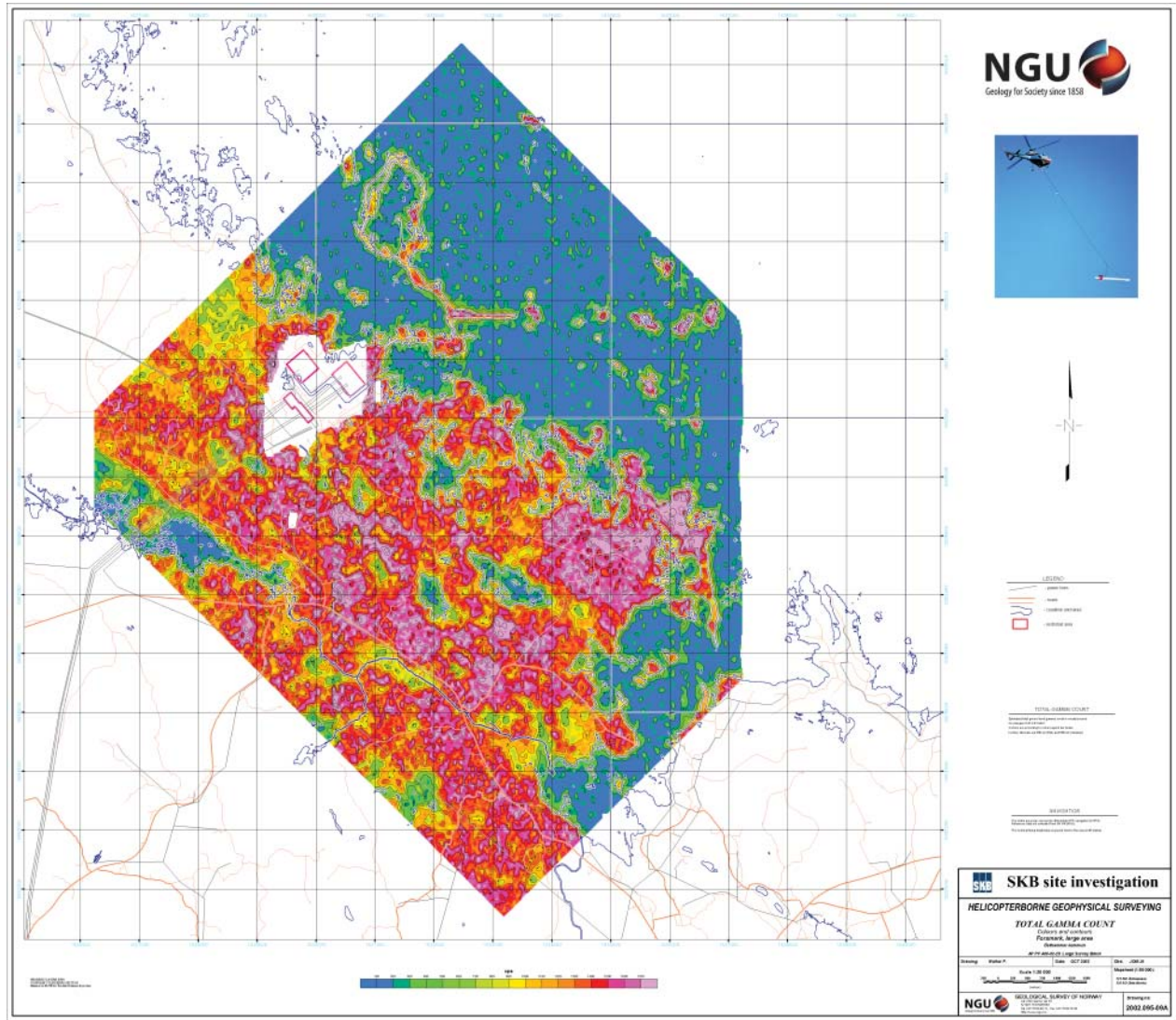


Figure F-9. Radiometric Corrected Total Count, North-South area. Map number 2002.095-09 A.

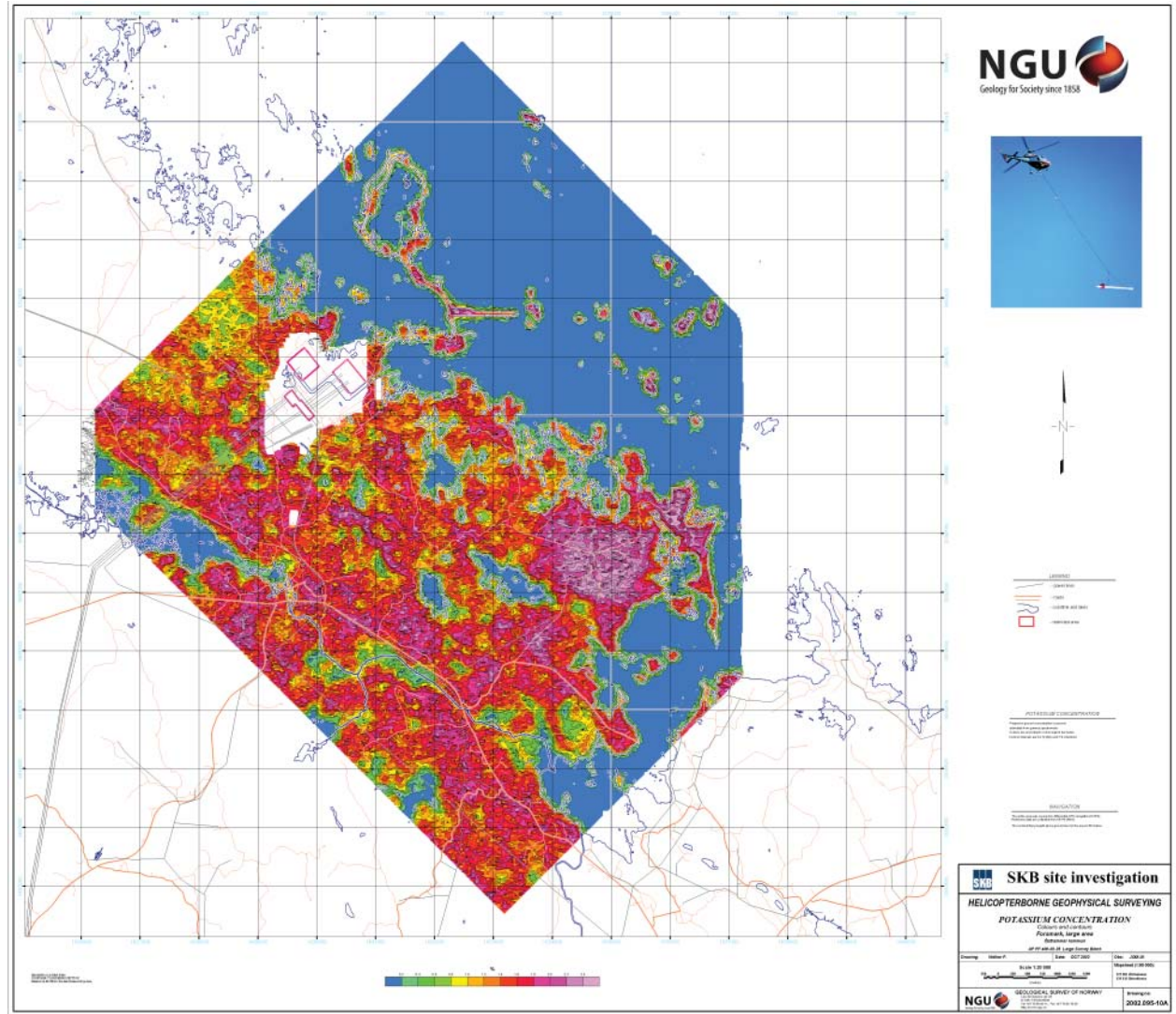


Figure F-10. Radiometric Potassium Concentration, North-South area. Map number 2002.095-10 A.

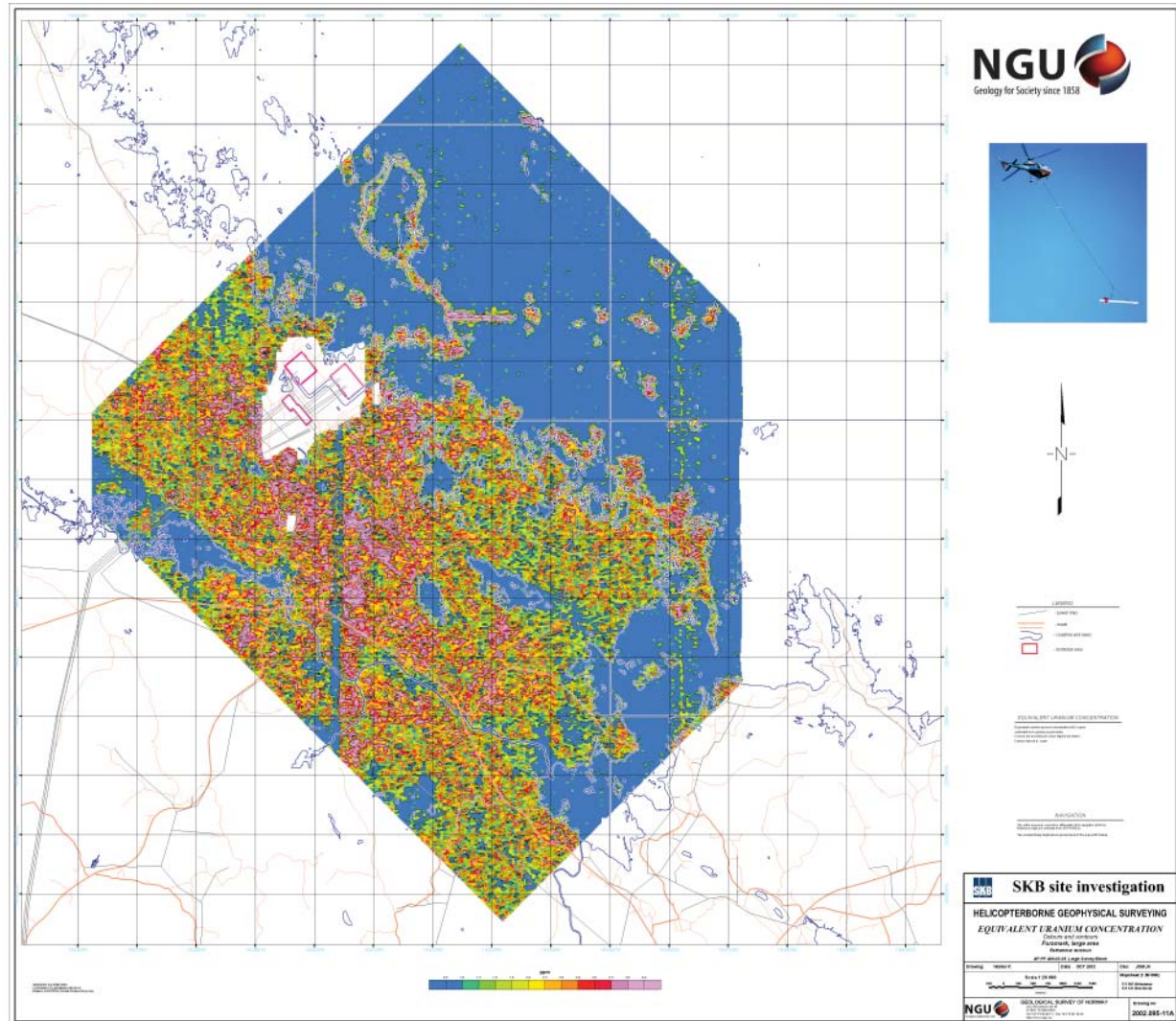


Figure F-11. Radiometric equivalent Uranium Concentration, North-South area. Map number 2002.095-11 A.

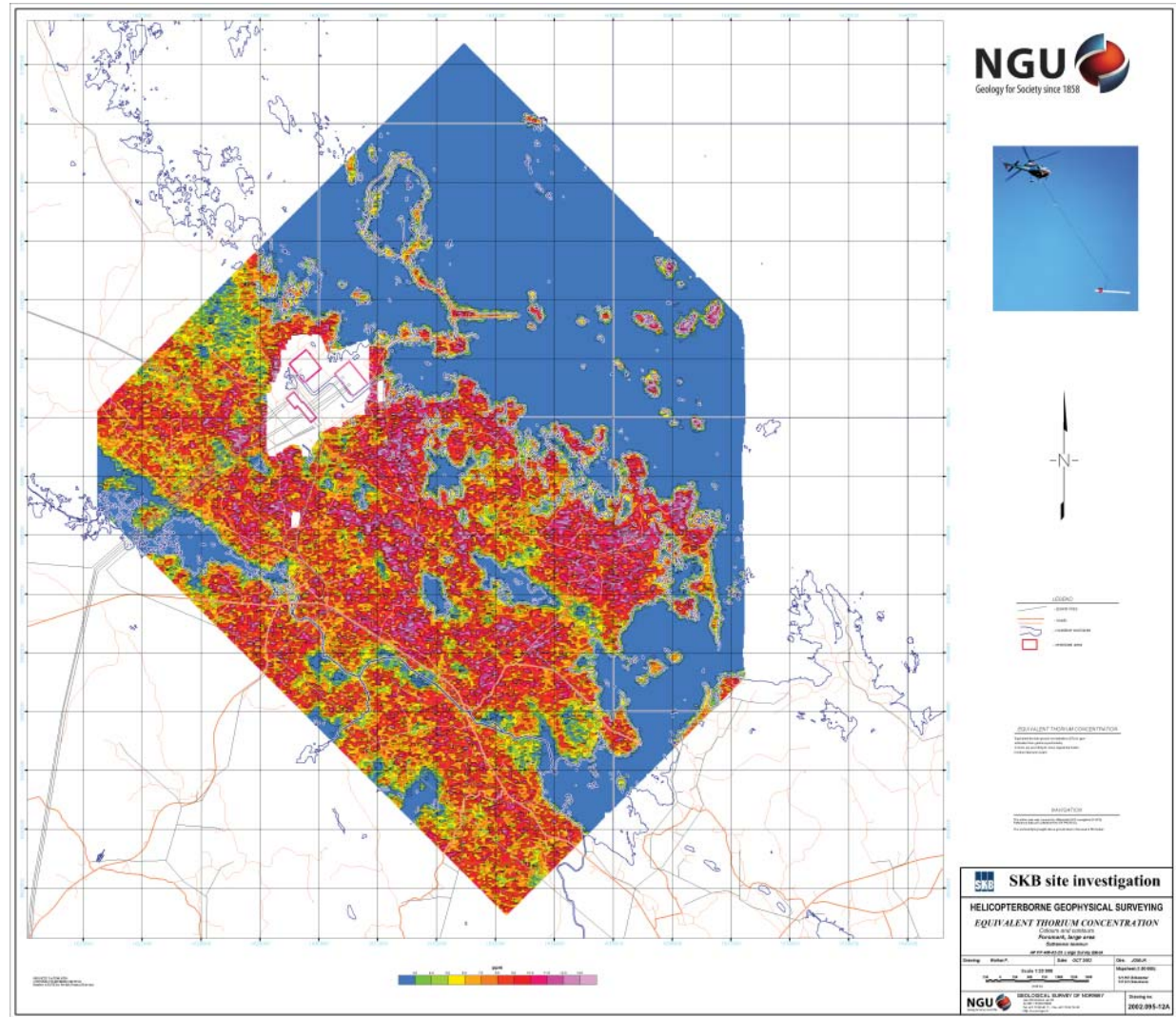


Figure F-12. Radiometric equivalent Thorium Concentration, North-South area. Map number 2002.095-12 A.

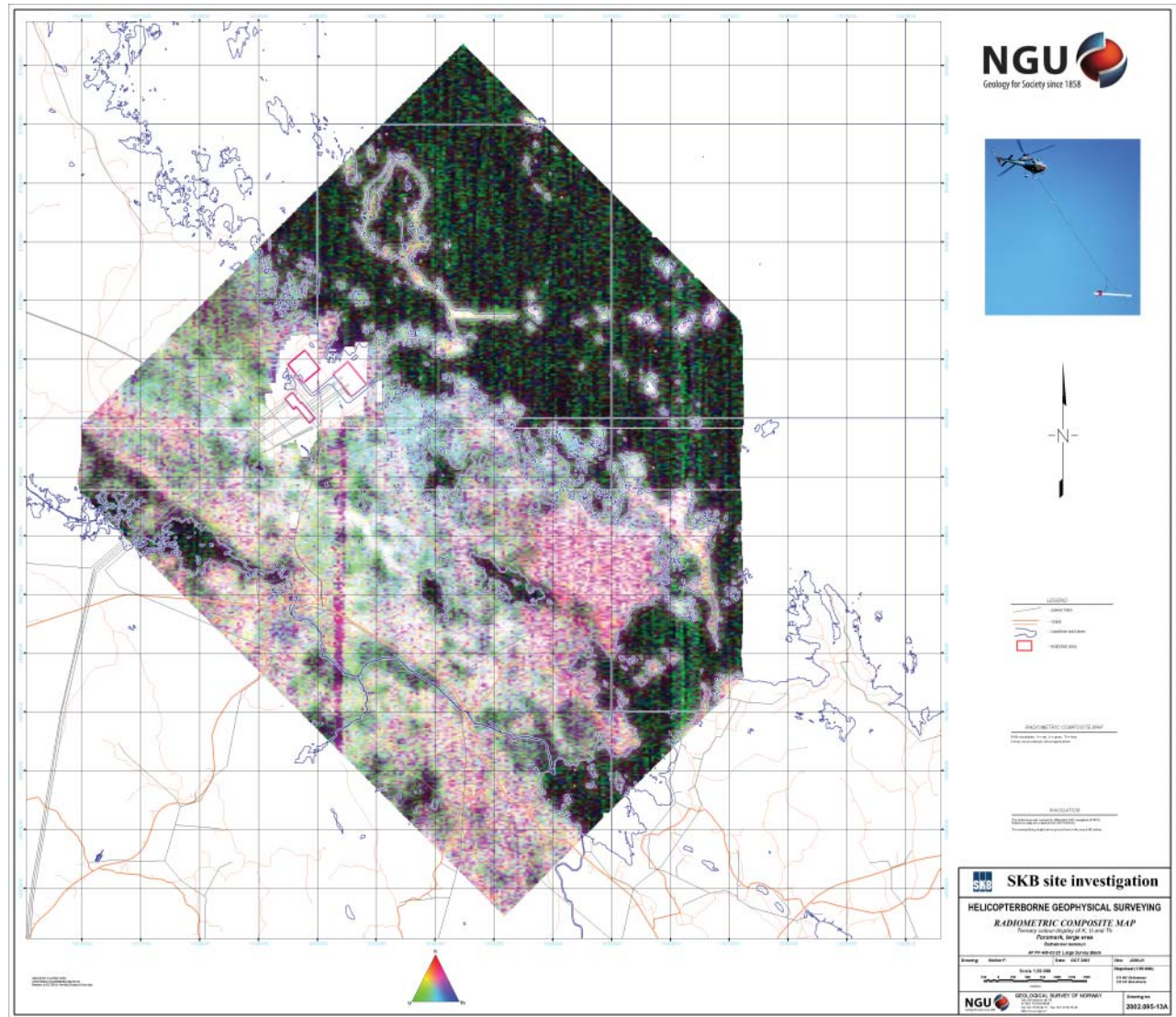


Figure F-13. Radiometric RGB Composite Map, North-South area. Map number 2002.095-13 A.

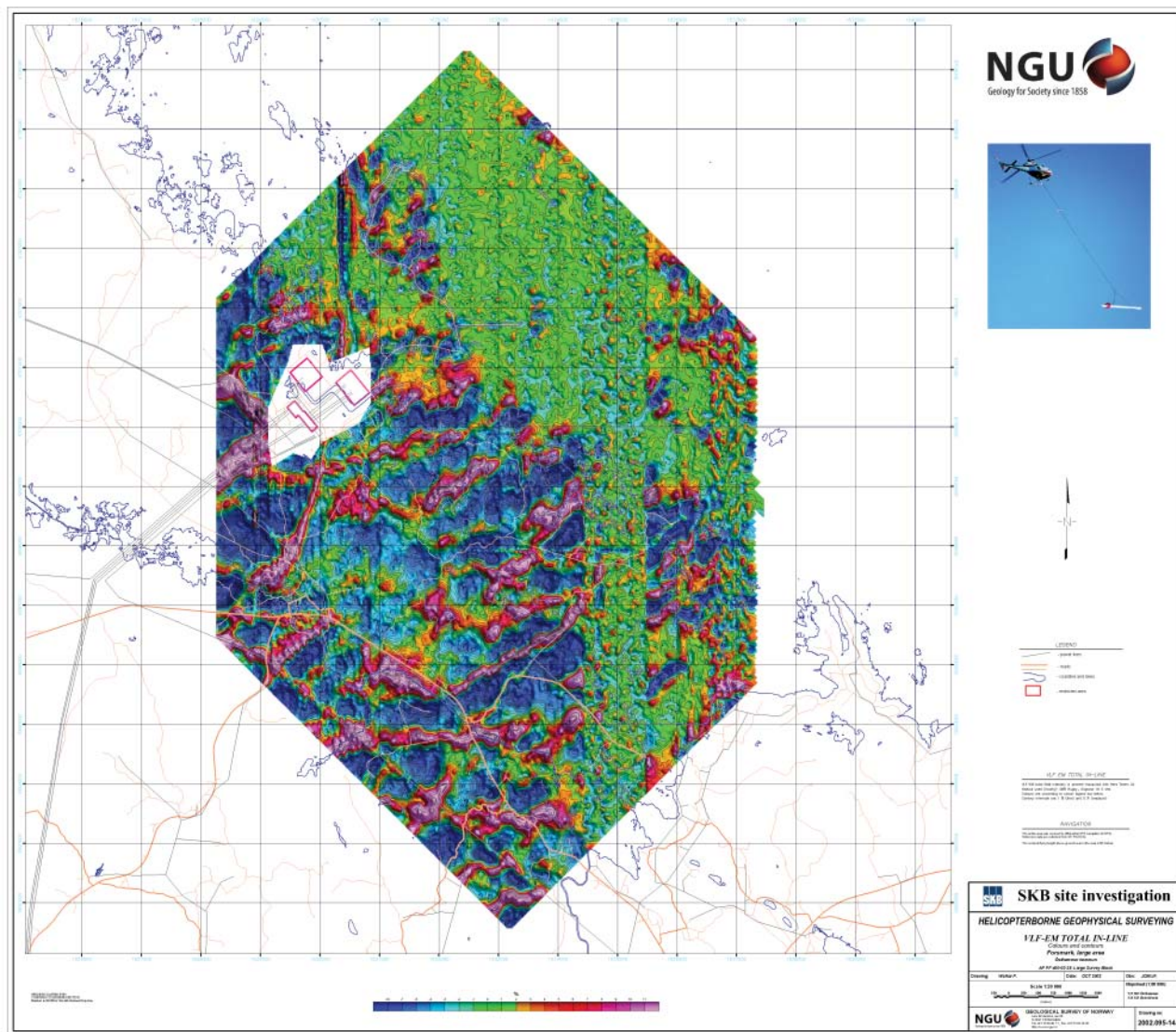


Figure F-14. VLF-EM Total In-Line, North-South area. Map number 2002.095-14 A.

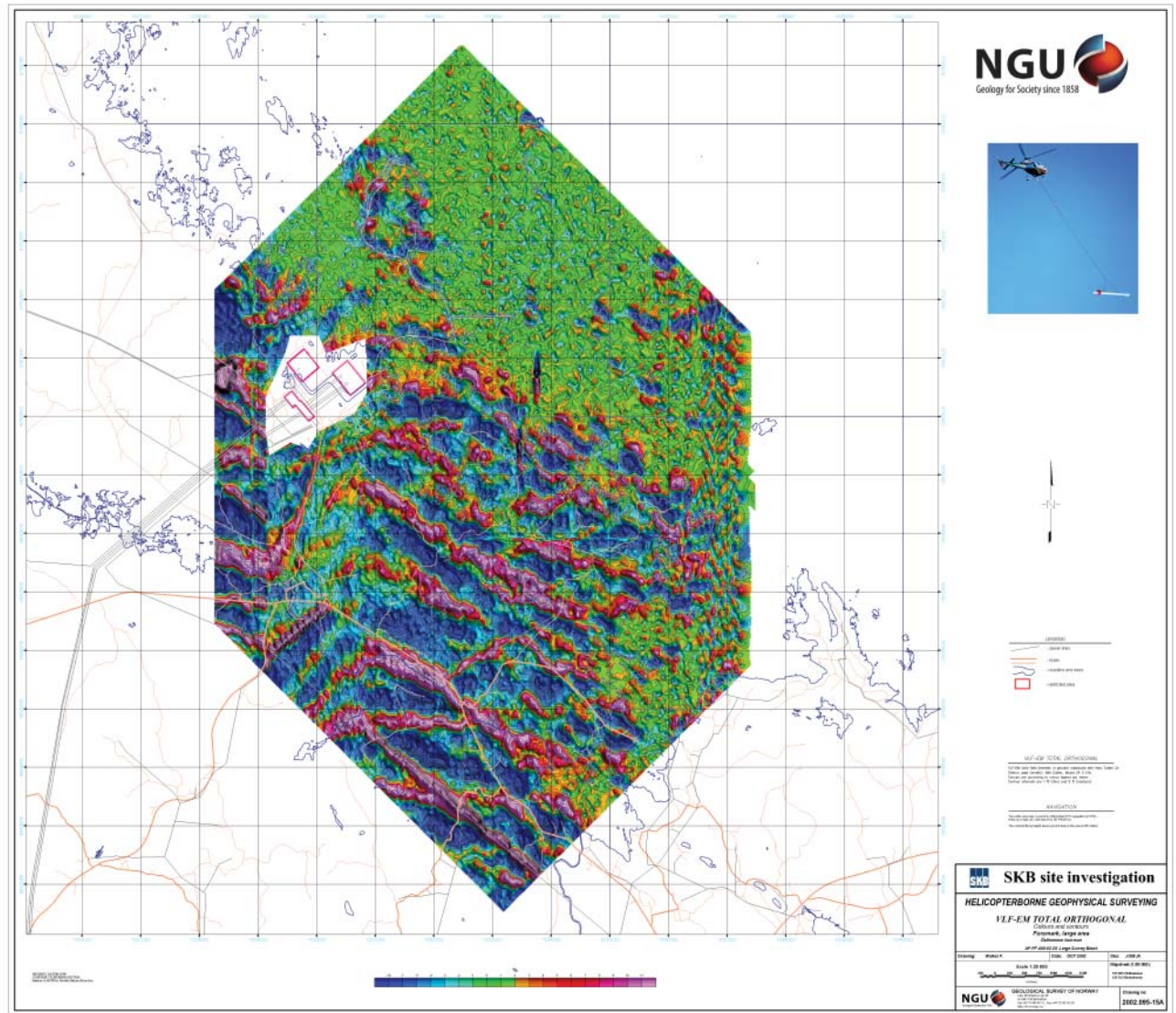


Figure F-15. VLF-EM Total Orthogonal, North-South area. Map number 2002.095-15 A.

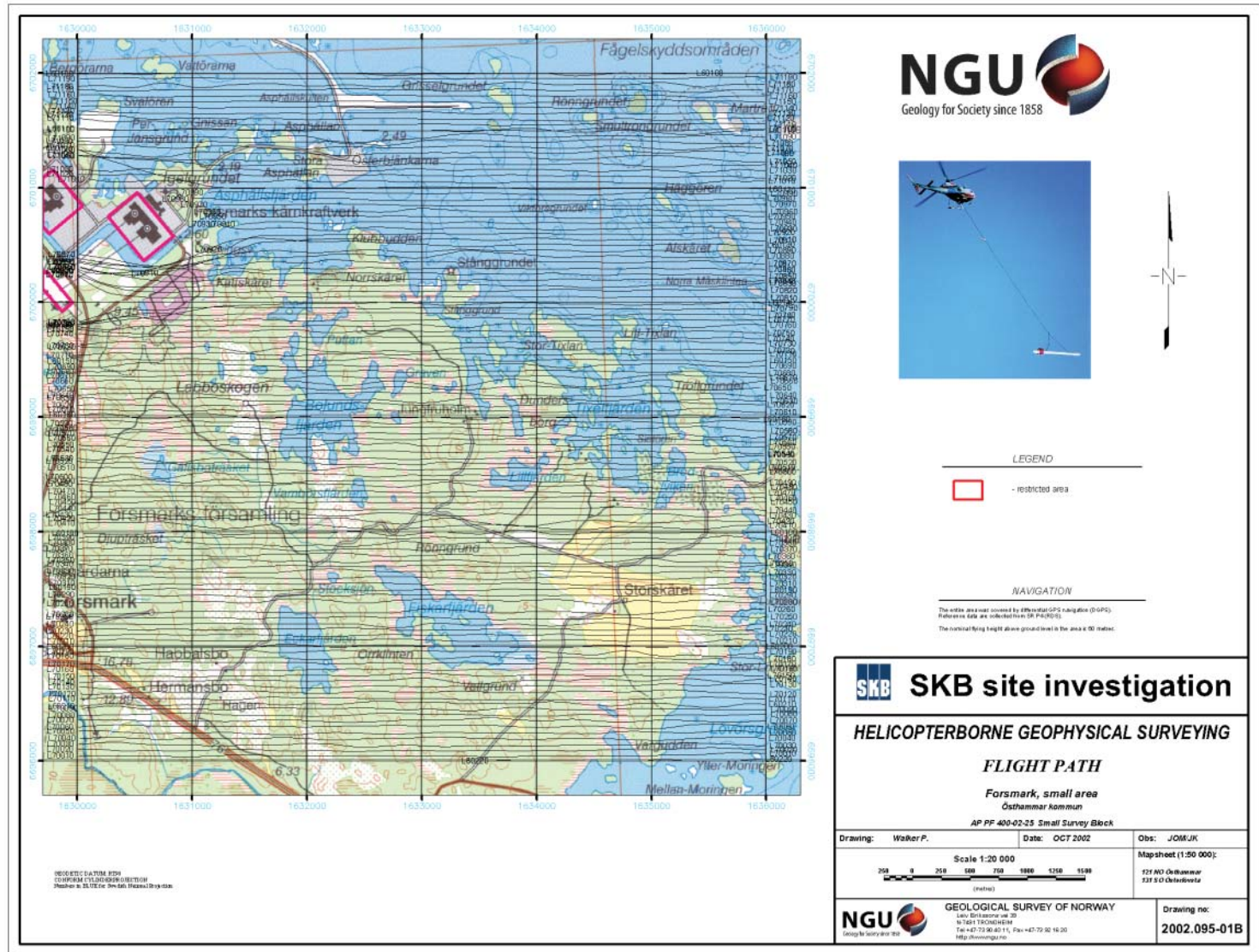


Figure F-16. Flight Path, East-West area. Map number 2002.095-01 B.

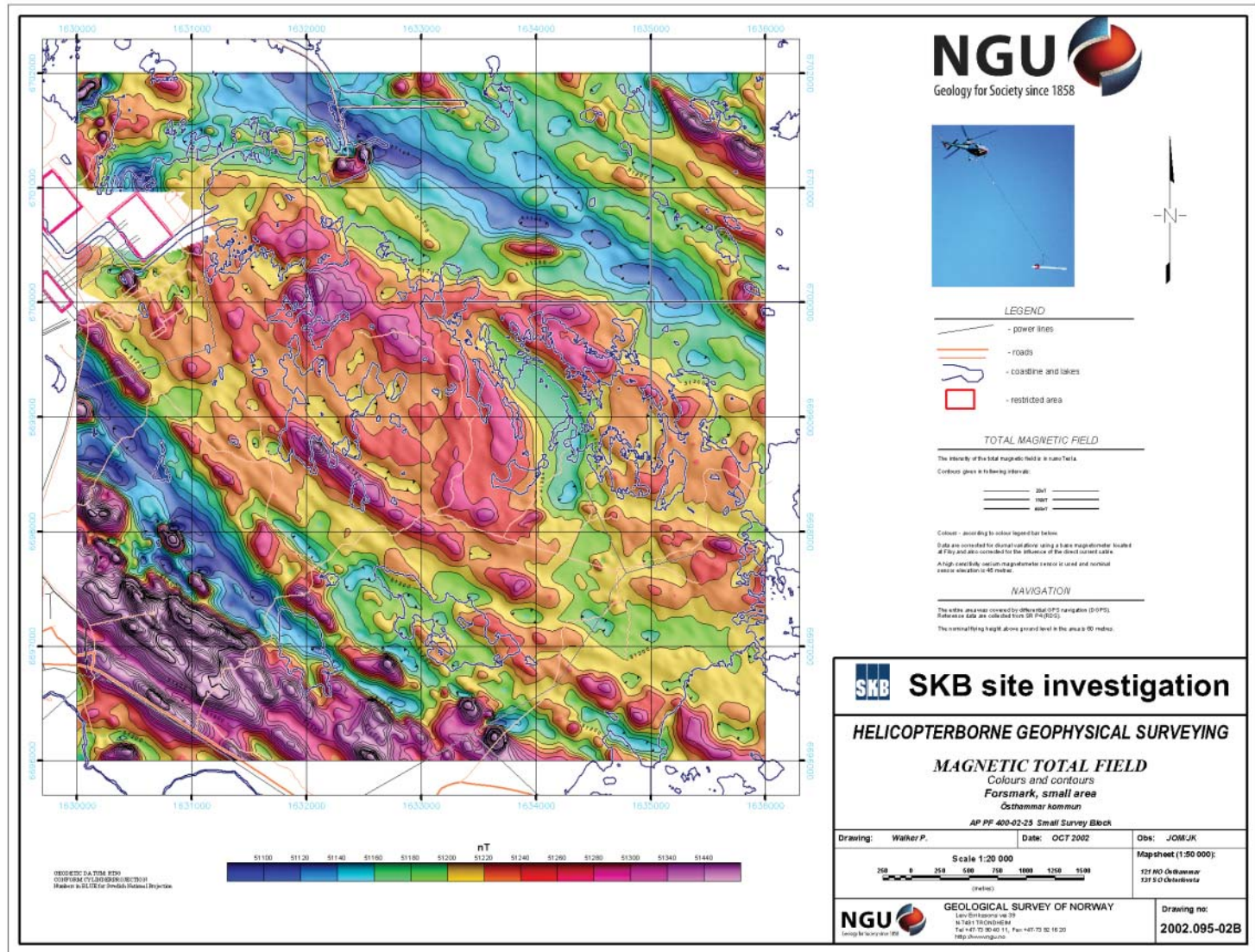


Figure F-17. Magnetic Total Field, East-West area. Map number 2002.095-02 B.

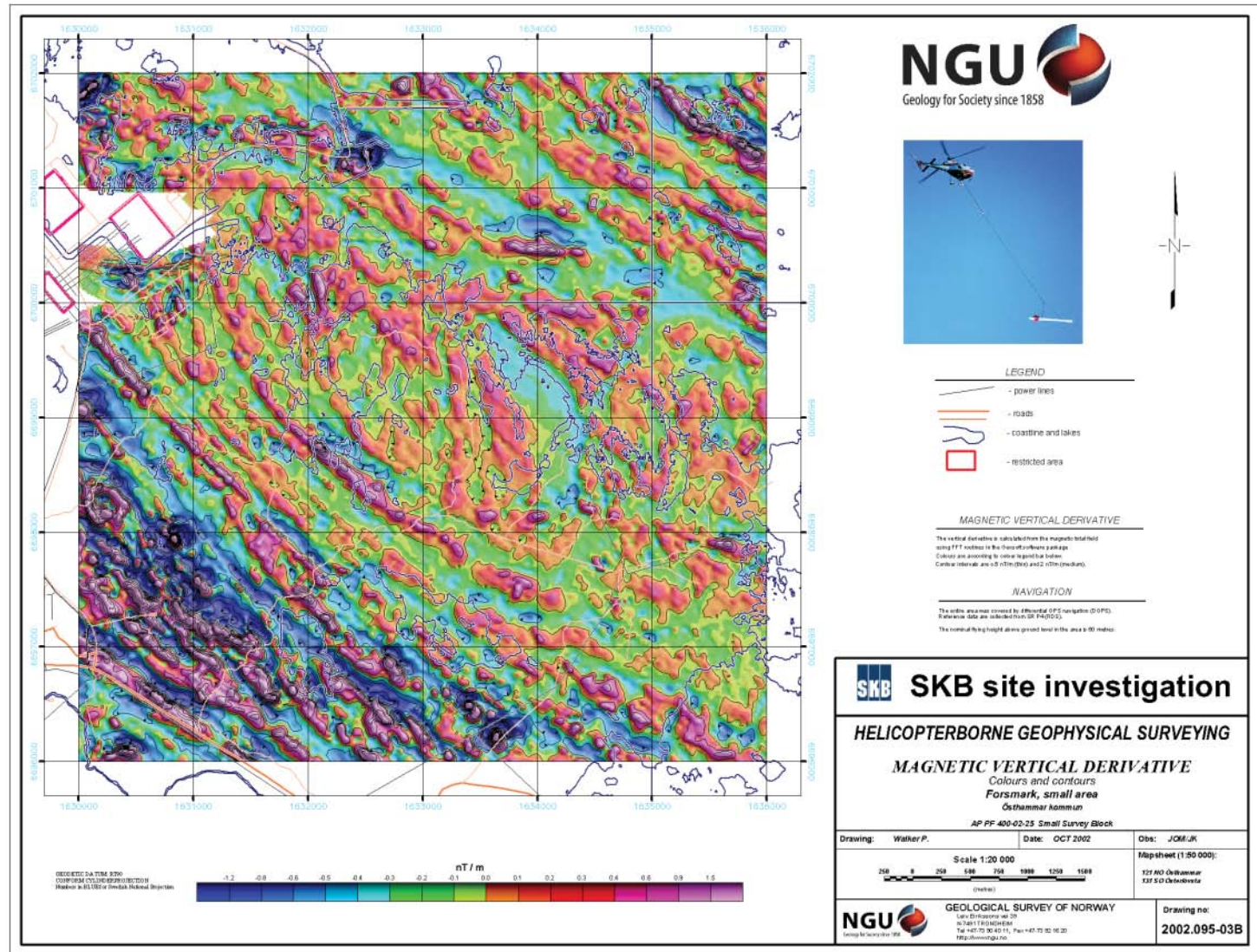


Figure F-18. Magnetic Vertical Derivative, East-West area. Map number 2002.095-03 B.

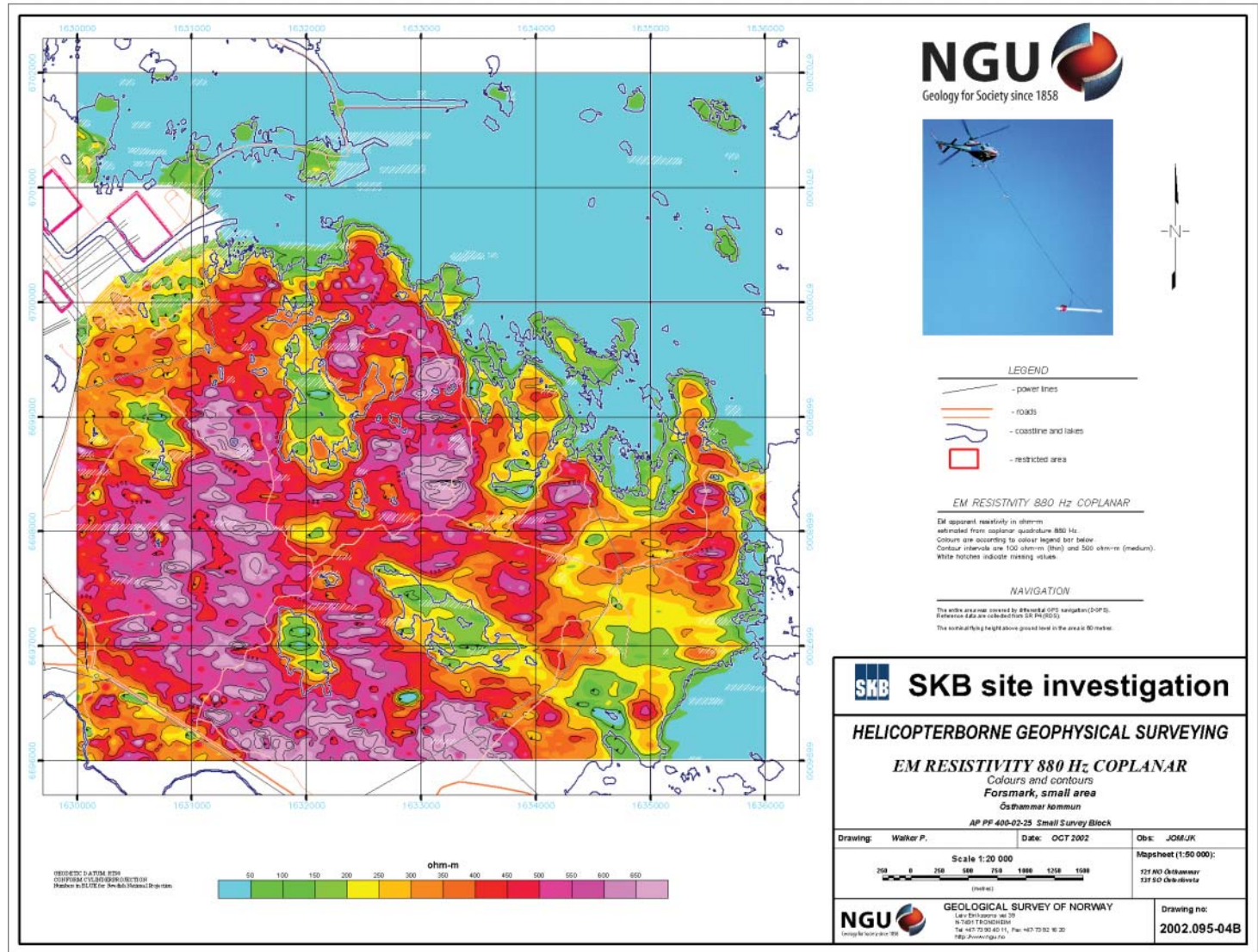


Figure F-19. EM Resistivity 880 Hz Coplanar, East-West area. Map number 2002.095-04 B.

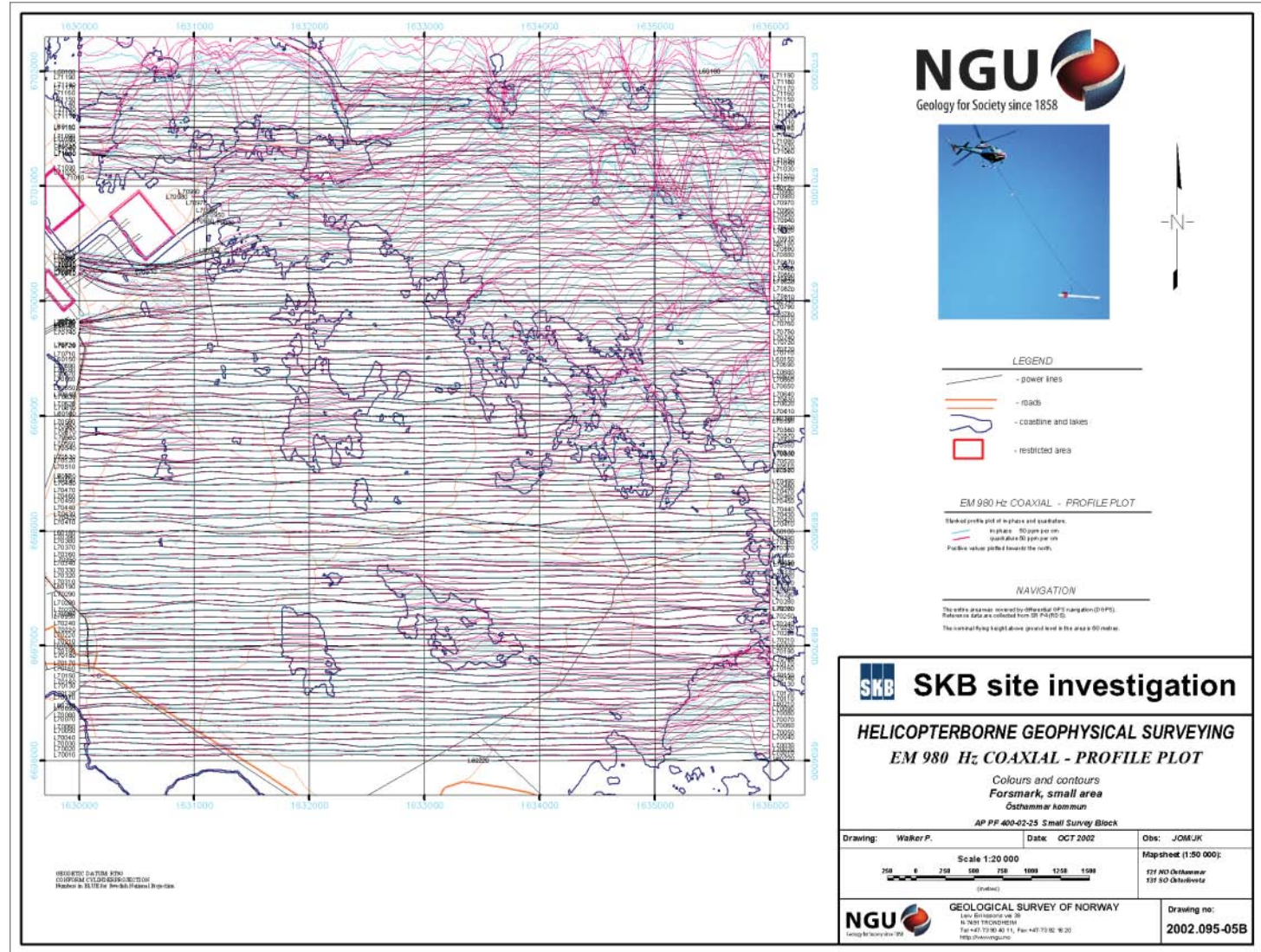


Figure F-20. EM Stacked Profiles 980 Hz Coaxial, East-West area. Map number 2002.095-05 B.

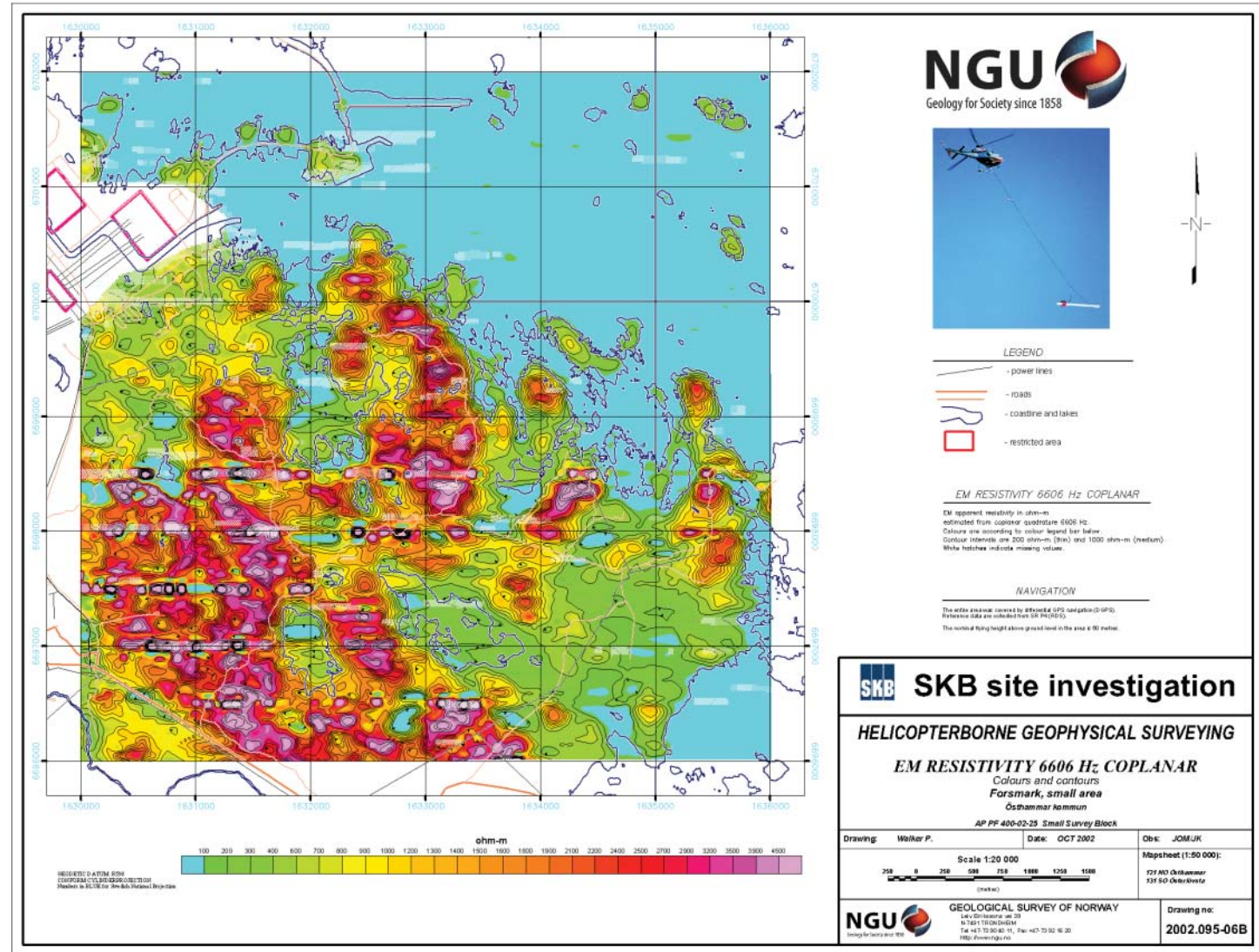


Figure F-21. EM Resistivity 6606 Hz Coplanar, East-West area. Map number 2002.095-06 B.

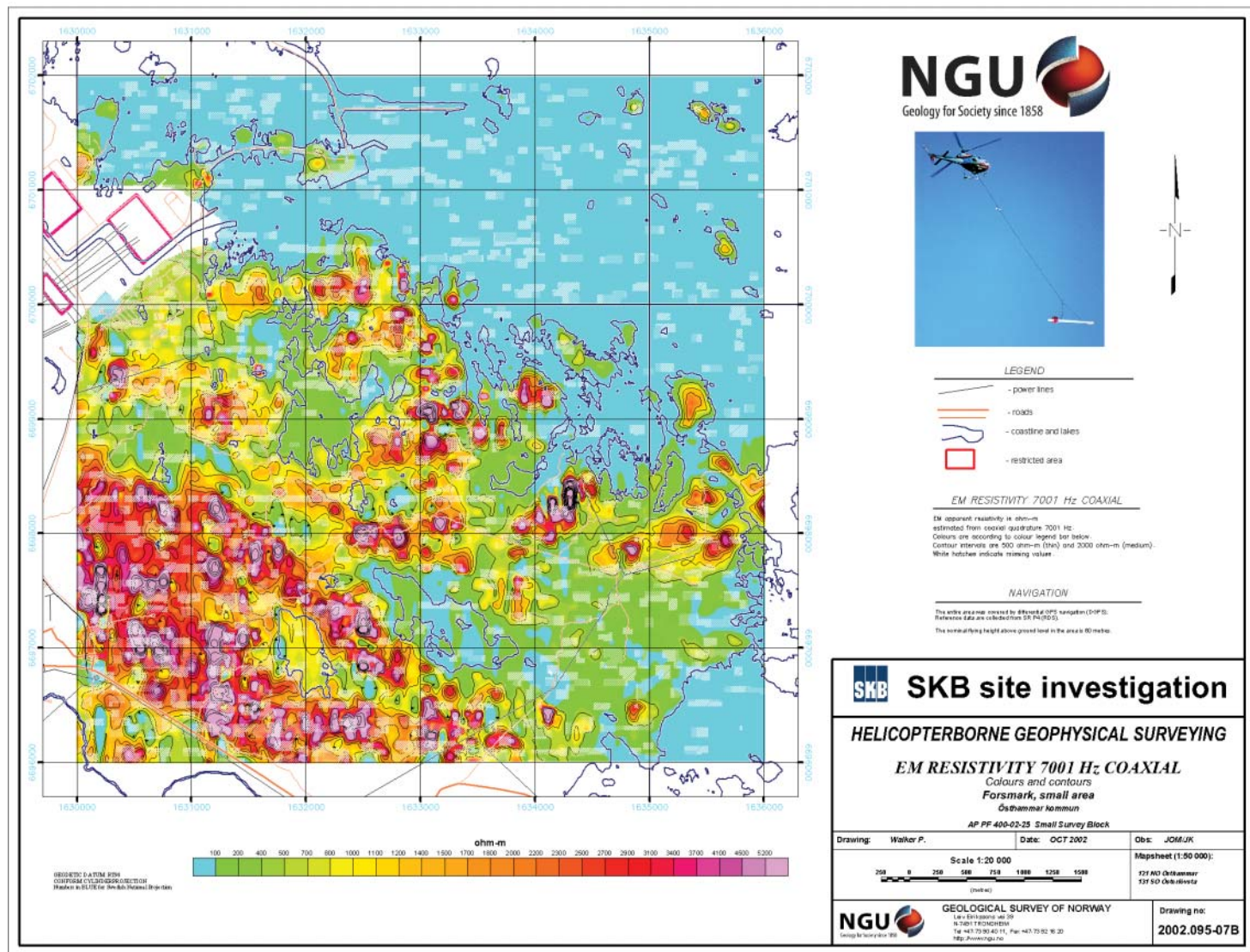


Figure F-22. EM Resistivity 7001 Hz Coaxial, East-West area. Map number 2002.095-07 B.

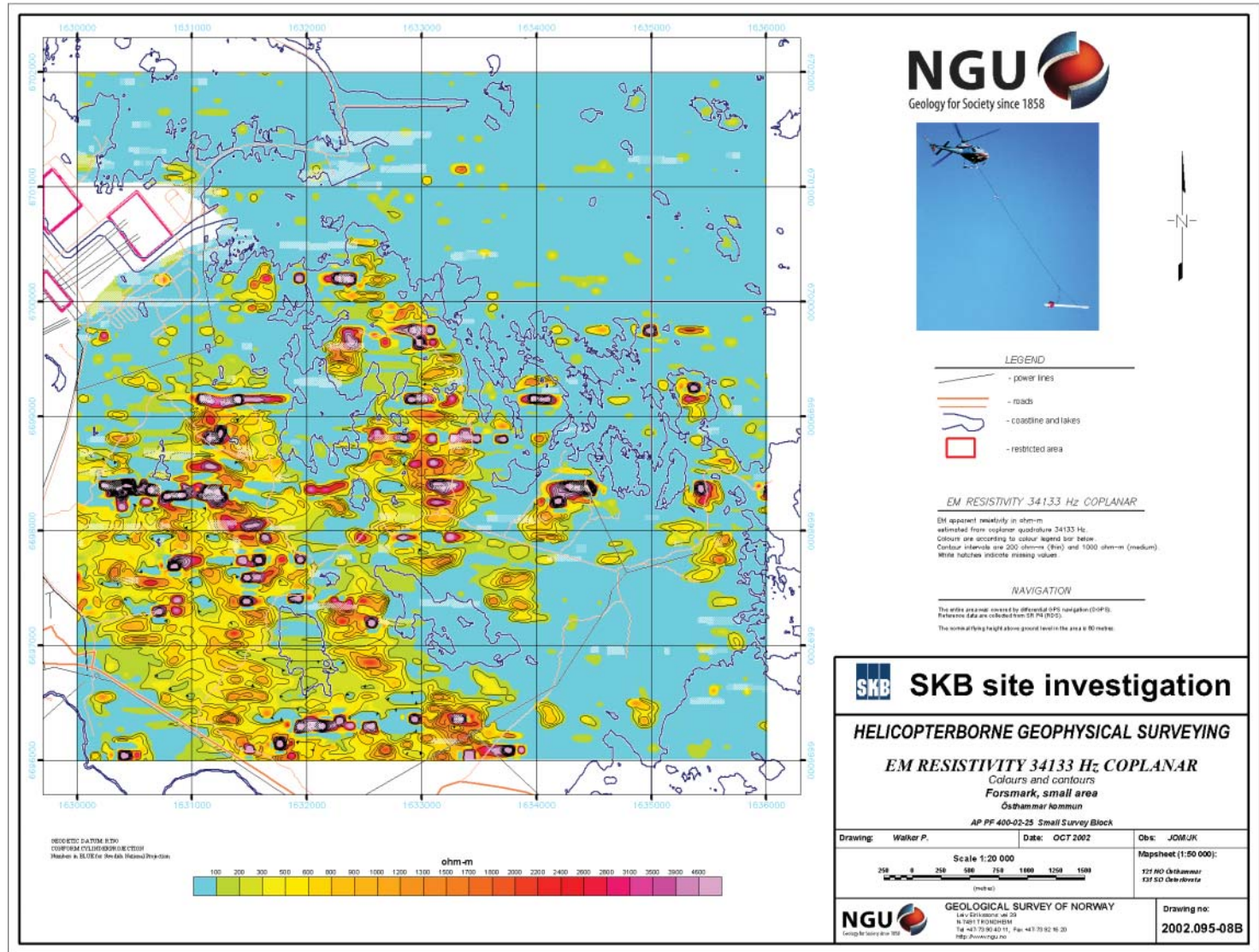


Figure F-23. EM Resistivity 34133 Hz Coplanar, East-West area. Map number 2002.095-08 B.

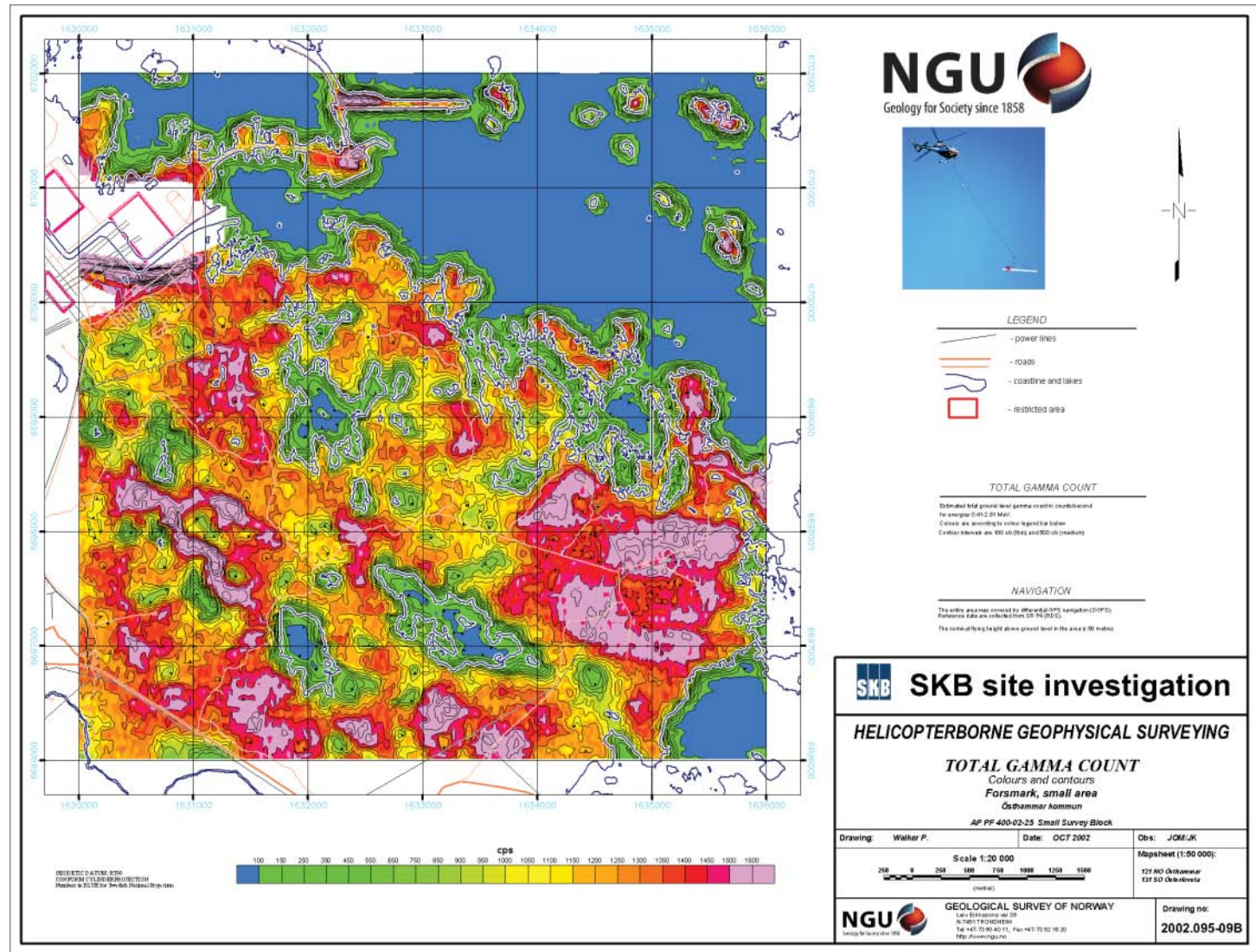


Figure F-24. Radiometric Corrected Total Count, East-West area. Map number 2002.095-09 B.

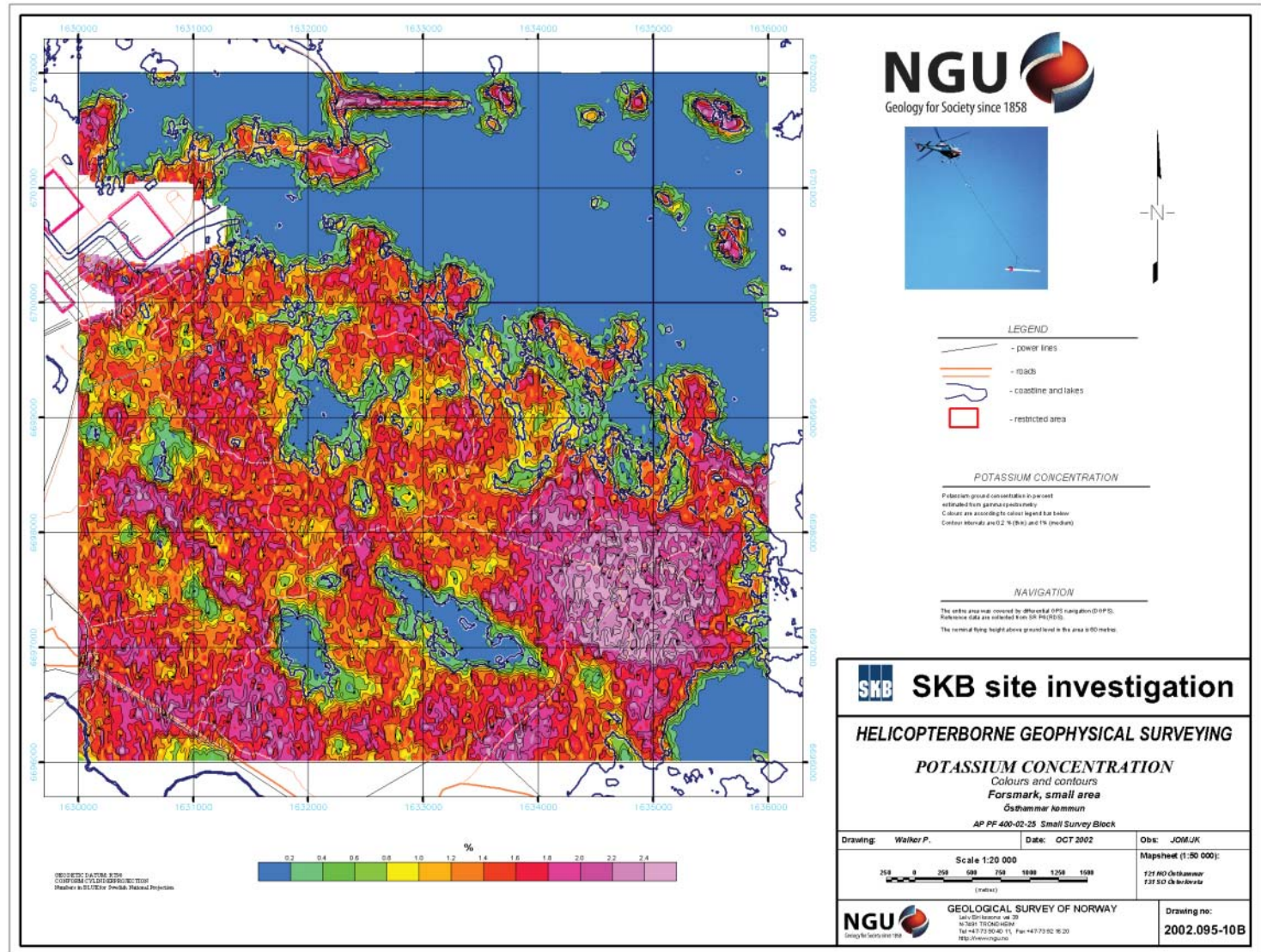


Figure F-25. Radiometric Potassium Concentration, East-West area. Map number 2002.095-10 B.

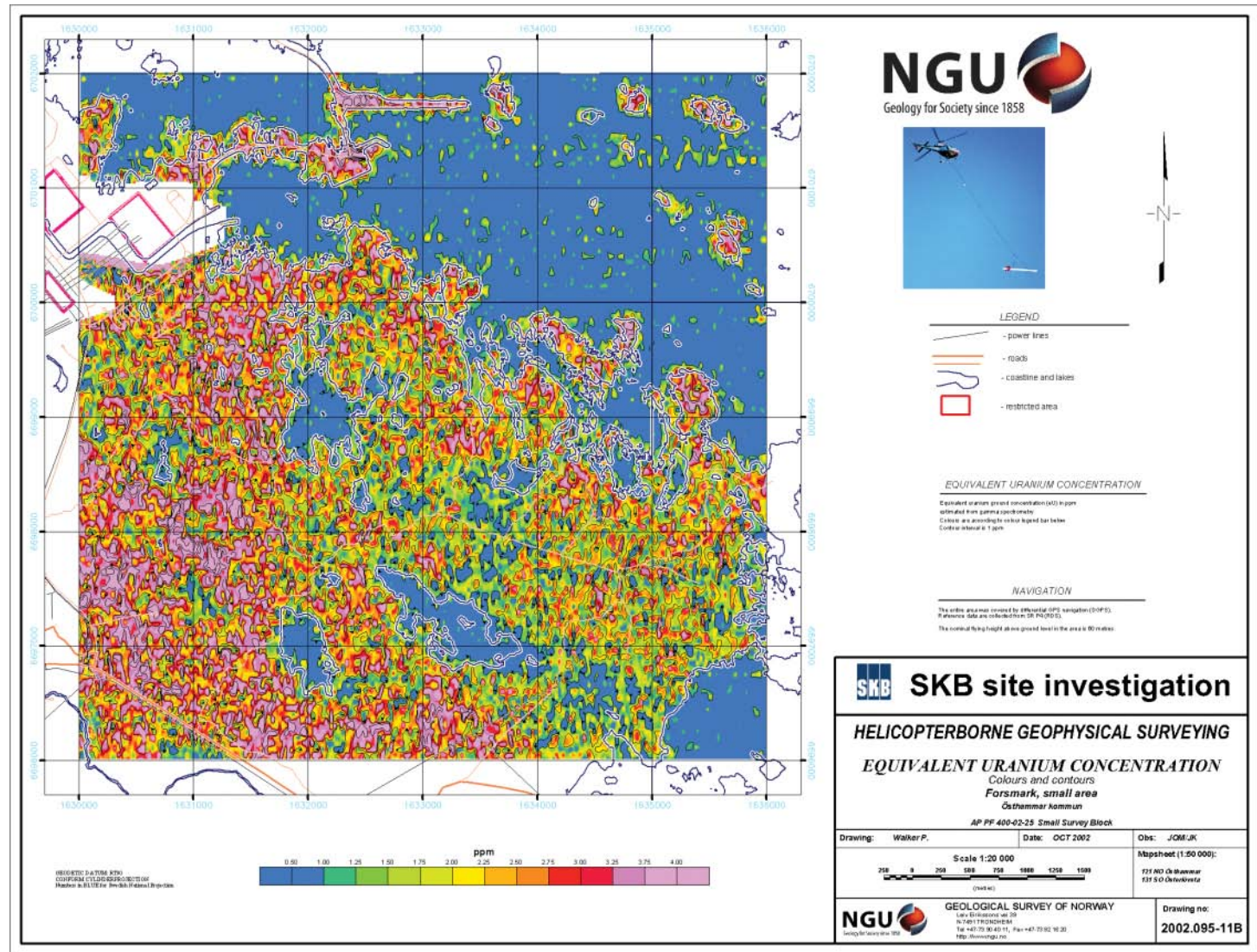


Figure F-26. Radiometric equivalent Uranium Concentration, East-West area. Map number 2002.095-11 B.

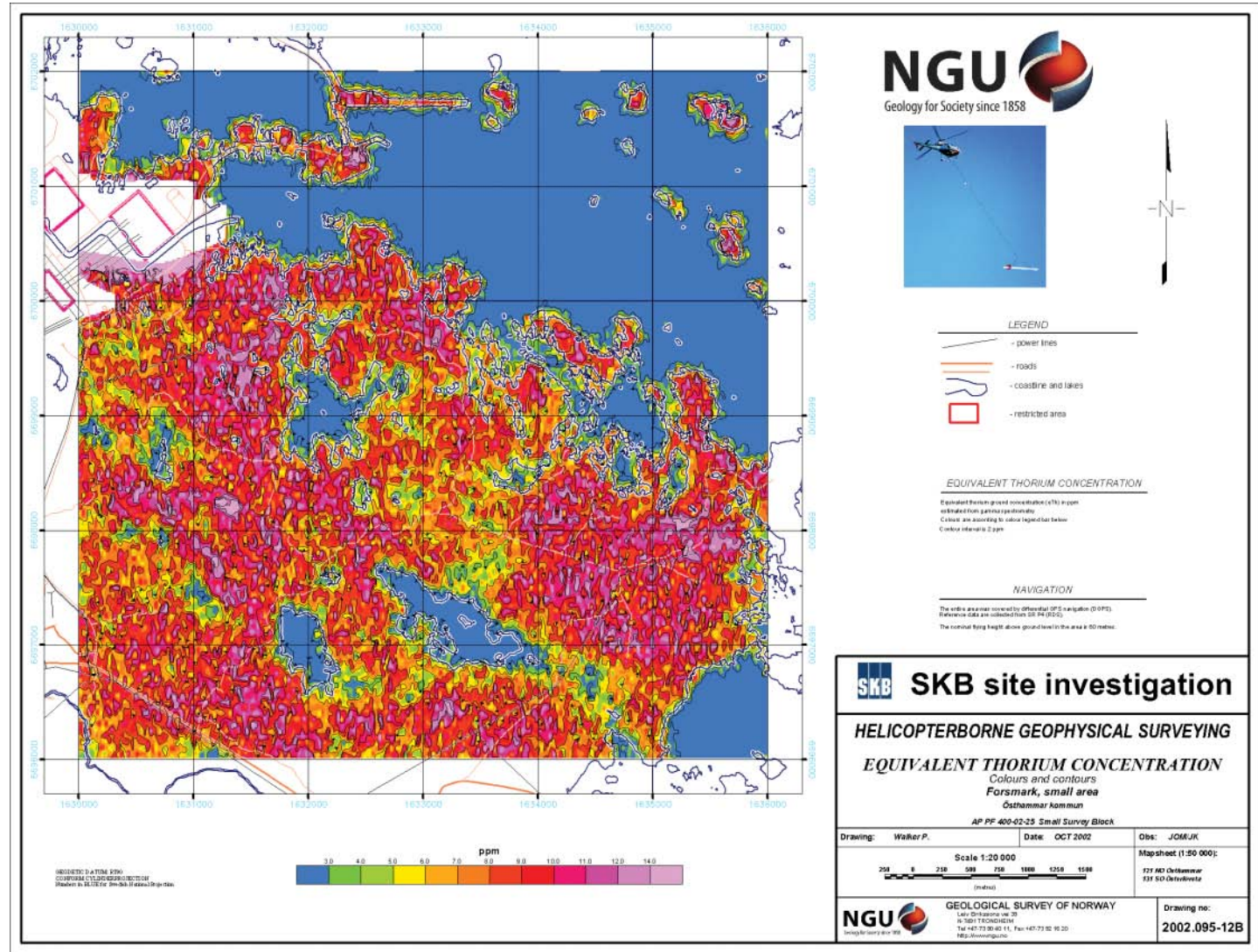


Figure F-27. Radiometric equivalent Thorium Concentration, East-West area. Map number 2002.095-12 B.

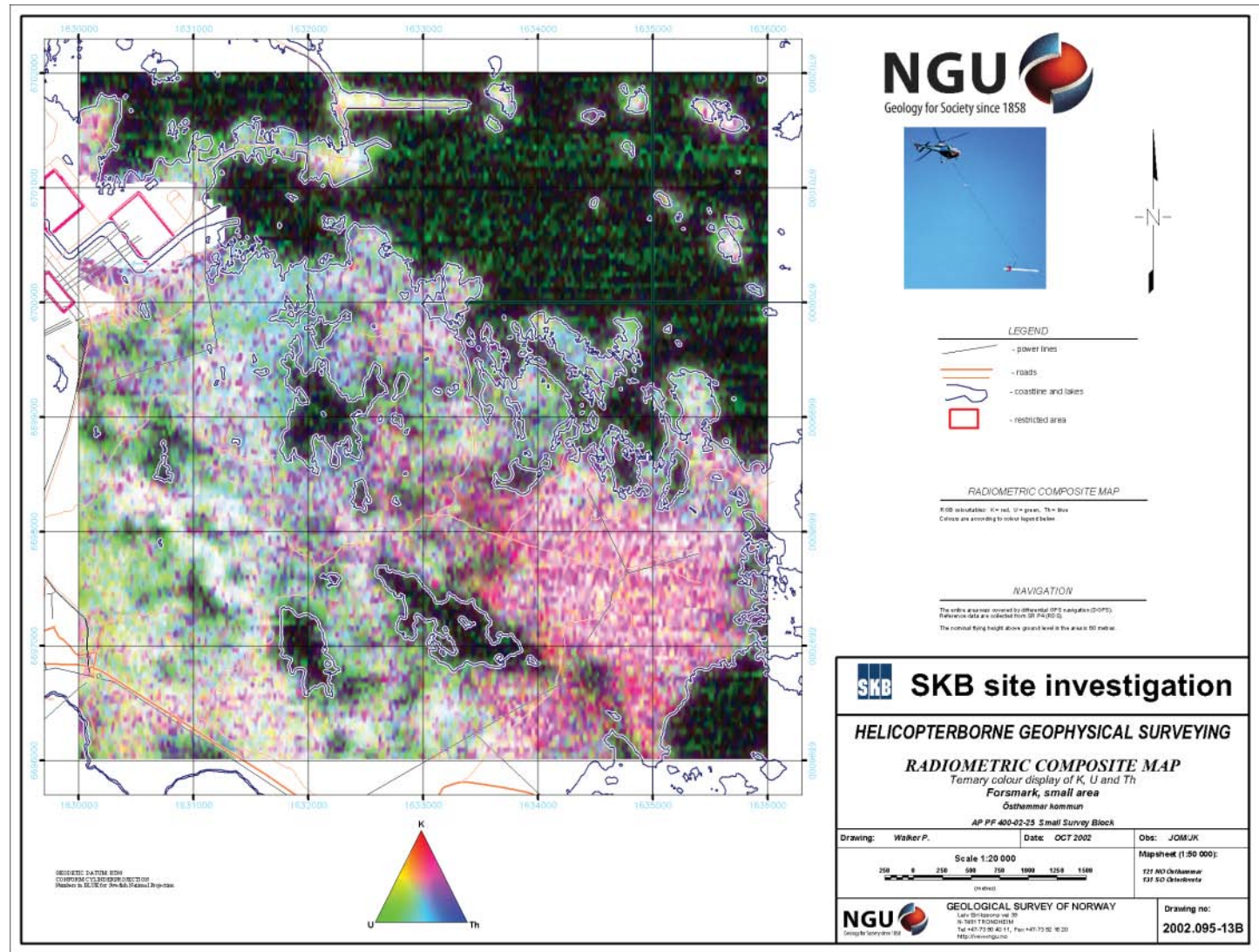


Figure F-28. Radiometric RGB Composite Map, East-West area. Map number 2002.095-13 B.

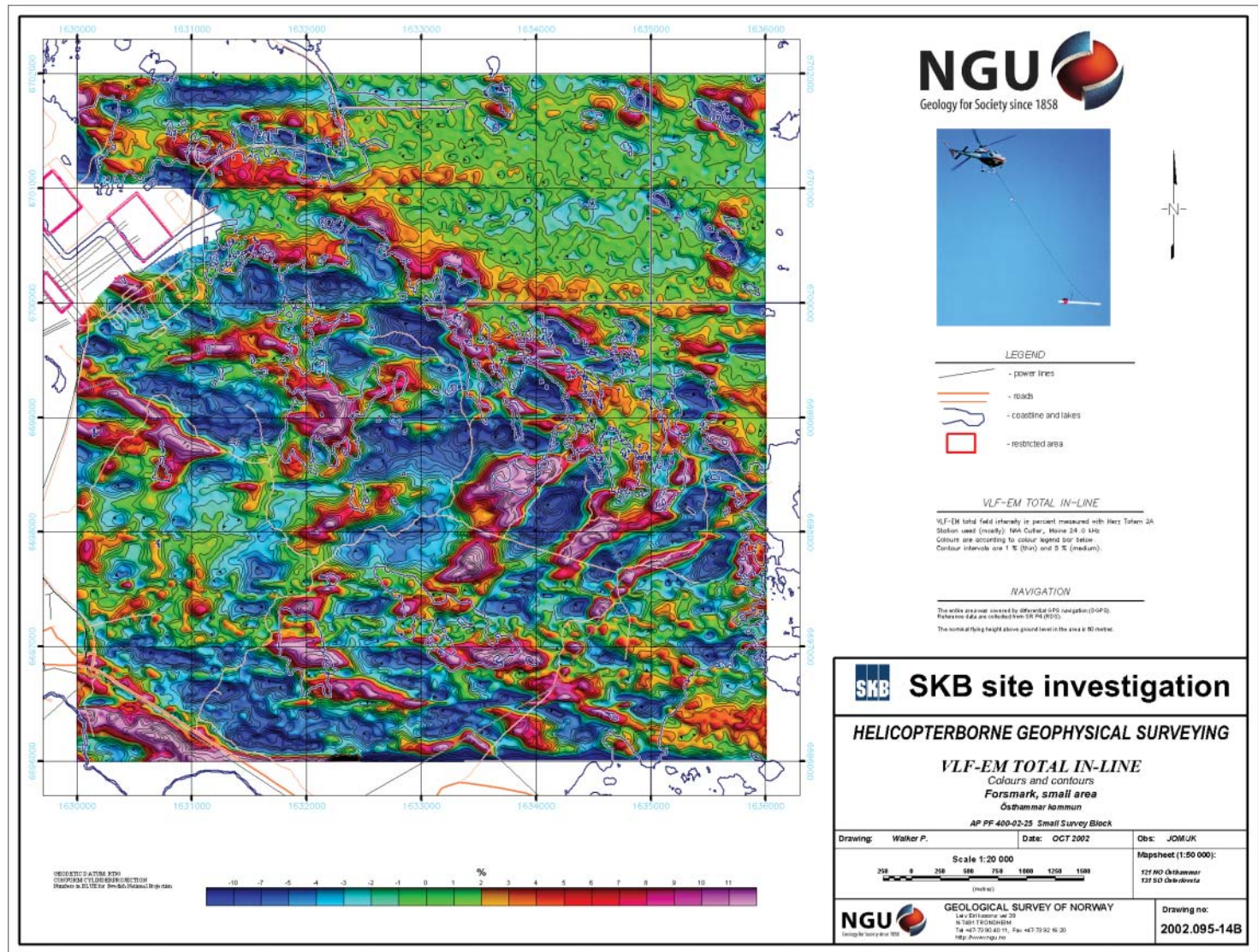


Figure F-29. VLF-EM Total In-Line, East-West area. Map number 2002.095-14 B.

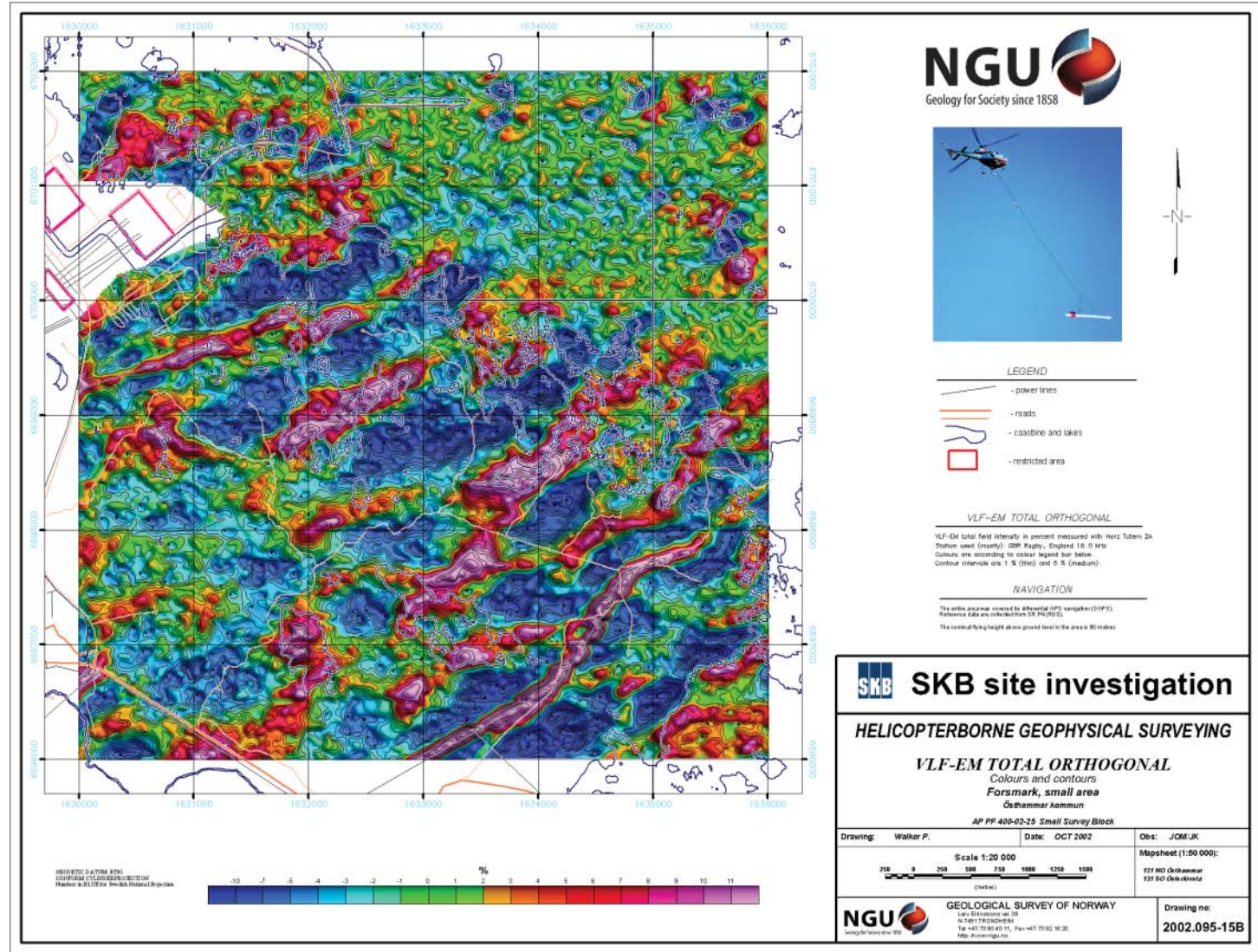


Figure F-30. VLF-EM Total Orthogonal, East-West area. Map number 2002.095-15 B.

Forsmark site investigation

Removal of DC power line influence on magnetic data in the Forsmark area

Hossein Shomali, Peter Hagthorpe, Sören Byström
Geological Survey of Sweden

January 2003

Keywords: DC, cable, nanoTesla, power line, microlevelling

Summary

As part of Svensk Kärnbränslehantering AB's (SKB) site investigations in the Forsmark area, geophysical measurements from helicopter have been carried out by the Geological Survey of Norway (NGU). Details about instrument tests, data acquisition, processing of data, map production and data delivery for the survey are described in section A of the present report.

The magnetic field data was severely influenced by the effect of a DC power line running on the sea bottom between Sweden and Finland, partly within the investigation area. Upon request from SKB, this effect has been, as far as possible, removed from the data set by the Geological Survey of Sweden (SGU).

Contents

1	Introduction	119
2	Processing steps	120
2.1	Preparation of a DC-current variations data file	121
2.2	Preparation of the original data	121
2.3	Estimation of the power-line location	122
2.4	Power-line correction	123
3	Results	124
3.1	Uncertainties	126
4	References	127

1 Introduction

This document reports the removal of the influence of a DC power line on magnetic data gained in a helicopter borne geophysical survey in the Forsmark site investigation area. The survey was carried out by the Geological Survey of Norway (NGU), according to activity plan AP PF 400-02-25 (SKB internal controlling document) and is one of the activities performed within the site investigations.

The magnetic field data was severely influenced by a DC power line, which runs on the sea bottom between Sweden and Finland. The Geological Survey of Sweden (SGU) was commissioned to, as far as possible, remove the influence of the power line.



Figure 1-1. Area covered by geophysical measurements from helicopter. Measurements are performed along north-south lines in the large diamond shaped area and along east-west lines in the smaller square area. The position of the DC cable can be seen in Figure 2-2.

2 Processing steps

The tool used for the processing was a standard PC computer with OASIS MONTAJ/ Geosoft software, and Matlab. Input data was XYZ files from NGU containing Co-ordinates, Dates, Time, Diurnal variation, Altitude above ground, Raw magnetic field and Magnetic field corrected for the diurnal variations.

The main task was to remove the influence from the DC power line. The basic principle for this correction is to calculate a correction value for each data point as a function of distance to the cable and actual current in the cable. However, some other corrections were also carried out. These corrections were:

- A few lines had an absolute offset with no connection to the DC power line. These lines were manually adjusted, see Table 2-1.
- In the data set received from NGU, the diurnal correction gave an incorrect value when GPS-data was missing. These data points were corrected by assigning the correct diurnal variation values, see Table 2-2.
- After the removal of the influence from the DC power line, microlevelling was performed on the data set. The limit was chosen to be 5 nT (nanoTesla).

Table 2-1. Lines with adjusted absolute value.

Line	Date	UTC-time	Added Value nT
1770	20020904	12.24–12.32	–3
60110	20020911	11.32–11.37	5

Table 2-2. Lines corrected for error in diurnal variation.

Line	Date	Time
560	20020829	08.48–08.51
970	20020917	09.01–09.04
1110	20020916	13.37–13.41
1350	20020908	09.58–10.06
1360	20020908	09.28–09.36
1410	20020908	09.41–09.48
2090	20020903	10.22–10.28
2320	20020917	14.46–14.50
2340	20020917	14.56–15.00
2380	20020917	15.16–15.20
2400	20020917	15.27–15.31
2430	20020917	15.42–15.46
70540	20020912	08.18–08.23
70550	20020912	08.32–08.36
70560	20020912	08.43–08.47
70890	20020913	11.32–11.36

2.1 Preparation of a DC-current variations data file

For each day during the airborne survey an analogue plot was received from Svenska Kraftnät (SVK). The plot showed the current in the DC cable during the day. According to these plots that present daily variations of the current (from Aug. 23 till Sep. 18 2002), in Amp. (Ampere), a file was generated that contains variations of current with respect to time. The resolution of the time and current are better than 5 minutes and 15 Amp, respectively. Fortunately, the uncertainty in time did not cause any correction problem.

This file was later used to add the corresponding current value to each grid point of the data set through a Fortran program written for this purpose. Some of the entries are as follows:

```
...  
20020828 03 03 255  
20020828 06 00 0  
20020828 14 00 150  
...
```

where the entries are “YearMonthDay”, “hour”, “minute” and “current” for a given period respectively.

2.2 Preparation of the original data

The original data set, delivered by NGU, had 7 columns as:

X	: x-values in metre (East-West),
Y	: y-values in metre (North- South),
MagFixLag	: magnetic data (nT) corrected for diurnal variation,
Date	: YearMonthDay,
UTCtime	: hour: minute: sec (utc),
RALTM	: altitude [†] (metre),
MAG_FIBY	: magnetic data from Fiby observation station (nT).

[†] The altitude data refer to the position of the helicopter, while the sensor used for measuring the total magnetic data was 30 metre below the helicopter. An attempt has been made to correct this with respect to the height of the power line. However, right above the power line, this uncertainty of the real height has caused some problems.

After visual inspection of the original data in OASIS, an ASCII-file was exported that contains the values above. Secondly, a Fortran program was used to check the time of each grid point with the time given in the file that contains variations of current with respect to time (described above), in order to assign a corresponding current value to each grid point. Therefore, an extra column was added which contains the amount of current in Amp. based on the time of measurement for each grid point.

2.3 Estimation of the power-line location

The position of the cable was only partly known, and in the end, the magnetic data itself gave the best position information.

The magnetic field shows an abrupt change around the power line, which is based on the amount of current. This can be used to find the location of the power line. Figure 2-1 shows the total magnetic field variations along the line “51160” as a sharp peak followed by a steep trough.

Various attempts were made to estimate the location of the power line by studying the magnetic field response:

(I): Horizontal gradient: This method failed to give an accurate location of the power line. The horizontal gradient method gives the centre of “peak-trough” as the position of the power line, which is not an accurate estimate. Since the magnetic field in the studied area is not vertical, the position of the power line does not coincide with the centre of the “peak-trough”.

(II): Analytic signal: For such cases as the current study, the best method to automatically estimate the location of the power line is thought to be the analytical signal. The implementation of this method did however not succeed, and due to the lack of time for further experiments, this method was abandoned.

(III): The procedure finally used in this project was to study the “peak-trough” characteristic feature of the data set and visually pick the location of the power line. It was assumed that the cable should be virtually straight without many changes in its strike.

The power line extension far outside the measured area was included in the final estimate of power line influence as depicted in the Figure 2-2.

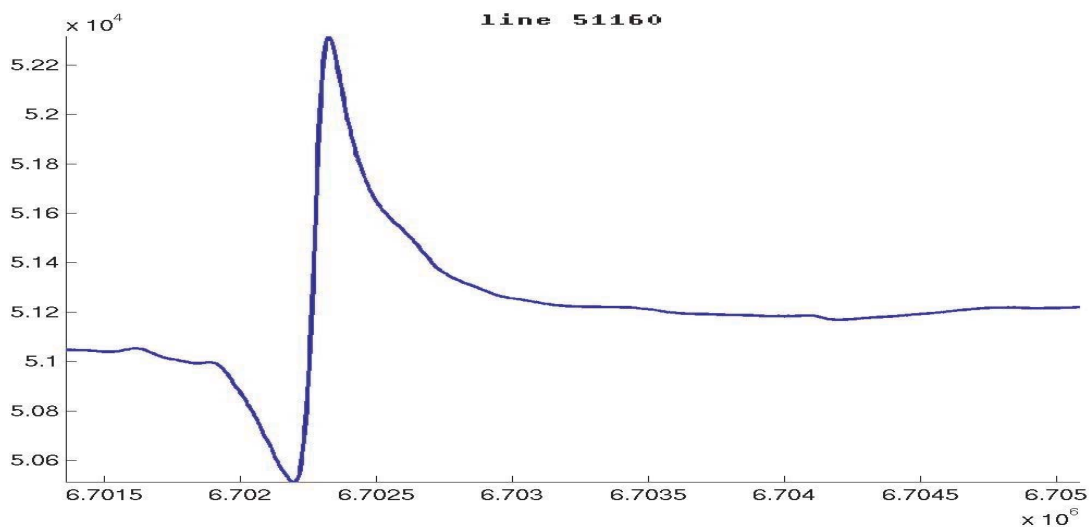


Figure 2-1. The magnetic field response over the DC cable (line 51160).

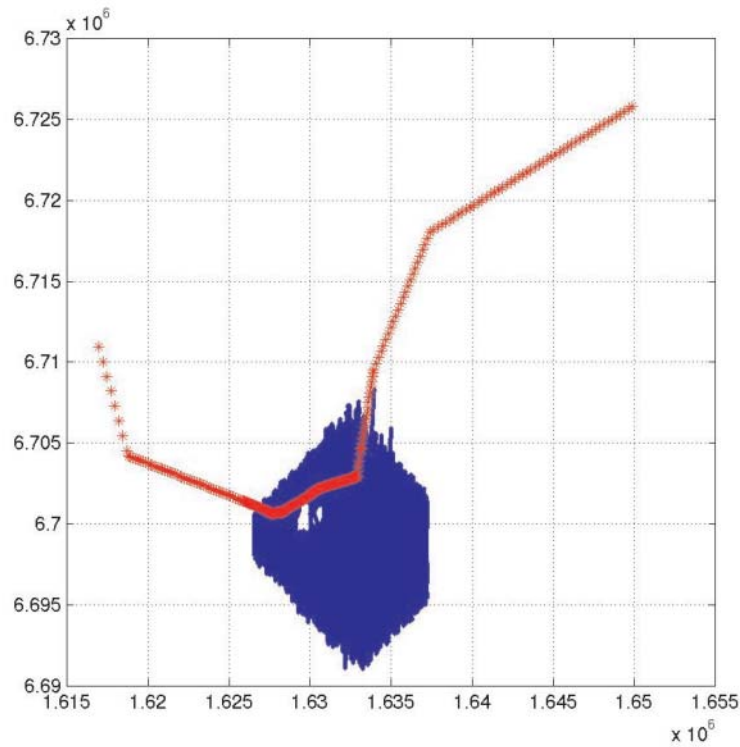


Figure 2-2. The position of the DC cable relative to the investigation area.

2.4 Power-line correction

After adding a proper current value to each grid point, the final data set was imported to “matlab” and the correction was done as follows:

The whole length of the estimated location of power-line was divided into different segments, and then for each segment and grid point (observation point) the magnetic field vectors (in x, y and z directions) were calculated based on “Biot-Savart law” as:

$$\vec{B}(p) = \frac{\mu_0 I}{4\pi} \int \frac{d\vec{l} \times (\vec{r}_2 - \vec{r}_1)}{|\vec{r}_2 - \vec{r}_1|^3}$$

where $\mathbf{B}(p)$ is the magnetic flux density (Tesla), μ_0 is the free space magnetic permeability ($\mu_0=4\pi \cdot 10^{-7}$), I is current (Amp.), $d\vec{l}$, \vec{r}_2 and \vec{r}_1 are source and observation point vectors. In this equation, $\mathbf{B}(p)$ is a vector with three components in East-West, North-South, and vertical directions. Subtracting calculated magnetic field components ($\mathbf{B}(p)$) from the observed magnetic field, removes the effect of the power-line from the data.

Detailed segments were used for the power line inside the area, whereas coarser segments were implemented outside the area while calculating the magnetic field effect of the power-line.

In conclusion, the magnetic effect of the power line was calculated for each grid point. For this calculation we have used the amount of current that was running in the power line at the time of measurement. Finally, for each grid point, the effect of the power-line has been corrected for by subtracting the observed magnetic field from the calculated magnetic field.

Close to the power line, there are some disturbances, which could not be removed. These disturbances may be due to some error in the location of the power-line, which to some extent is due to the oscillations of the sensor (see also Section 3.1).

3 Results

Corrected data has been sent back to NGU and are also delivered to SKB on a CD marked “SGU, Forsmark site investigation, AP PF 400-02-25”. The data is delivered in two files:

- Forsmark_EW_Cable_April2003.XYZ East-west flying area.
- Forsmark_NS_Cable_April2003.XYZ North-south flying area.

The data in the files has the following parameters:

X	x-values in metre (East-West).
Y	y-values in metre (North- South).
MagFiby_Cor	Corrected diurnal variation.
Date	YearMonthDay.
Mag_noCable	Magnetic field data after cable reduction, corrected diurnal variation and adjustment of absolute values.
Mag_Fin	Magnetic field data after microlevelling within 5 nTesla.
Mask	Data is either 1 or dummy. 1 corresponds to valid data. Dummy corresponds to data straight over the cable.
Mag_Fin_Mask	Magnetic field data after microlevelling within 5 nTesla. Finally masked to hold dummies directly over the power line.
UTCTIME	Time in Hours, Minutes and seconds.
RALTM	Altitude in metre above ground.

All magnetic data are delivered in the unit of nanoTesla (nT).

Figures 3-1 to 3-4 show data before and after removal of the DC cable effect.

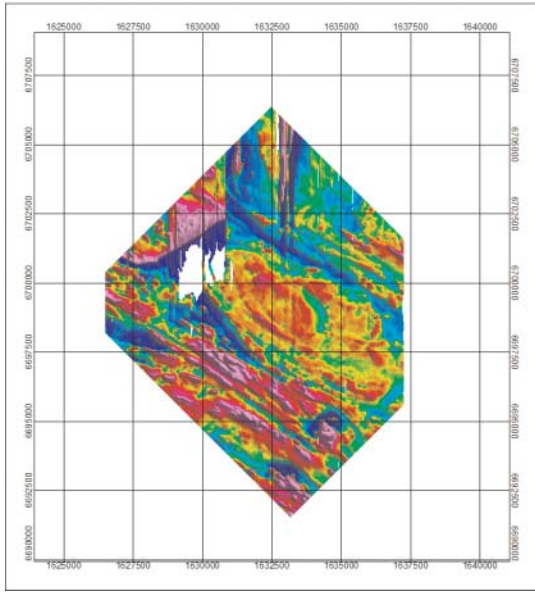


Figure 3-1. Magnetic field before correction. N-S flight direction.

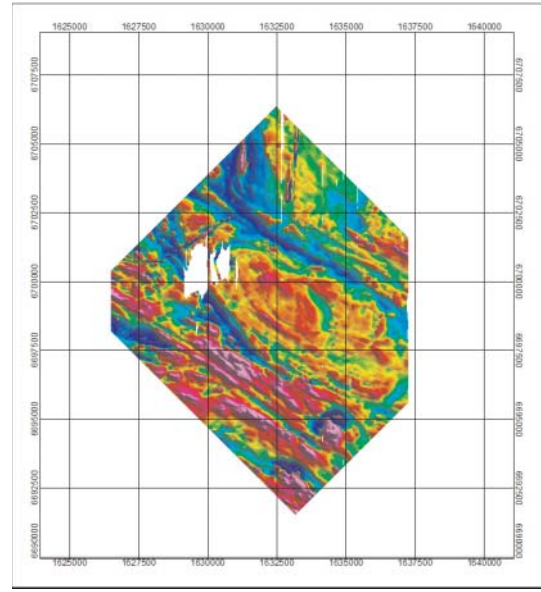


Figure 3-2. Magnetic field after correction. N-S flight direction.

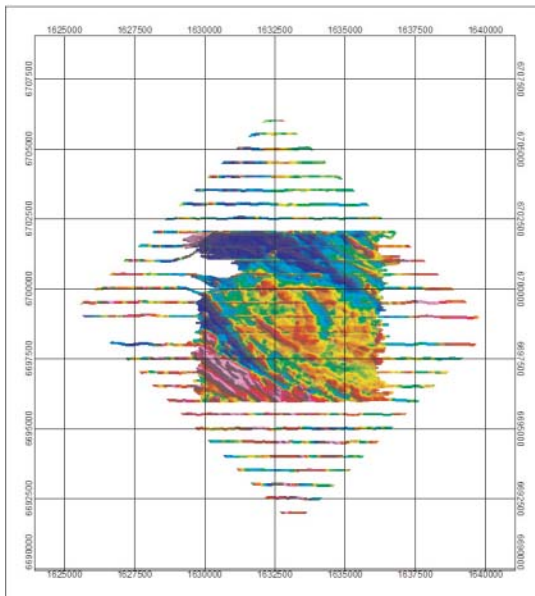


Figure 3-3. Magnetic field before correction. E-W flight direction.

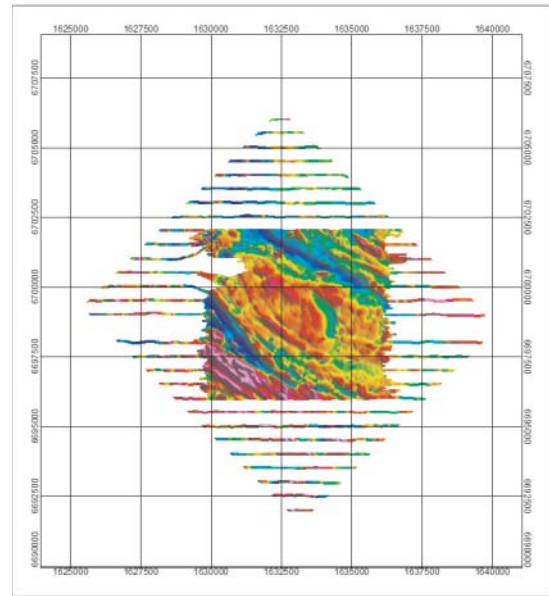


Figure 3-4. Magnetic field after correction. E-W flight direction.

3.1 Uncertainties

Uncertainties in the reduction of the DC power line influence arise from:

1. Absolute value of current in the DC cable. The information from Svenska Kraftnät was an analogue plot for each day. The accuracy in data selected from these plots is in the order of 5 to 15 A corresponding to an uncertainty in the order of tenths of nT straight over the cable and 1 to 2 nT 1000 metres away.
2. Uncertainties of the sensor position relative to the GPS sensor. Straight over the cable this could give an error of more than 100 nT. 1000 m away from the cable this effect is negligible.
3. Uncertainties of the distance from the sensor to the cable. Straight over the cable this could give an error of more than 100 nT. 1000 m away from the cable this effect is negligible.

These uncertainties imply that right over the cable it is more or less impossible to get a total reduction of the DC power line effect in magnetic field data. A kilometre away from the power line, these uncertainties are virtually negligible.

4 References

- (I) “Matlab” function to calculate “Biot-Savart law” was received from:

Valana L Wells, Ph.D. Associate Professor
Department of Mechanical and Aerospace Engineering
Arizona State University, Box 876106
Tempe, AZ 85287-6106
USA
<http://ceaspub.eas.asu.edu/aero/mae461/downloads.htm>

- (II) Text books used in this study :

Blakely R J, 1995. Potential theory in Gravity and magnetic applications. Cambridge university press.

Cooper G R J, 2002. Advanced potential field data processing. Helsinki University.

Gharibi M, 2000. Electromagnetic studies of the continental crust in Sweden. Ph.D. thesis, Uppsala University, Sweden.

- (III) Some Cshell-scripts, matlab functions, and a Fortran program that have been written for this purpose.

Forsmark site investigation

Correction of uranium data in the Forsmark area

Sören Byström
Geological Survey of Sweden

April 2003

Keywords: Geophysics, helicopter, radiometrics, Uranium, levelling

Summary

As part of Svensk Kärnbränslehantering AB's (SKB) site investigations in the Forsmark area, geophysical measurements from helicopter have been carried out by the Geological Survey of Norway (NGU). Details about instrument tests, data acquisition, processing of data, map production and data delivery for the survey are described in section A of the present report.

In the final data delivery from NGU, a few lines in the radiometric data set were not properly levelled for radon in the air. The lines are 1060, 1070, 1080 and 1090, all flown N-S. The Geological Survey of Sweden (SGU) has, on request from SKB, levelled the uranium data on the lines in question.

Contents

1	Introduction	135
2	Processing steps	136
3	Data delivery	137

1 Introduction

This document reports the correction of uranium data gained in a helicopter borne geophysical survey in the Forsmark site investigation area. The survey was carried out by the Geological Survey of Norway (NGU), according to activity plan AP PF 400-02-25 (SKB internal controlling document) and is one of the activities performed within the site investigations.

In order to enable proper interpretation of the data, the uranium data on a few lines needed levelling to compensate for anomalous concentrations of radon in the air. The levelling was carried out by the Geological Survey of Sweden and applies to lines 1060, 1070, 1080 and 1090 in the area flown N-S (see Figure 1-1).

SGU have upon request from SKB carried out the levelling of uranium data.



Figure 1-1. Area covered by geophysical measurements from helicopter. Measurements are performed along north-south lines in the large diamond shaped area and along east-west lines in the smaller square area.

2 Processing steps

The work carried out comprises five steps, as described below. The tools used are a standard PC computer and Geosoft OASIS MONTAJ software. The five processing steps are:

1. Statistics was run on the Uranium window on the downward looking detector and the upward looking detector. This was done on a number of lines in the area where the radon problem occurred, as well as on a number of lines without radon problem.
2. Based on the statistics, a correction factor was estimated. This estimation was basically done by trial and error.
3. The correction factor was used to create new uranium values. Data was gridded and by visual inspection the correction factor was adjusted until the lines to be levelled showed no visual radon effects.
4. The final new uranium values were imported to the original database from the new uranium grid.
5. Data delivered is the original radiometric data set (as delivered from NGU) with a new channel "UR_COR" added. "UR_COR" is a copy of the original "UCORR_LAG" except for the corrected lines 1060,1070,1080,1090.

3 Data delivery

Corrected data have been delivered to SKB, on a CD labelled “SGU, Forsmark site investigation, AP PF 400-02-25”. The data is delivered in one file:

NS_FORSMARK_SPM_CO2.XYZ

The data file is a copy of the file named NS Forsmark Radiometric.xyz, as delivered from NGU, with one additional column named “UR_COR”, which is a copy of the original “UCORR_LAG” except for the corrected lines 1060, 1070, 1080 and 1090.

Thus the file contains the following channels:

Flight		Flight number
Date		Date YMMDD; Y = year, MM = month, DD = Day of month
UTCtime		Universal time Hours:Minutes:Seconds.Decimal_seconds
recnum		Internal record number, ordinal, per flight; incremented at 0.1 per tenth of a second
X_RT90FIXINT	metres	X, RT90 corrected
Y_RT90FIXINT	metres	Y, RT90 corrected
RT90_LAT	deg:min:sec	Latitude, RT90, based on X_RT90FIXINT
RT90_LONG	deg:min:sec	Longitude, RT90, based on Y_RT90FIXINT
RALTM	metres	Radar altimeter, unfiltered
TCEXP_LAG	micoR/hr	Exposure
TCCORR_LAG		Apparent total count concentration, /Geosoft, 2001/
UCORR_LAG	ppm	Apparent U concentration
THCORR_LAG	ppm	Apparent Th concentration
KCORR_LAG	%	Apparent K concentration
TEMP	Degrees C	Temperature
BARO	mBar	Barometric altimeter
UR_COR	ppm	Apparent U concentration, leveled by SGU